DYNAMIC MODELING OF AN UNDERGROUND GAS STORAGE FACILITY

HISTORY MATCHING AND PREDICTION

by
Karakoz Kozhakhmetova

A thesis submitted to the Department of Mineral Resources and Petroleum Engineering of the Mining University of Leoben in partial fulfilment of the requirements for the degree of Master of Science (Petroleum Engineering).

Vienna, Austria

Date_____

Signed: _____
Karakoz Kozhakhmetova

Approved: _____
Dr. Johannes Pichelbauer
Thesis Advisor

Leoben, Austria

Date_____

_____
Univ.-Prof. Dipl.-Geol. Ph.D. Stephan Matthai
Professor and Head,
Chair of Reservoir Engineering

I declare in lieu of oath, that I wrote this thesis and performed the associated research myself, using only literature cited in this volume.

_____ _____

Date Karakoz Kozhakhmetova

ABSTRACT

The Haag field in the Molasse Basin in Upper Austria is a depleted dry gas reservoir that was converted to underground gas storage. Three horizontal wells have been drilled to implement a gas storage facility. During their development many areas are subject to uncertainties. This work investigates the overall range of uncertainty in well performance prediction.

Well performance is calculated by semi-analytical and numerical approaches. For the semi-analytical approach a software package of Petroleum Experts, PROSPER, is used. The inflow performance of a well is calculated based on a specified well model. The three models applied are Kuchuk and Goode, Goode and Wilkinson, and Babu and Odeh. Further work is then based on Kuchuk and Goode model.

The numerical approach is based on the finite difference method, and the simulation software of Schlumberger, ECLIPSE. The simulation model used is the history matched model of the gas storage facility.

Inflow performance curves for different scenarios were determined by these two approaches and the results of the two approaches are then compared. The inflow performance curves calculated semi-analytically are considered to be more realistic, because they are based on models specifically developed for horizontal wells. Therefore, these inflow performance curves are used as reference curves.

The calculations indicate that the inflow performance calculated numerically is too optimistic compared to the semi-analytical approach. Thus, the inflow performance of horizontal wells, calculated numerically, needs to be corrected for future simulation forecasts. However, it is not possible to determine a general correction factor. Performance must be evaluated for each well individually. For this task it is recommended to construct semi-analytically inflow performance models.

KURZFASSUNG

Das ausgeförderte Gasfeld Haag liegt im Molasse Becken in Oberösterreich und wurde in einen Untertage Erdgasspeicher umgewandelt. Zu diesem Zweck wurden drei horizontale Speicherbohrungen abgeteuft. Bei der Entwicklung eines Untertage Gasspeichers existieren verschiedene Bereiche in denen man mit Unsicherheiten in der Bestimmung der notwendigen Daten und Parameter konfrontiert ist. Diese Arbeit behandelt die Unsicherheiten im Bereich der Berechnungen der Sondenkapazitäten.

Die Sondenkapazitäten wurden mit semi-analytischen und numerischen Ansätzen berechnet. Für den semi-analytischen Ansatz wurde das Software Packet von Petroleum Experts, PROSPER, verwendet. Die Berechnungen basieren auf verschiedenen Horizontalsondenmodellen, die verwendeten drei Modelle sind von Kuchuk & Goode, Goode & Wilkinson, and Babu & Odeh. Für die weiteren Berechnungen in dieser Arbeit wurde das Modell von Kuchuk & Goode verwendet.

Der numerische Ansatz basiert auf der Finite Differenz Methode, die Simulationssoftware von Schlumberger, ECLIPSE, wurde hierfür benutzt. Das verwendete Simulationsmodell ist das an den historischen Daten geeichte Modell des Gasspeichers.

Mit diesen zwei Ansätzen wurden „Inflow Performance“ Kurven (IPR Kurven) für unterschiedliche Szenarien ermittelt und die Ergebnisse verglichen. Da der semi-analytisch Ansatz auf Modellen, entwickelt speziell für Horizontalsonden basiert, wurden diese IPR Kurven als Referenzwerte verwendet.

Die Auswertung hat gezeigt, dass die numerisch berechneten Sondenkapazitäten der horizontalen Speichersonden zu optimistisch waren. Daher müssen diese Werte korrigiert werden um zuverlässige Modelle für Vorhersagen zu erhalten. Es ist jedoch nicht möglich, einen allgemeinen Korrekturfaktor zu finden, deshalb muss dieser Faktor für jede Sonde individuell bestimmt werden. Es wird daher empfohlen jeweils semi-analytische IPR Modelle zu erstellen um den notwendigen Korrekturfaktor für die numerischen Berechnungen bestimmen zu können.

TABLE OF CONTENTS

LIST OF FIGURES

LIST OF TABLES

ACKNOWLEDGMENTS

I would like to express my sincere appreciation to the Rohöl – Aufsuchungs AG and its employees for their support of this thesis. I would specifically like to thank my mentor, Dr. Johannes Pichelbauer for his valuable suggestions and assistance, and lots of patience. I must also acknowledge MSc. Bernhard Griess, whose expertise, understanding and patience, added considerably to my graduate experience. Particular thanks to Dr. Ralph Hinsch and MSc. Wolfdietrich Jilg for taking the time to explain the geology of the field.

Further, I would like to extend my thanks to Professor Stephan Matthai, for his advice and guidance in writing this thesis.

I'm very grateful to Mr. Arnold Wahl for providing me this great and unique opportunity and financial support to get an academic degree in Austria.

I would like to express my deepest gratitude to my parents and my American family, Bidgoods, for their incredible support and love in all good and hard times.

Very special thanks go out to my friend, Pavel, who supported me fully in this process and has been an endless source of encouragement throughout the years I have known him.

Finally, I would like to thank God.

1 INTRODUCTION

RAG builds an underground gas storage using the depleted gas reservoir HOF3 in the Haag gas field. Schlumberger DCS and other consulting companies proved the convenience of the Haag field for storage operation by performing integrated reservoir studies. The further detailed design and the development of underground gas storage was done using a dynamic reservoir simulator.

During this kind of work different areas are subject to strong uncertainties in regard of storage development. For example, the determinations of long-term pressure development because of the uncertainty in the aquifer support, the correct modulation of the water-gas contact movement during the storage cycles. Well performance predictions lack relevant historic dynamic data as the potential of storage wells is usually an order of magnitude larger than that of existing production wells for which data exist.

The aim of this work is to evaluate the range of uncertainty in well performance predictions in case of the Haag underground gas storage and to develop recommendations for future gas storage developments.

The subsurface part of the gas storage Haag consists of three horizontal storage wells, drilled in 2008, and three vertical wells, mainly used for observation purposes but also used as back-up storage wells.

Well performance and productivity were calculated by a semi-analytical and numerical approach.

For the semi-analytical approach a software package from Petroleum Experts (IPM-PROSPER) was used. For each well a so called “Integrated Production Model” was constructed, each based on a different well model. IPR curves for various operating conditions were calculated. The impact of changing skin, permeability and effective well length on performance of the storage wells has been evaluated as well.

The numerical approach is based on the finite difference method. The simulation software ECLIPSE from Schlumberger was employed in numerical approach. The dynamic simulation model for the gas storage was used to calculate comparable well performance data by simulating withdrawal scenarios with the same operating conditions as in the analytical case.

The results of the semi-analytical and numerical approach were compared and recommendations to improve well performance predictions of future simulation models were derived.

2 FIELD DESCRIPTION

The Haag field is located in one of RAG's concessions of the Molasse Basin in Upper Austria (See Fig. 2.1, Fig. 2.2). The Molasse Basin is a foreland basin, which, from Oligocene onwards was in compression due to the Alpine Orogeny (See Fig. 2.3). This field was discovered in 1981 by exploration well HAAG-001 and has been extended with the wells HAAG-002 and HAAG-003 in the gas bearing horizon 'HOF-3' close to the Hall formation. The depositional environment of the gas bearing sands is of deep marine character. The reservoirs are part of a turbiditic channel belt which was fed from different source points. The dominant sediment transport direction in this particular reservoir was from west to east along the northern flank of the Northern Calcareous Alps. The reservoir comprises channel deposits which pinch out and are flanked by shale as well as sloping fan deposits that pinch out towards the north. HAAG-001 has been drilled through 5.0 m (MD) net gas sands, HAAG-002 through 12 m (MD) and HAAG-003 through 5.9 m (MD) net gas in the HOF-3 horizon. The average porosity is 30 % and average permeability is in the range of 250 mD. The field has an East-West trend with dimensions of 1500 m and 3000 m in the N-S and E-W directions respectively.

Proven GIIP is 420 Mio. m^3(Vn) and the estimated ultimate recovery is 405.5 Mio. m^3(Vn). Production histories and previous studies i.e. simulations of the reservoir have shown negligible connate water in the system. However, HAAG-002 has a secondary gas-water contact at -460.8 m TVDSS.

Table 2-1: Summary of reservoir characteristic in Haag field

GIIP proved [Mio.m^3(Vn)]	**420**
Ultimate Recovery [Mio.m^3(Vn)]	**405,5**
Reservoir Depth [m]	**985**
Initial Reservoir Pressure [bara]	**91**
Net Thickness [m]	**5 - 12**
Reservoir N/S [m]	**1500**
Reservoir E/W [m]	**3000**
Average Porosity [%]	**30**
Permeability [mD]	**250**

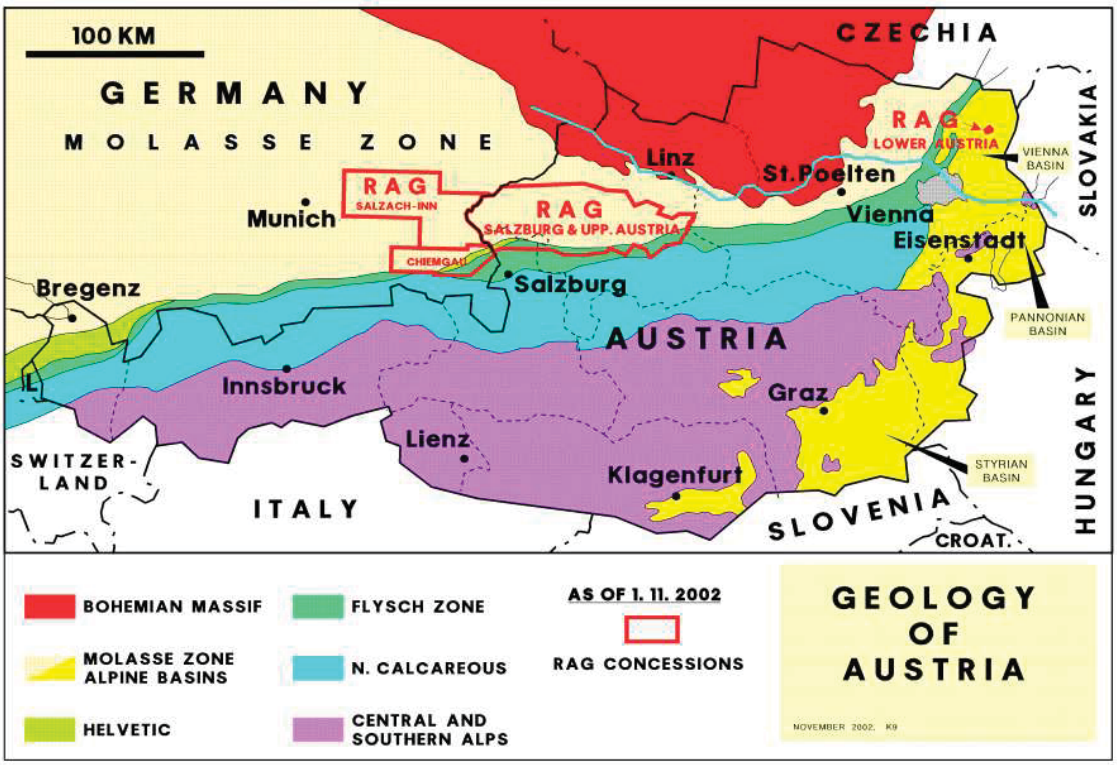

Figure 2-1: RAG Concessions on a Geological Map of Germany and Austria (after RAG)

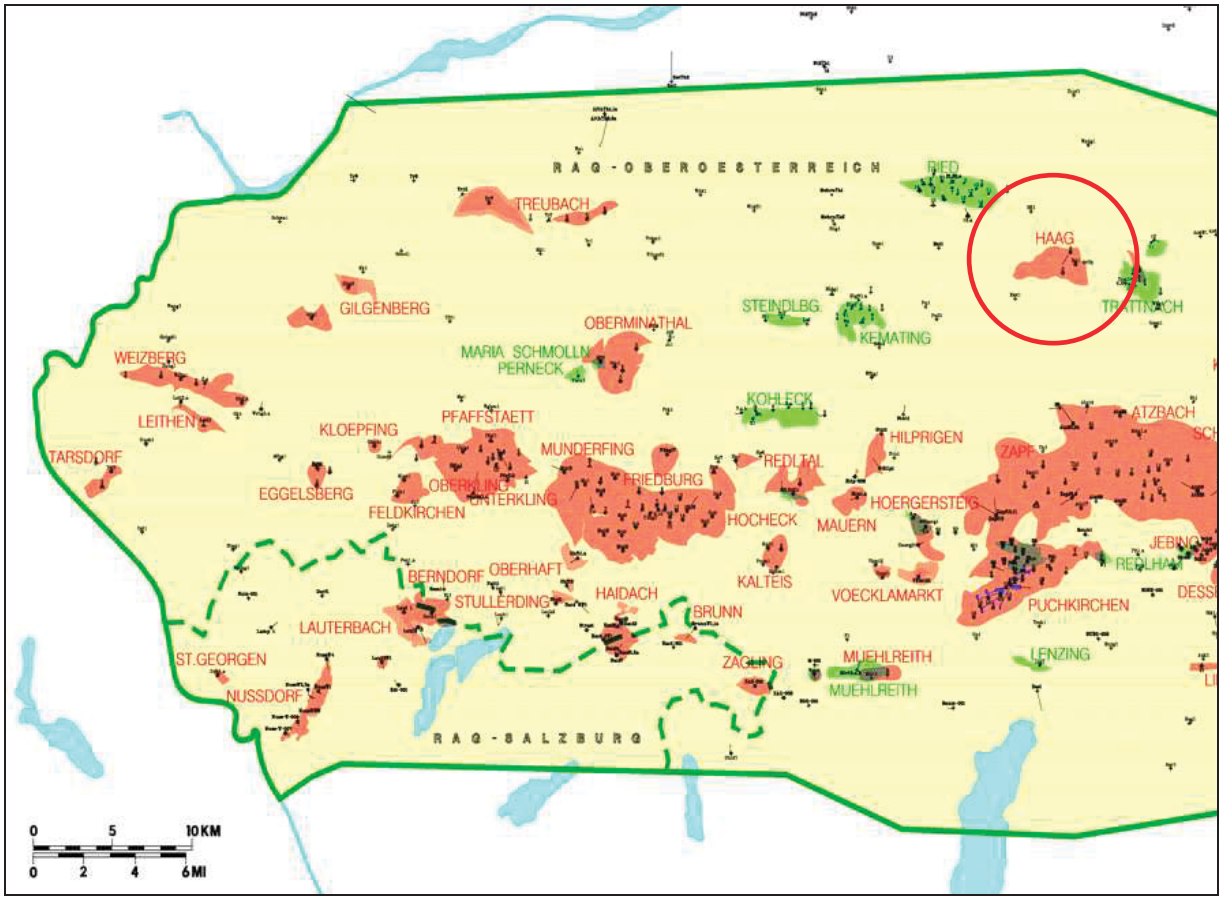

Figure 2-2: Location of Haag Field in RAG's Austrian Concession (after RAG)

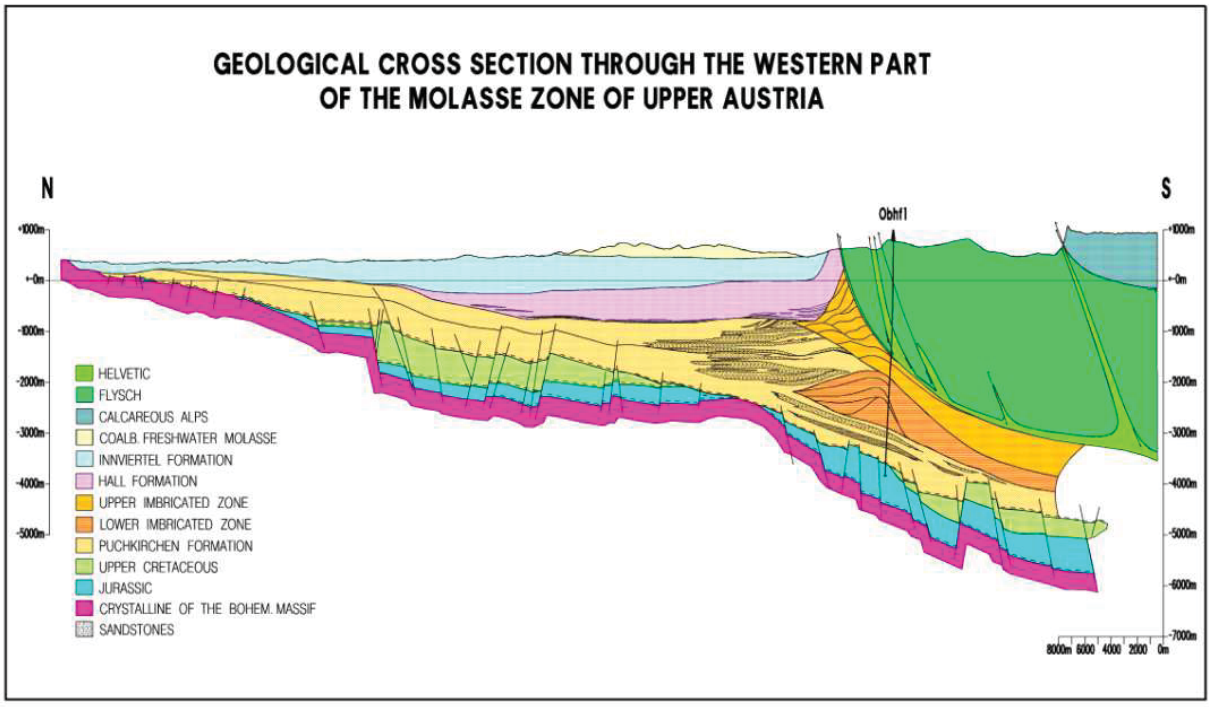

Figure 2-3: Geological cross-section through the Molasse Basin (after RAG)

3 FIELD DATA

The Haag dry gas reservoir started producing in mid-1983 through HAAG-001. In 1986 two more vertical wells, HAAG-002 and HAAG-003, were drilled. In 1993 HAAG-001 reached peak production of about 107103 [Sm^3/d], while HAAG-002 and HAAG-003 peak production of $75x10^3$ [$m^3(Vn)/d$] and $85x10^3$ [$m^3(Vn)/d$)] was reached in 1991 and 1994 respectively. At the end of February 2005, the production from all three wells was below $14x10^3$ [$m^3(Vn)/d$]. The surface limit for production was about $190x10^3$ [$m^3(Vn)$], which was attained in mid-1994.

It was decided to convert this depleted field to gas storage. Three horizontal wells were drilled to serve as injection/withdrawal wells. The main reason for deciding for horizontal wells was the relative thin thickness of the reservoir. It is difficult to drain large volumes using vertical wells since the contact area is small. Horizontal wells provide an alternative to achieve long penetration lengths in the formation. Another reason would also be the high permeability of the reservoir. In high-permeability gas reservoirs, wellbore turbulence limits the deliverability of a vertical well. To reduce turbulence near the wellbore, the only alternative is to reduce the gas velocity around the wellbore. This can be partly achieved by fracturing a vertical well. However, fracturing is not very effective in a high-permeability reservoir, because proppants themselves have a limited flow capacity, which may be comparable to that of the reservoir rock. The most effective way to reduce gas velocity around the wellbore is to reduce the amount of gas production per unit well length. This can be accomplished by using horizontal wells. The long wells may produce less gas per unit well length than a vertical well, but total horizontal-well production can be higher than for a vertical well because of the long length. Thus, horizontal wells provide an excellent method to minimize near-wellbore turbulence, and at the same time, improve total gas production from a well.

3.1 Data Review

3.1.1 Geological Model

The geology department of RAG has constructed a geological model, which forms the basis of the simulation model used in this study.

The reservoir deposits of the Haag Storage are part of the Hall Formation (Burdigalian), which belongs to the deposits of the Northern Alpine Foreland Basin (NAFB), commonly referred to as Molasse Basin[2].

The NAFB is a classical foreland basin, fetching the erosional products of the evolving Alpine orogen to the south, starting in upper Eocene times (Nachtman and Wagner, 1987). Kuhlemann and Kempf[2] stated "In the Swiss and German Molasse Basin a typical succession of marine to continental shelf deposits characterise the basin fill. In contrast, the eastern Bavarian and Upper Austrian part of the Molasse Basin maintain constant deep marine conditions from Rupelian to Burdigalian".

Borowski et al.[4] reported that a major unconformity at the base of the Burdigalian (Base of Hall Group) marks a major erosional event likely corresponding to the end of northward thrusting in of the tectonic units to the south of the basin. After the deposition of the basal beds of the Hall Group, which are deposited only in the central trough of the basin, a system of sedimentary wedges infills the morphological trough left behind by the Base Hall unconformity, prograding from southwest to northeast (See Fig. 3-1). Whether the Hall Group deposits of this system reflect delta sediments with storm reworking or still deep marine deposits is still under debate (Hinsch 2008). The reservoir deposits of the Haag storage belong to this system. The most common interpretation at RAG is that the sandstones represent turbiditic deposits at the toe of the prograding wedges, shed from the south. The Haag area is located at the northern slope of the Hall formation basin. Here, the prograding wedges directly down- and onlaps onto the basal Hall unconformity (See Fig. 3-1). The gas bearing sandstones of the Haag storage are called HOF-3 sands and are usually correlated between the Haag field and the Tratnach field further to the east, where they were encountered water bearing.

In reflection seismic data, the top HOF-3 level is represented by an impedance decrease (trough, red colour in RAG convention). In the area of the Haag storage, this level is characterized by a very high amplitude level, which is a result of the thick sand accumulation.

The former gas trap of the Haag field is mainly a stratigraphic trap, defined by pinch out of the sandstones towards the north, east and west in combination with the deposits dipping towards the south. Parts of the northern pinch out of the Haag field seem to be controlled by east-west striking normal faults, rooting in the Mesozoic deposits and the basement. The top and lateral seal is build by shales of the Hall Group.

The reservoir model was build by using the mapped and depth converted HOF-3 reflector and the amplitude information to constrain pinch outs and reservoir thickness in the field. Well logs were used to define reservoir and non-reservoir facies. The up-scaled logs were used to guide and constrain object based facies modelling in Petrel.

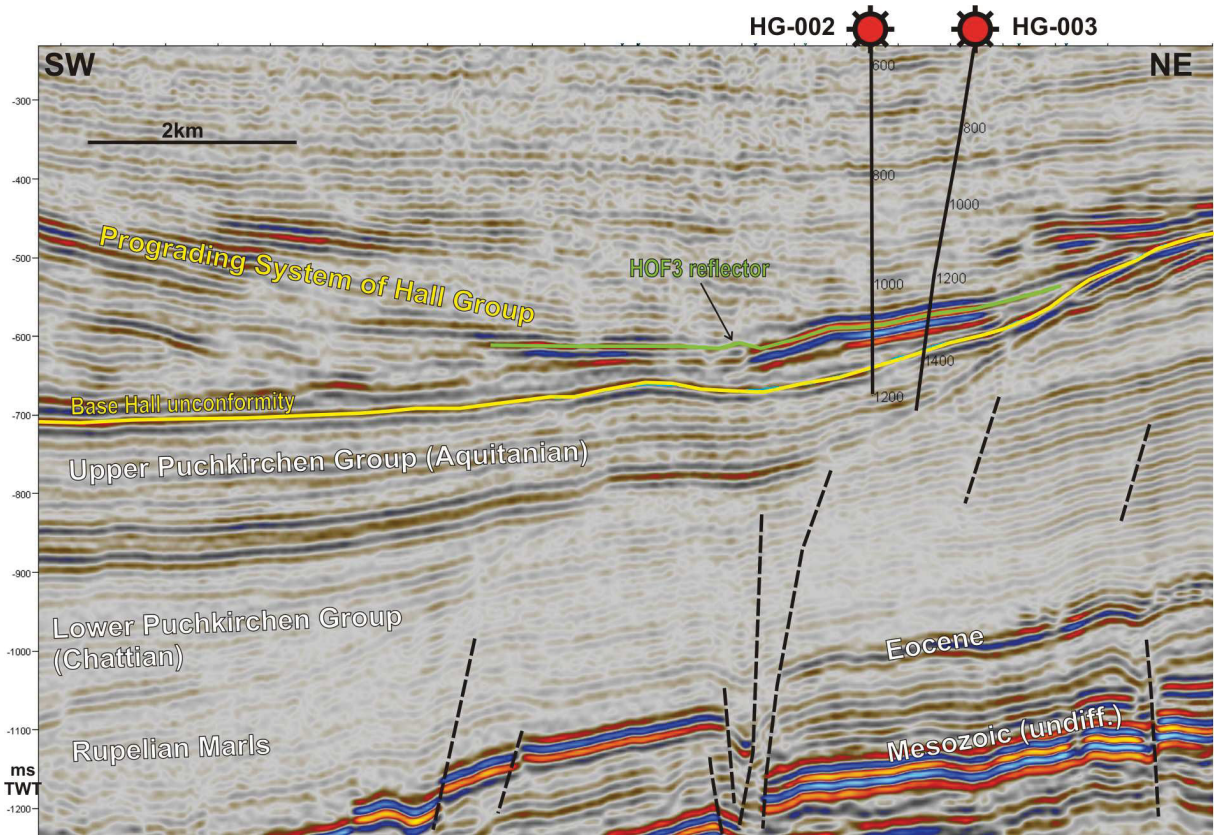

Figure 3-1: Interpreted 3-D reflections seismic section showing the geological setting of the Haag Field at the northern Slope of the Molasse Basin (after RAG).

After completion of HGSP-001, 002 and 003 the static model was updated. An additional zone (Zone 1) has been created comprising a suspected initial layer in top-section of HGSP-001. Zone 1 has a shale (non-reservoir) base. The Figure 3-2 illustrates the updated static model with the Zone 1. The next following figures show the top and base model. The facies modelling in Petrel was used for distribution of reservoir heterogeneity. The properties from upscaled well logs were used for distributing the reservoir facies by using a stochastic method. The main reservoir, Zone 2, has 72 % sand (reservoir) and 28 % shale (non-reservoir). The quality of the facies distribution in the main reservoir is shown in the histogram table. The percentages of reservoir, upscaled cells and well logs are well matched (see Fig. 3-5).

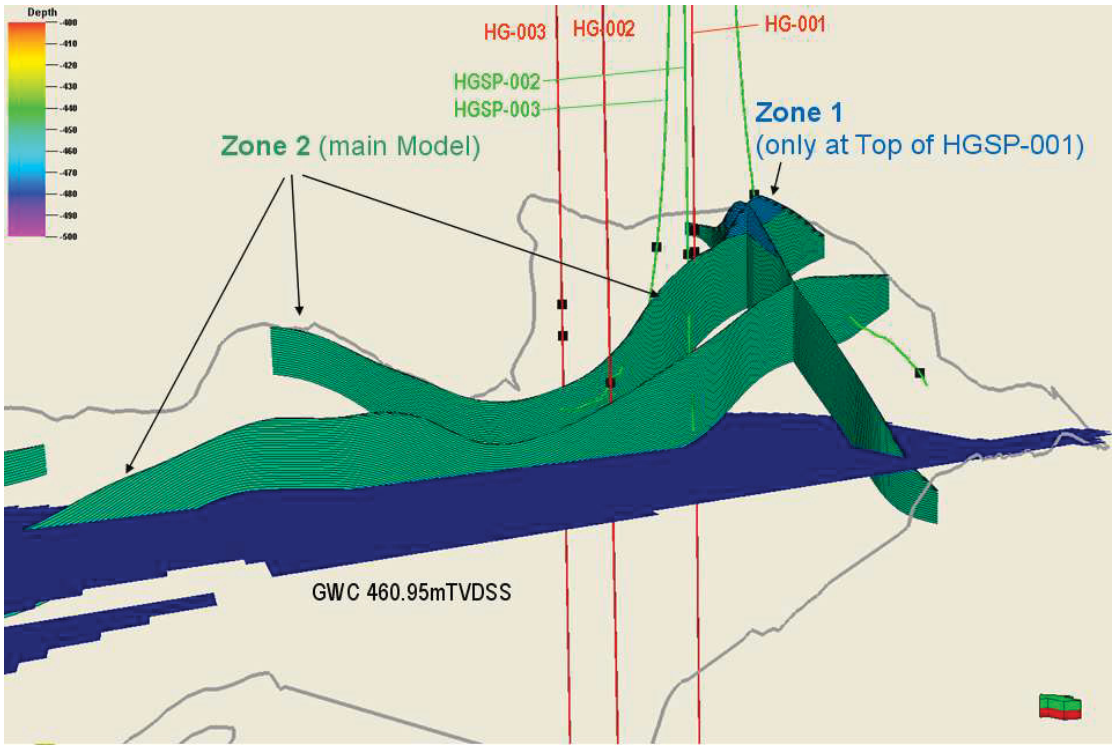

Figure 3-2: Static model with the Zone 1

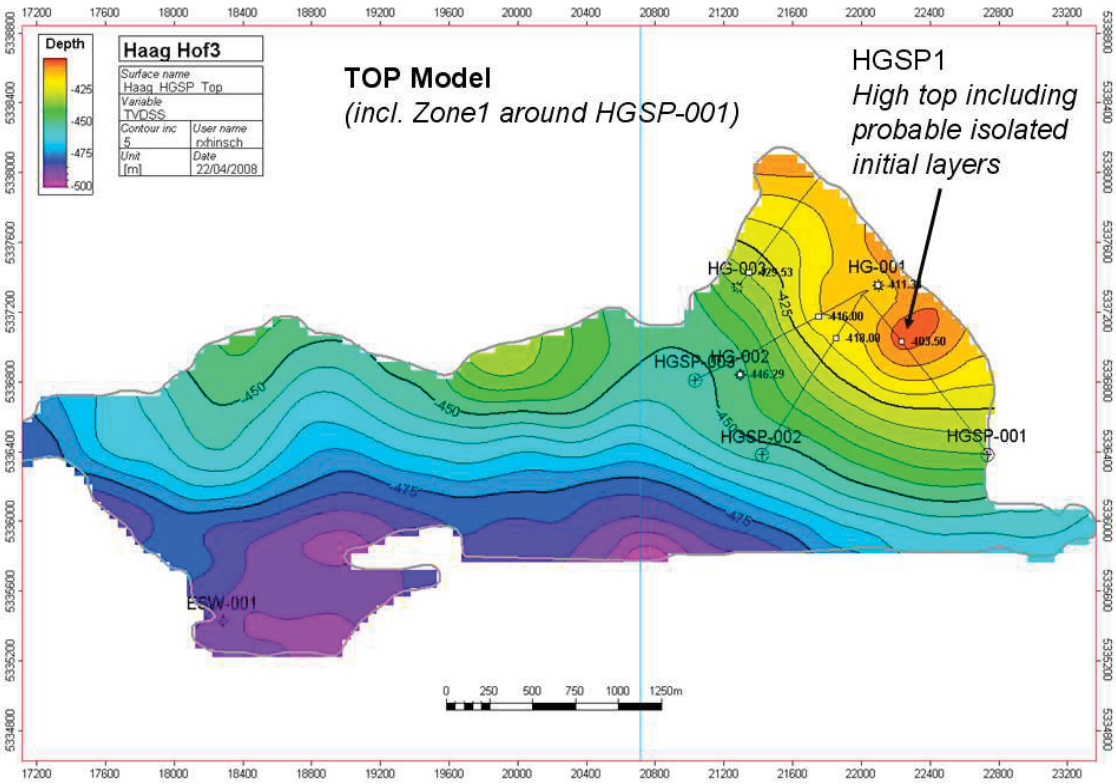

Figure 3-3: Top model

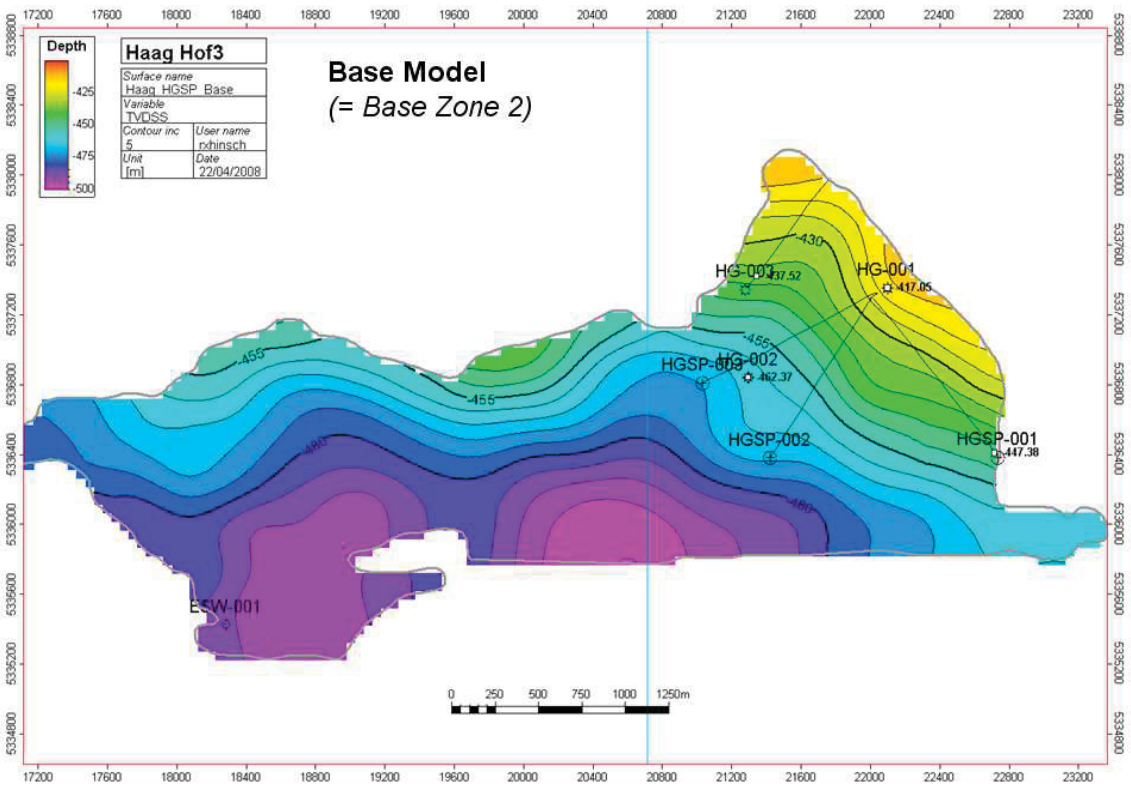

Figure 3-4: Base model

Figure 3-5: Histogram of facies distribution

The figure below depicts the overall distribution of reservoir and non-reservoir in the Haag field.

Figure 3-6: Sand and shale distribution in the reservoir

3.1.2 Petrophysical Data

Petrophysical properties were obtained from available logs of wells in the Haag reservoir. The properties which were input to the model were based on the results of petrophysical analysis performed by Schlumberger.

The porosity-permeability relationship is plotted in the following figure. This correlation is analogous to the porosity-permeability correlation of the neighbor field Puchkirchen located about 35 km away from the Haag field.

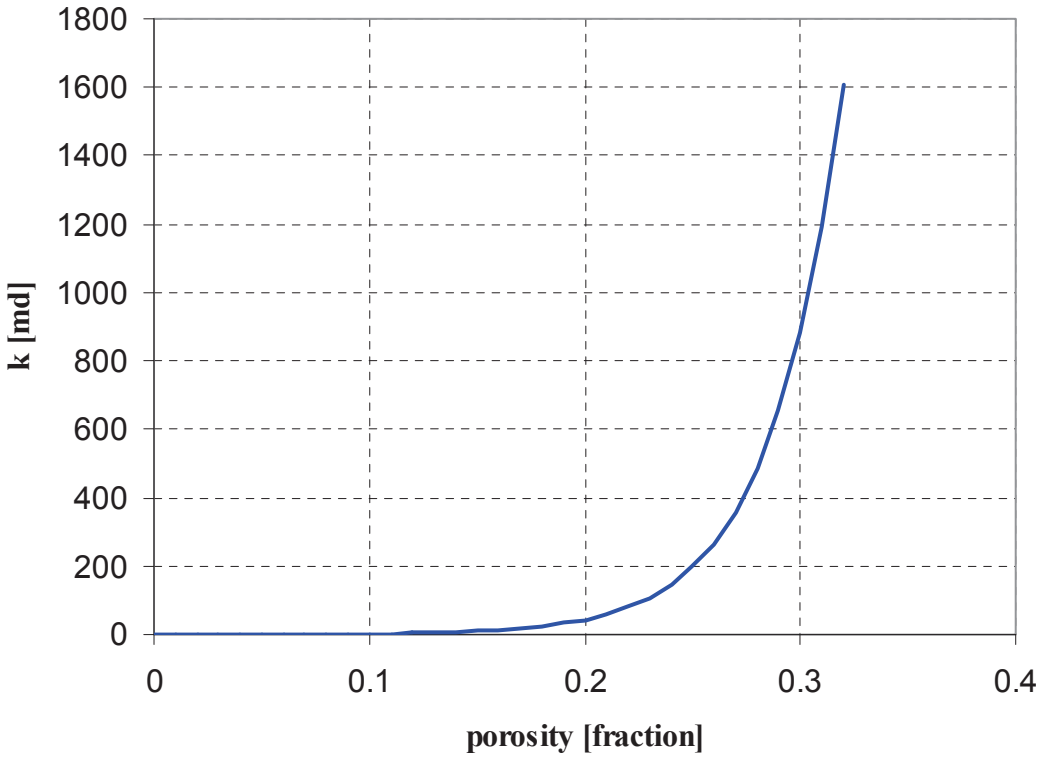

Figure 3-7: Permeability vs. Porosity

3.1.3 Initial Data

Initial pressure at datum depth of 411 m was 91 bars and initial temperature was 43 °C. The initial gas-water contact (GWC) was at 465 m TVDSS, which was defined from the observed GWC in well logs of HAAG-002.

3.1.4 SCAL Data

Relative Permeability curves were calculated using the Corey gas-water correlation method (see Appendix A). Capillary pressure curves were obtained on the basis of log data.

3.1.5 PVT Data

The Haag reservoir fluid analysis report indicates about 99 % of methane. Therefore, a specific gravity of 0.562 was used for calculations. Water salinity is 15000 ppm.

The Z-factor was calculated by using Standing and Katz method. The formation volume factor was computed with Z-factor correlation. (See Appendix B and C)

3.1.6 Well Data

Completion intervals of vertical and horizontal wells are tabulated below. The HGSP-001 was drilled from July 27th till 27th of August in 2008. The well was drilled down to depth of 1933

[mMD] which is 1033 [mTVDss]. Then the second storage well HGSP-002 was drilled from 30th of August till 3rd of October in 2008. HGSP-002 was drilled to final depth of 1900 [mMD] that is 1037 [mTVDss]. The third storage well was drilled in the fall of the same year, namely from 6th of October till 11th of November, down to depth of 1988 [mMD] which is equal to 1034 [mTVDss]. The sequence of completions in the reservoir was built into the Petrel model for each well.

Table 3-1: Completion Intervals for Haag vertical wells

Well	Year	Completion Interval [m] (MD)	Net Perforation [m]
HAAG-001	1983	984 - 987.5	3.5
HAAG-002	1986	1071.3 - 1084.0	4
HAAG-003	1986	1301.5 - 1311.0	9.5

Table 3-2: Completion Intervals for Haag horizontal wells

Well	Year	Completion Interval [m] (MD)	Net Perforation [m]
HGSP-001	2008	1192.46 - 1893.38	504.6
HGSP-002	2008	1094.52 - 1782.41	469.69
HGSP-003	2008	1181.44 - 1865.14	604.8

3.1.7 Production Data

Gas production data versus time of old vertical wells were provided up to March 2005. The production records showed that perforated pay intervals of the wells had produced gas rates of up to 200,000 [m³(Vn)/d]. The wells could have been produced higher rate but there was a limiting surface constraint.

3.1.8 Pressure Data

Reservoir pressure data provided by RAG had been gathered by RAG since the field start. The data used for estimating the reservoir pressure had been taken mainly from the flowing measurements. The pressure data had already been screened by RAG to eliminate unreliable data.

4 WELL PERFORMANCE AND PRODUCTIVITY – ANALYTICAL APPROACH

Well performance was examined analytically using the PROSPER software package. Two different models were used for each well and for different well model scenarios.

4.1 Description of reservoir models used for vertical wells

Since there are only production data, but no well test data for the three vertical wells, HAAG-001, HAAG-002 and HAAG-003 are available, the input data for IPR and VLP calculations were limited, as a result the number of models available in PROSPER was also limited to two models, namely *Jones* and *Petroleum Experts*.

Jones (1976)

The *Jones* equation for gas is a modified form of the Darcy equation which allows for both laminar and turbulent flow pressure drops. The Jones equation can be expressed in the form of:

$$p_{res}^{\ 2} - p_{wf}^{\ 2} = bq + aq^2 \qquad (4\text{-}1)$$

where b is a laminar flow coefficient and aq is a turbulence coefficient for gas wells. They are calculated from the reservoir properties or can be determined from a multi-rate test[6]. The definitions for a and b can be derived from the equation for radial pseudo-steady state gas flow, which is given as[7]

$$p_{res}^{\ 2} - p_{wf}^{\ 2} = \frac{1.424\mu ZTq}{kh}\left(\ln 0.472\frac{r_e}{r_w} + s\right) + \frac{3.16\times10^{-18}\beta\gamma_g ZT}{h^2}\left(\frac{1}{r_w} - \frac{1}{r_e}\right)q^2 \qquad (4\text{-}2)$$

where p_{res} … average formation pressure [psi]

p_{wf} … Flowing well pressure [psi]

q … Gas flow rate [Scf/d]

r_e … Well radius [ft]

r_w … Well radius [ft]

h … Producing formation thickness [ft]

s … Skin effect excluding turbulence effects [dimensionless]

Z … Dimensionless gas compressibility coefficient

T … Reservoir temperature [°R]

μ … Viscosity [cp]

k … Permeability [md]

β … Turbulence factor [ft^{-1}]

γ_g … Gas gravity

The darcy term is

$$b = \frac{1.424\mu ZT}{kh}\left(\ln 0.472\frac{r_e}{r_w} + s\right) \tag{4-3}$$

and, the term $\frac{1}{r_e}$ can be neglected since it is usually very small, then a is

$$a = \frac{3.16\times10^{-18}\beta\gamma_g ZT}{h^2 r_w} \tag{4-4}$$

Petroleum Experts

The *Petroleum Experts* inflow option for gas and condensate, in PROSPER, uses a multi-phase pseudo pressure function to allow for changing gas and condensate saturations around the wellbore. It assumes that no condensate banking occurs and that all the condensate that drops out is produced. Transient effects on productivity index are accounted for.

Petroleum Experts offers several choices in terms of defining permeability. User can define either effective permeability or total permeability at connate water saturation. In case of defining total permeability, the effective permeability will be calculated depending on the given connate water saturation. The following diagram illustrates how PROSPER treats effective and absolute permeabilities:

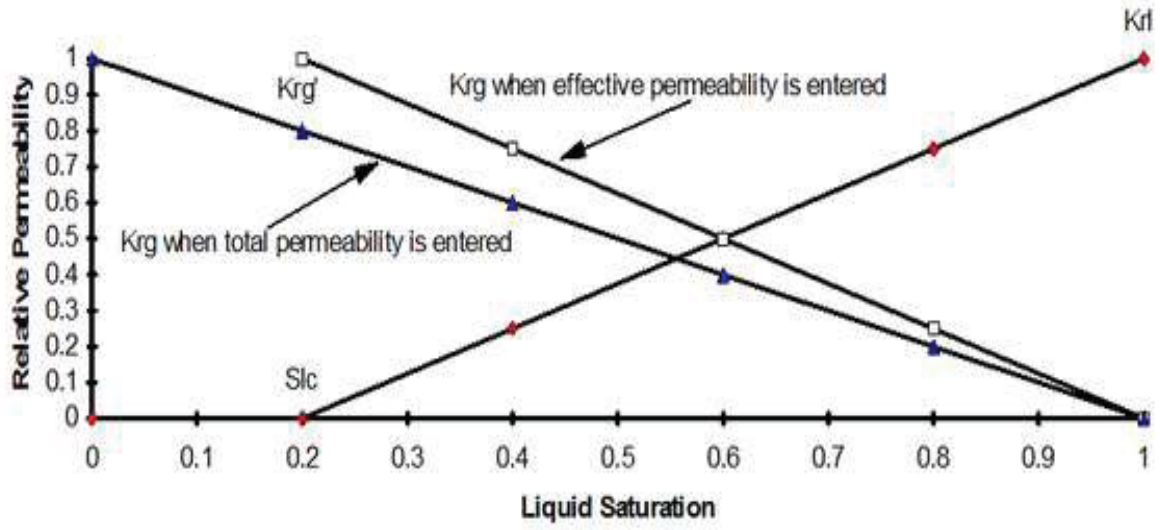

Figure 4-1: Petroleum Experts IPR Relative Permeabilities model[6]

4.1.1 Comparison of the models for the three vertical wells in production phase

The highest production rate out of these three vertical wells was between 2500 – 4300 [m³(Vn)/h]. Rates within the practical range of 0 – 10000 [m³(Vn)/h] were used for the comparison of models.

IPR curves for HAAG-001

The Fig. 4-2 illustrates the IPR curves for HAAG-001 using the *Jones (1976)* equation and *Petroleum Experts*. The input parameters for both models are tabulated in the following table:

Table 4-1: Input parameters in both models at p_{res}=91 [bara] and T= 42°C

Parameters	Value
Reservoir permeability	150 [md]
Reservoir thickness	5.1 [m]
Skin	8.4
Wellbore radius	4.25 [inches]

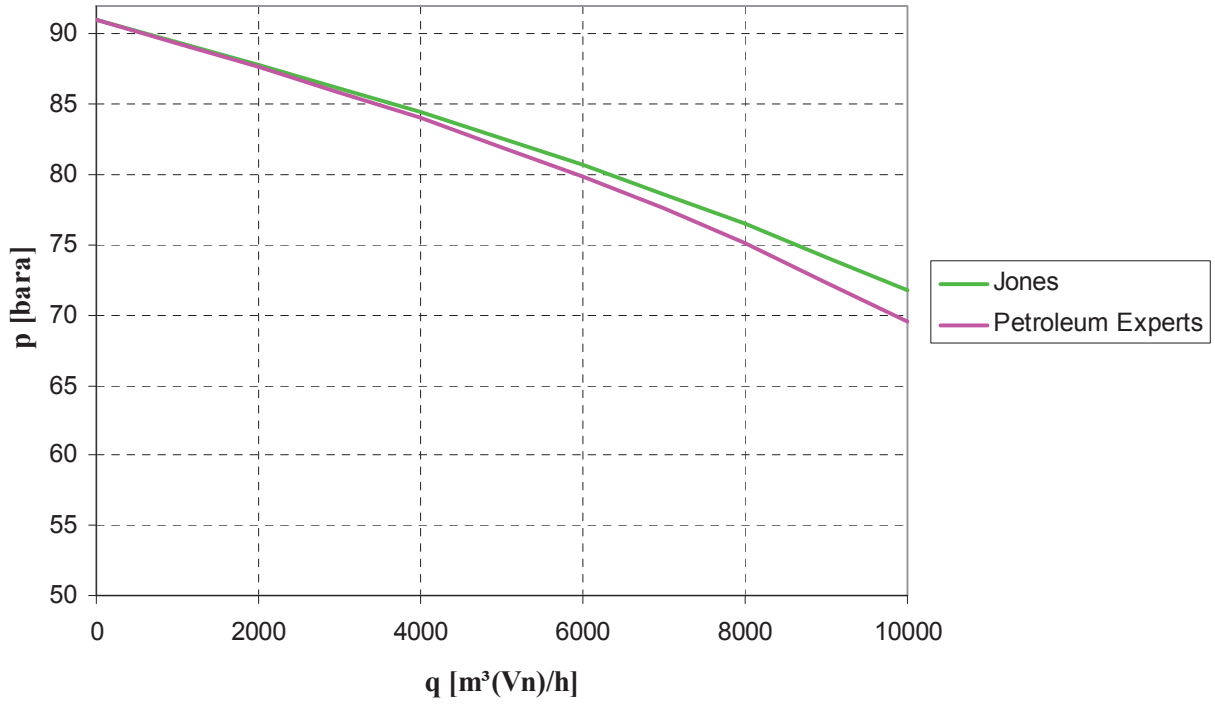

Figure 4-2: Comparison of IPR models for HAAG-001

IPR curves for HAAG-002

The Fig. 4-3 illustrate the comparison IPR curves for HAAG-002 using the *Jones (1976)* equation and *Petroleum Experts*. The input parameters for both models are tabulated in Table 4-2.

Table 4-2: Input parameters in both models at p_{res}=91 [bara] and T= 42°C

Parameters	Value
Reservoir permeability	150 [md]
Reservoir thickness	12.7 [m]
Skin	17
Wellbore radius	4.25 [inches]

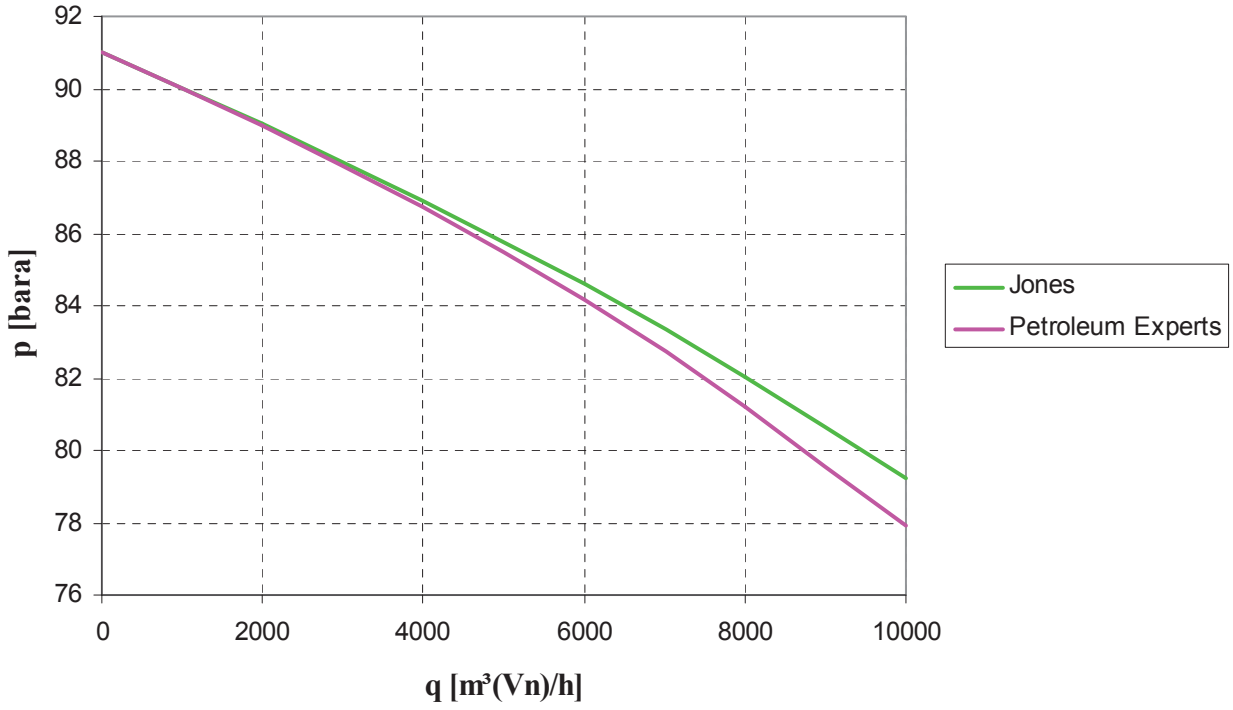

Figure 4-3: Comparison of IPR models for HAAG-002

IPR curves for HAAG-003

The following figure illustrates the IPR curves for HAAG-003 using the *Jones (1976)* equation and *Petroleum Experts*. The input parameters for both models are tabulated in the table below.

Table 4-3: Input parameters in both models at p_{res}=91 [bara] and T= 42°C

Parameters	Value
Reservoir permeability	150 [md]
Reservoir thickness	9.9 [m]
Skin	17.5
Wellbore radius	4.25 [inches]

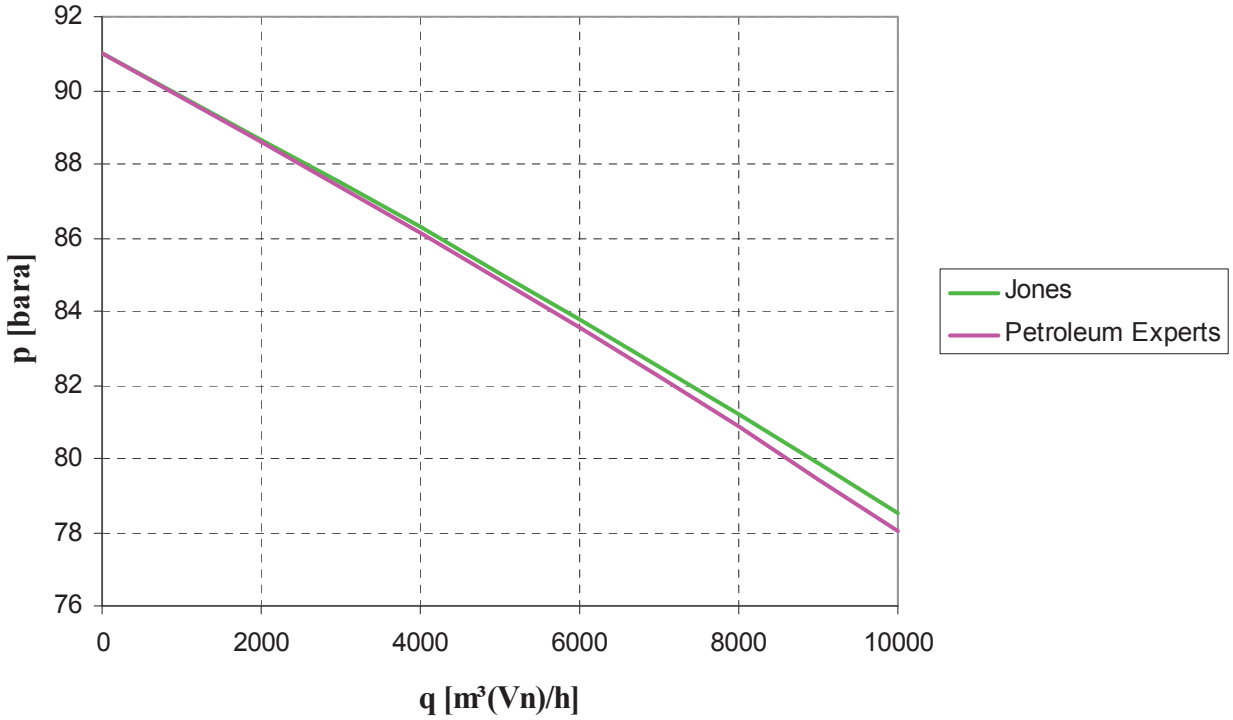

Figure 4-4: Comparison of IPR models for HAAG-003

4.1.2 Discussion of results for vertical wells in production phase

In general, both models deliver approximately same AOFs for each well, and the trend of both IPR models are similar. There is a slight difference to see between the both IPR models in regions, which most likely will not be achieved in practical implementation.

The *Petroleum Experts* IPR allows for the reduction in effective permeability resulting from liquid production in gas and condensate wells, i.e. it takes liquid production into account. If a reservoir has liquid production, then *Petroleum Experts* delivers more accurate IPR curve than the *Jones (1976)* equation.

4.1.3 Comparison of the models for the three vertical wells in injection phase

The Haag field was completely depleted, and pressure build up was necessary to be able to drill the three horizontal storage wells. Pressure build up was performed starting with July 2007 until September 2009 using the three vertical wells, HAAG-001, HAAG-002 and HAAG-003. The same models were applied for building the injection IPR curves for the vertical wells.

IPR curves for HAAG-001

In the following figure the injection IPR curves built by using *Jones (1976)* and *Petroleum Experts* models are compared.

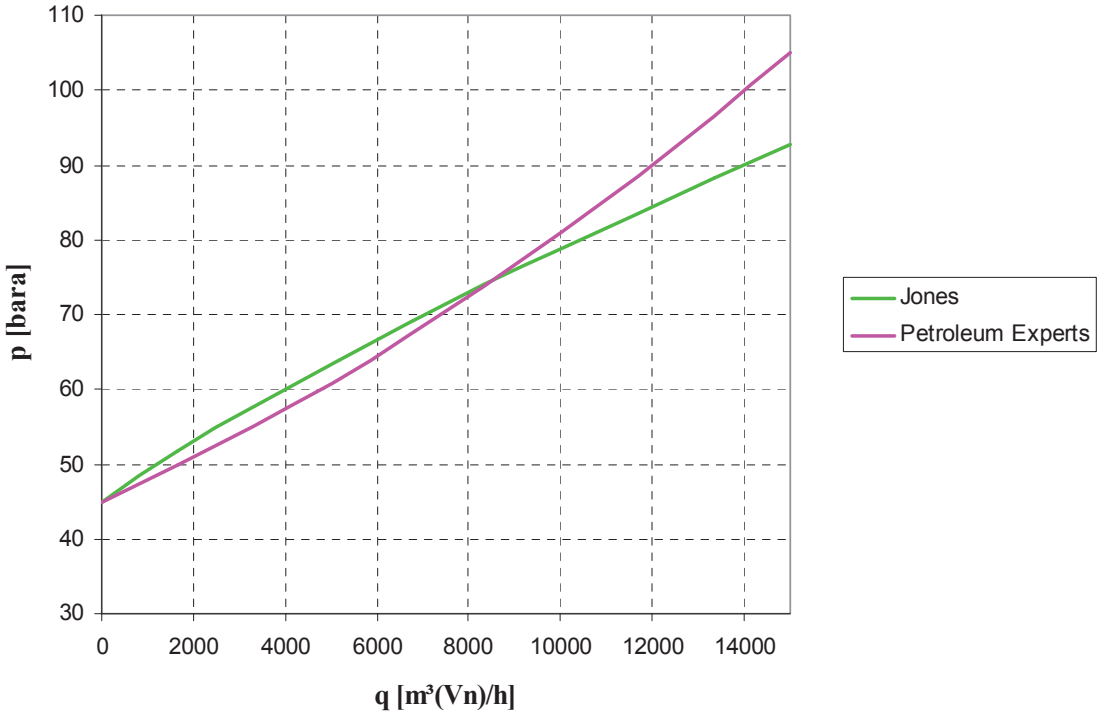

Figure 4-5: Comparison of IPR models for HAAG-001 in injection phase

Table 4-4: Input parameters in both models at p_{res}=45 [bara]

Input data		
Reservoir permeability	150	[md]
Reservoir thickness	5.1	[m]
Drainage area	472548	[m²]
Wellbore radius	4.25	[inches]
Perforation interval	3.5	[m]
Porosity	0.3	fraction

IPR curves for HAAG-002

In the figure below the injection IPR curves calculated with *Jones (1976)* and *Petroleum Experts* models are compared:

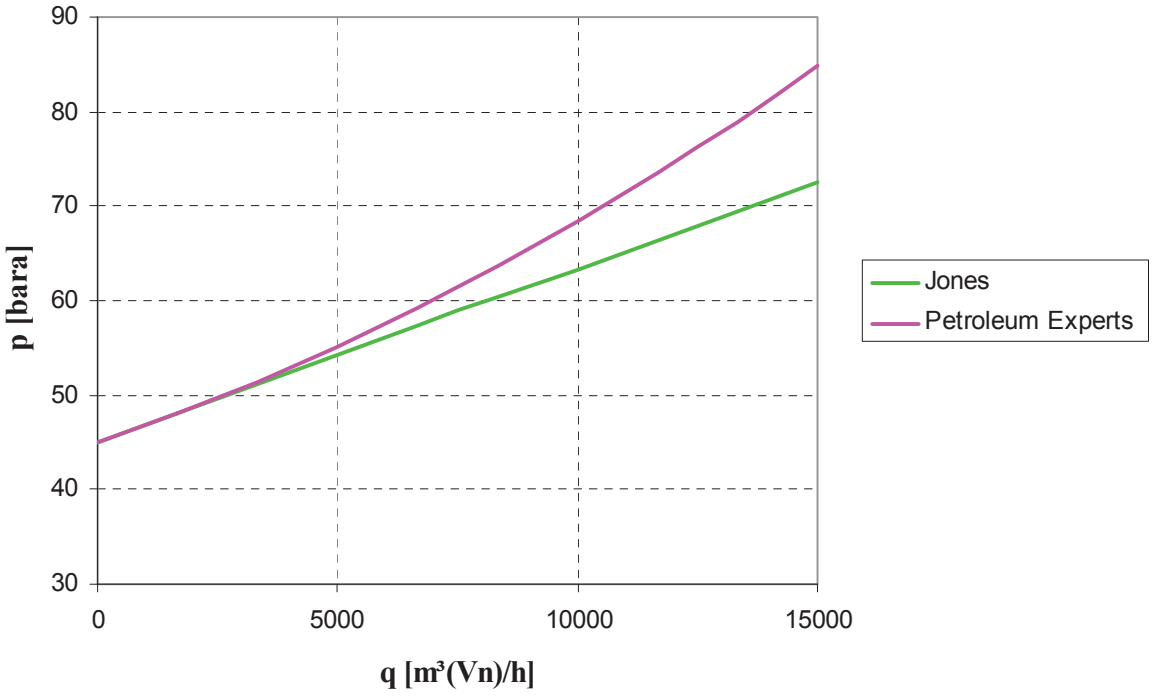

Figure 4-6: Comparison of IPR models for HAAG-002 for the injection phase

Table 4-5: Input parameters in both models at p_{res}=45 [bara]

Input data		
Reservoir permeability	150	[md]
Reservoir thickness	12.7	[m]
Drainage area	708822	[m²]
Wellbore radius	4.25	[inches]
Perforation interval	4	[m]
Porosity	0.3	fraction

IPR curves for HAAG-003

The Fig. 4-7 depicts the comparison of two injection IPR curves constructed using Jones and Petroleum Experts models.

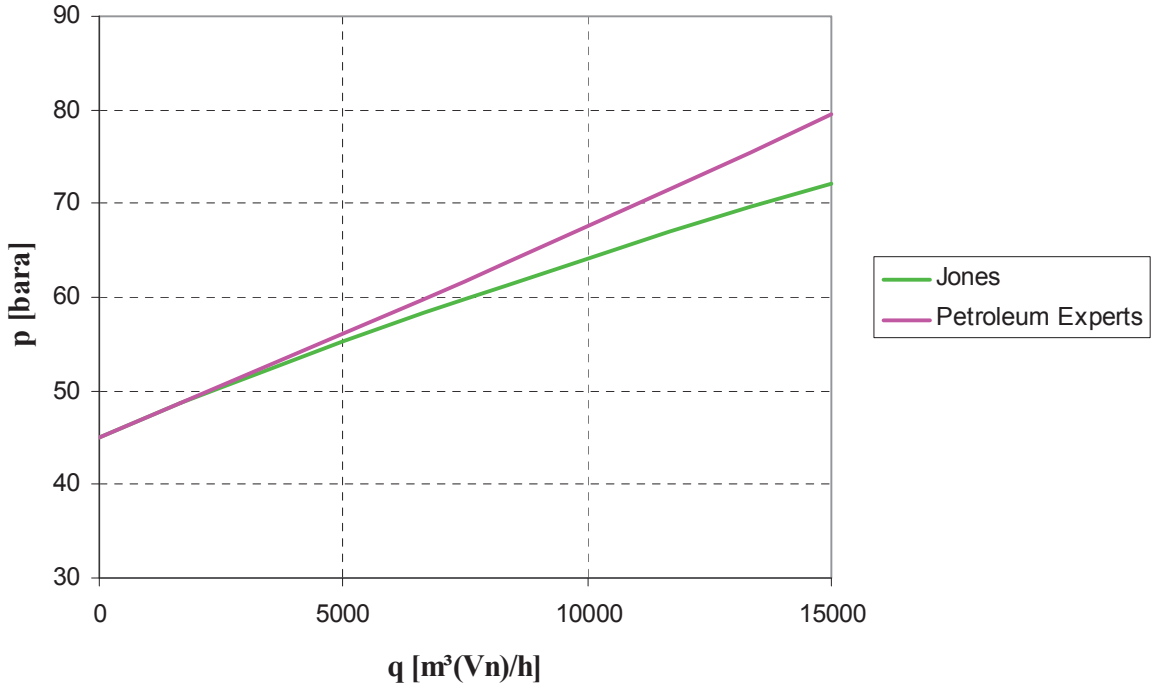

Figure 4-7: Comparison of IPR models for HAAG-003 for the injection phase

Table 4-6: Input parameters in both models at p_{res}=45 [bara]

Input data		
Reservoir permeability	150	[md]
Reservoir thickness	9.9	[m]
Drainage area	31416	[m²]
Wellbore radius	4.25	[inches]
Perforation interval	9.5	[m]
Porosity	0.2	fraction

4.1.4 Discussion of results for vertical wells in injection phase

For HAAG-001 the Jones follows almost a linear trend compared to Petroleum Experts, which follows the exponential trend. They intersect at a rate of about 8300 [m³(Vn)/h]. In case of HAAG-002 and HAAG-003 the two models show same trend up to 5000 [m³(Vn)/h] rate. Above this rate *Petroleum Experts* results in faster pressure increase with increasing rate i.e. *Jones* gives more optimistic results for the injection phase through the vertical wells. Both of the models give results in a scope, which practically allows the consideration of being them

same. To compare the models we need to suppose a scope within which results are considered to be equal. Thus this scope permits a practical comparison of results.

4.2 Inflow Performance of Horizontal Wells

As around the world interest in drilling horizontal wells to increase productivity has grown, several methods to calculate pseudo-steady productivities of horizontal wells for single-phase flow have been introduced in the literature. Unfortunately, most of them contain unacceptable simplifying assumptions. In this work three types of these methods are used to construct inflow performance curves in semi-analytical approach with PROSPER. They are less restrictive than other methods appeared in the literature. These three treatments are Kuchuk & Goode, Goode & Wilkinson, and Babu & Odeh. In all these methods, the reservoir is assumed to be bounded in all directions and the horizontal well is located arbitrarily within a rectangular bounded drainage area.

4.2.1 Kuchuk and Goode method (1991)

The inflow performance of a well is related to the pseudo-steady-state or steady-state behavior. For a reservoir with no-flow boundaries, the difference between the average pressure of the reservoir and the wellbore pressure draws near a constant value, which is called the pseudo-steady-state pressure. This applies for a reservoir with no-flow boundaries. If the reservoir is bounded above and/or below by a constant-pressure boundary (e.g., gas cap or strong aquifer) then at long times, the difference between the pressure at the boundary and the pressure in the well will become a constant, called the steady-state pressure. When the pseudo-steady- or steady-state is normalized with respect to the stabilized well flow rate, it provides a measure of the pressure drawdown required to flow a unit volume per unit time. The dimensionless pseudo-state pressure, p_{wD}, for the no flow case is defined as

$$p_{wD} = \frac{2\pi k_H h}{q\mu}\left(\bar{p}(t) - p_w(t)\right) \tag{4-5}$$

where $\bar{p}(t)$ = average reservoir pressure at time t

$p_w(t)$ = pressure at the wellbore

$k_H = \sqrt{k_x k_y}$

For the constant pressure boundary case,

$$p_{wD} = \frac{2\pi k_H h}{q\mu}\left(p_e - p_w(t)\right) \tag{4-6}$$

where p_e = pressure at the constant-pressure boundary.

The inflow performance is often expressed as

$$J = 7.08\times10^{-3}\,\frac{k_H h}{\mu B_o (p_{wD} + S_m^{\,*})} \qquad \text{In oilfield units – [STB/d-psi])} \tag{4-7}$$

In this formula $S_m^{\,*}$ is defined as

$$S_m^{\,*} = \left(\frac{h}{2L_{1/2}}\right)\sqrt{\frac{k_x}{k_z}}\cdot S_m \tag{4-8}$$

where S_m, the usual van Everdingen mechanical skin, is related to the pressure drop across the skin region, Δp_s, by

$$S_m = \left(\frac{2\pi L_{1/2}\sqrt{k_y k_z}}{\mu q}\right)\Delta p_s \tag{4-9}$$

This is necessary because p_{wD} has been made dimensionless with respect to the formation thickness, not the length of the well over which the pressure drop owing to skin occurs.

As already mentioned above, most of the inflow-performance formulas for horizontal wells presented in the literature make certain limiting assumptions about the well. Particularly, the well length has been assumed to be long compared with the formation thickness and to be short compared with the dimensions of the drainage area; and the well is required to be in the center of the drainage volume. Goode, P.A. and Kuchuk, F. J.[8] have presented formulas for evaluating the inflow performance of a horizontal well in a rectangular drainage region of uniform thickness and do not need the assumptions mentioned above. The well is assumed to be parallel to the x direction and it can be placed anywhere within the drainage volume, as shown in Fig. 4-8, which gives all the relevant parameters. All boundaries are closed to flow (no flow) except the top boundary, which may be a no-flow or constant-pressure boundary.

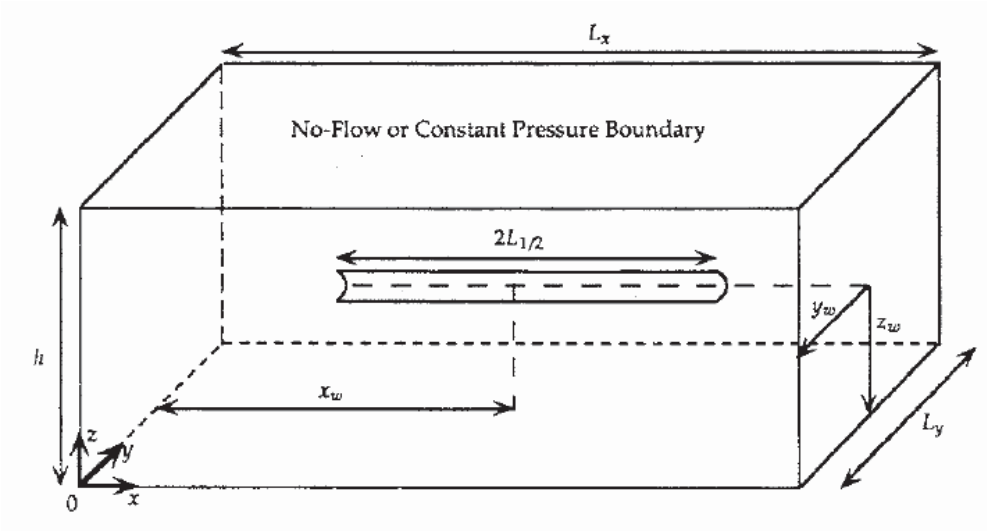

Figure 4-8: Horizontal-well model[8]

The only other assumption required is that, if the well is not long compared to with the scaled reservoir thickness $\left(h\sqrt{k_x/k_z}\right)$, the distance from the well to any lateral boundary must be large relative to the distance from the well to the top and bottom boundaries. In practice this is not an unduly restrictive assumption, unless the vertical permeability is extremely low, which in any event would make the reservoir a poor candidate for development with horizontal wells. The pseudo-steady-state pressure is given by

$$p_{wD} = \frac{2\pi L_y}{L_x}\sqrt{\frac{k_x}{k_y}}\left(\frac{1}{3}-\frac{y_w}{L_y}+\frac{{y_w}^2}{{L_y}^2}\right)+\frac{2{L_x}^2}{\pi^2{L_{1/2}}^2}\sum_{n=1}^{\infty}\frac{1}{n}{\Xi_x}^2(1+\xi)+S_{zD} \tag{4-10}$$

where

$$S_{zD} = -\frac{h}{2L_{1/2}}\sqrt{\frac{k_x}{k_z}}\left\{\ln\left[\frac{\pi r_w'}{h}2\sin\left(\frac{\pi z_w}{h}\right)\right]+\sqrt{\frac{k_x}{k_z}}\frac{h}{L_{1/2}}\left(\frac{1}{3}-\frac{z_w}{h}+\frac{{z_w}^2}{h^2}\right)\right\} \tag{4-11a}$$

$$r_w' = \left(\frac{r_w}{2}\right)\left(1+\sqrt{\frac{k_z}{k_y}}\right) \tag{4-11b}$$

$$\xi = \frac{2e^{\alpha L_y}+e^{\alpha(L_y-y_w)}+e^{\alpha y_w}}{1-e^{\alpha L_y}} \tag{4-11c}$$

$$\alpha = -\frac{2n\pi}{L_x}\sqrt{\frac{k_x}{k_y}} \tag{4-11d}$$

And

$$\Xi_x = \frac{1}{n}\sin\left(n\pi\frac{L_{1/2}}{L_x}\right)\cos\left(n\pi\frac{x_w}{L_x}\right) \tag{4-11e}$$

Although Eq. 4-10 contains an infinite series, it is not difficult to calculate because the series converges rapidly.

4.2.2 Goode and Wilkinson method (1991)

This method expands the work of Kuchuk and Goode[8] to include the effects of having only a portion of the well open. The same horizontal well model as in Kuchuk & Goode is considered. The well produces through n_p open intervals, with segment i of length $2L_i$ centered at x_i (Fig. 4-9).

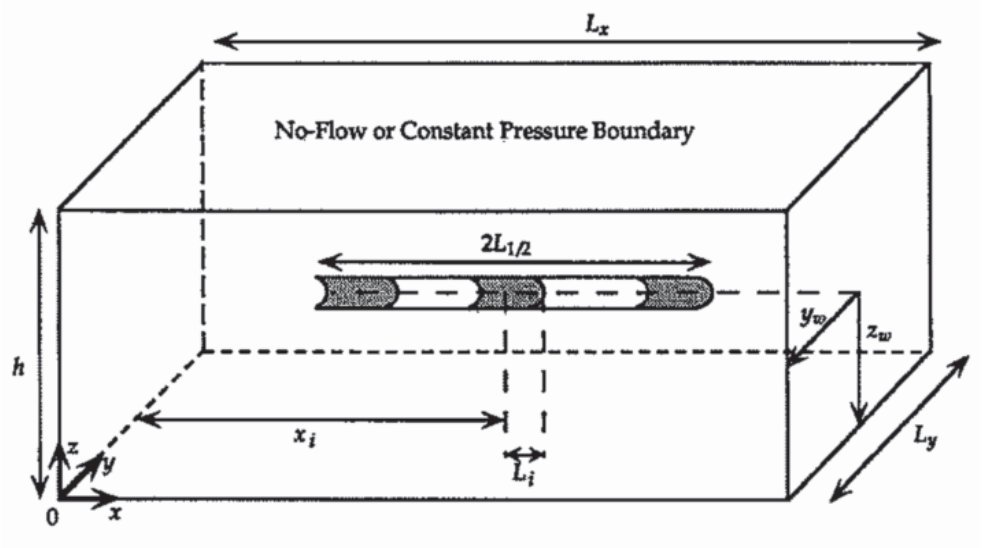

Figure 4-9: Schematic of partially open horizontal well[9]

Goode and Wilkinson[9] consider the inflow pressure as a sum of two pressure drops, namely a 2D fracture contribution and a 3D well contribution:

$$p_{ID} = p_{xyD} + S_{zD} \tag{4-12}$$

The first part, p_{xyD}, is the dimensionless pressure in the x and y plane resulting from considering the well as a set of fractures that fully penetrate the formation:

$$p_{xyD} = \frac{2\pi L_y}{L_x}\sqrt{\frac{k_x}{k_y}}\left(\frac{1}{3} - \frac{y_w}{L_y} + \frac{{y_w}^2}{{L_y}^2}\right) + \frac{2{L_x}^2}{\pi^2 {L_p}^2}\sum_{n=1}^{\infty}\frac{\Xi_n}{n^3}\left(\sum_{i=1}^{n_p}\cos\frac{n\pi x_i}{L_x}\times\sin\frac{n\pi L_i}{L_x}\right)^2 \tag{4-13}$$

where

$$\Xi_n = \left\{1 + \exp(-2\alpha_n L_y) + \exp(-2\alpha_n y_w) + \exp\left[-2\alpha_n (L_y - y_w)\right]\right\} \Big/ \left[1 - \exp(-2\alpha_n L_y)\right] \tag{4-14}$$

$$\alpha_n = \frac{n\pi}{L_x}\sqrt{\frac{k_x}{k_y}} \tag{4-15}$$

And L_p is the total open half-length of the well,

$$L_p = \sum_{i=1}^{n_p} L_i \tag{4-16}$$

The second term, S_{zD}, is the geometric skin that results because the well does not fully penetrate the formation and flow must converge near the well:

$$S_{zD} = \frac{h}{2L_p}\sqrt{\frac{k_x}{k_z}}\left[-\ln\left(\frac{2\pi r_w'}{h}\sin\frac{\pi z_w}{h}\right)-\frac{n_p h}{L_p}\sqrt{\frac{k_x}{k_z}}\left(\frac{1}{3}-\frac{z_w}{h}+\frac{{z_w}^2}{h^2}\right)\right]+2\sum_{k=1}^{\infty}F_w^*(\beta_k)\cos^2\frac{k\pi z_w}{h} \tag{4-17}$$

where

$$r_w' = \frac{1}{2}\left(1+\sqrt{\frac{k_z}{k_y}}\right)r_w \tag{4-18}$$

$$\beta_k = \frac{\pi^2 k^2}{h^2}\frac{k_z}{k_x} \tag{4-19}$$

and the function F_w^* is defined as

$$F_w^*(\beta) = \frac{1}{{L_p}^2}\int_{\sqrt{\beta}}^{\infty}\frac{\partial u}{\sqrt{u^2-\beta}}\frac{1}{2u^2}\sum_{i=1}^{n_p}\left[\exp(-2uL_i)+4\sum_{j<i}\exp\left(-u\left|x_j-x_i\right|\right)\times\sinh uL_i\sinh uL_j\right] \tag{4-20}$$

These formulas were obtained with the uniform-flux, line-source solution and by averaging the pressure along the well length.

4.2.3 Babu and Odeh method (1987)

Babu and Odeh[10] derived the following equation for horizontal well pseudo-steady state flow potential, i.e. productivity of a horizontal well:

$$q = \frac{7.08\times10^{-3}\,b\sqrt{k_z k_x}\left(p_{av}-p_{wf}\right)}{B\mu\left(\ln\frac{\sqrt{A}}{r_w}+\ln C_H-0.75+S_R\right)} \tag{4-21}$$

where

q = Flow rate, [STB/day]

b = Width of drainage volume, [ft]

k_x, k_z = Permeability in the x and z-directions, respectively, [md]

p_{av} = Average pressure in the drainage volume of the well, [psi]

p_{wf} = Average flowing bottom hole pressure of the well, [psi]

B = Formation volume factor, [RB/STB]

μ = Viscosity, [cp]

C_H = Geometric factor, dimensionless

A = Drainage area = ah, [ft²]

r_w = Wellbore radius, [ft] and

S_R = Skin due to restricted entry to flow: occurs only when the well length L < b.

S_R is a function that depends on the well length. $S_R = 0$ when $L = b$ (the fully penetrating case). Eq. 4-21 assumes there is no mechanical skin. If this happens, then S_R would become $(S_R + S_f)$, where S_f is skin due to damage or improvement around the wellbore.

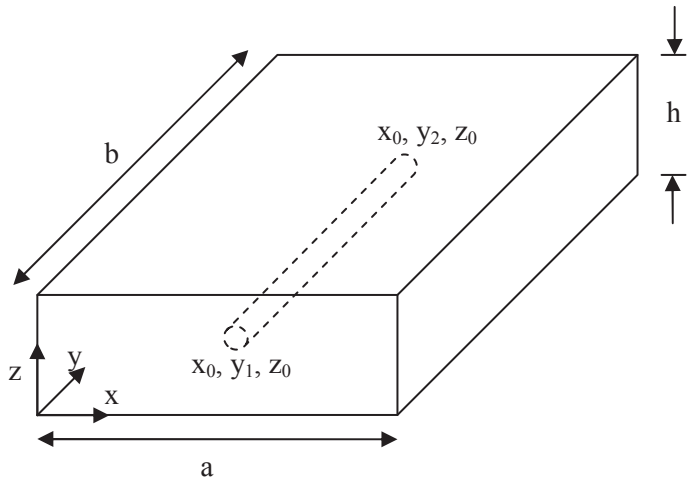

Figure 4-10: Drainage volume of horizontal well[9]

The above figure depicts the drainage volume of the horizontal well. The coordinates (x_0, y_1, z_0) and (x_0, y_2, z_0) refer to the location of the beginning and the end of the well, respectively. Since the productivity index (P.I.) is $q/\Delta p$, the P.I. using Eq. 4-18 is defined as

$$P.I. = \frac{7.08\times10^{-3} b\sqrt{k_x k_z}}{B\mu\left(\ln\frac{C_H\sqrt{A}}{r_w} - 0.75 + S_R\right)} \tag{4-22}$$

These equations above contain two parameters C_H and S_R, which are functions of the aspect ratio, i.e. the relative magnitude of *a*, *b*, and *h*; the values of k_x, k_y, and k_z; and the location of the well. Here, $\ln C_H$ is defined as

$$\ln C_H = 6.28\frac{a}{h}\sqrt{\frac{k_z}{k_x}}\left(\frac{1}{3} - \frac{x_0}{a} + \frac{{x_0}^2}{a^2}\right) - \ln\left[\sin\frac{180^\circ z_0}{h}\right] - 0.5\ln\left[\frac{a}{h}\sqrt{\frac{k_z}{k_x}}\right] - 1.088 \tag{4-23}$$

Again, x_0 and z_0 are the x and z coordinates of the well.

The value of partial penetration skin factor S_R depends upon the following two conditions:

Case 1: $\frac{a}{\sqrt{k_x}} \geq \frac{0.75b}{\sqrt{k_y}} > \frac{0.75h}{\sqrt{k_z}}$ and **Case 2:** $\frac{b}{\sqrt{k_y}} \geq \frac{1.33a}{\sqrt{k_x}} > \frac{h}{\sqrt{k_z}}$

It is assumed that *a* and *b* will be orders of magnitude larger than *h* so that $\left(\frac{h}{\sqrt{k_z}}\right)$ is always less than $\left(\frac{a}{\sqrt{k_x}}\right)$ and $\left(\frac{b}{\sqrt{k_y}}\right)$. If this does not hold, the exact solution shows that there will be a loss in productivity in drilling a horizontal well instead of vertical well.

Case 1:

As stated previously, $S_R = 0$ when $L = b$. If L<b, then

$S_R = PXYZ + PXY$

Here, the *PXYZ* component is due to the degree of penetration, i.e. to the value of *L/b*, and *PXY* component is due to the location of the well in the x-y plane. The skin component due to the z-location is negligible and is ignored.

The *PXYZ* component:

$$PXYZ = \left(\frac{b}{L} - 1\right)\left[\ln\frac{h}{r_w} + 0.25\ln\frac{k_x}{k_z} - 1.05\right] \tag{4-24}$$

The *PXY* component:

$$PXY = \frac{2b^2}{Lh}\sqrt{\frac{k_z}{k_y}}\left\{f\left(\frac{L}{2b}\right) + 0.5\left[f\left(\frac{4y_0 + L}{2b}\right) - f\left(\frac{4y_0 - L}{2b}\right)\right]\right\} \tag{4-25}$$

where

$$f\left(\frac{L}{2b}\right) = -\left(\frac{L}{2b}\right)\left[0.145 + \ln\left(\frac{L}{2b}\right) - 0.137\left(\frac{L}{2b}\right)^2\right] \tag{4-26}$$

The evaluation of $f\left(\frac{4y_0 + L}{2b}\right)$ and $f\left(\frac{4y_0 - L}{2b}\right)$ depends on their arguments i.e. $\left(\frac{4y_0 + L}{2b}\right)$ and $\left(\frac{4y_0 - L}{2b}\right)$. If $\left(\frac{4y_0 + L}{2b}\right)$ or $\left(\frac{4y_0 - L}{2b}\right) \leq 1$, Eq. 4-23 is used. In this case $\left(\frac{L}{2b}\right)$ is replaced by $\left(\frac{4y_0 + L}{2b}\right)$ and/or $\left(\frac{4y_0 - L}{2b}\right)$. On the other hand, if the argument is > 1 then for $\left(\frac{4y_0 + L}{2b}\right) > 1$, one computes:

$$f\left(\frac{4y_0+L}{2b}\right)=\left(2-\frac{4y_0+L}{2b}\right)\left[0.145+\ln\left(2-\frac{4y_0+L}{2b}\right)-0.137\left(2-\frac{4y_0+L}{2b}\right)^2\right] \quad (4\text{-}27)$$

and for $\left(\frac{4y_0-L}{2b}\right)>1$,

$$f\left(\frac{4y_0-L}{2b}\right)=\left(2-\frac{4y_0-L}{2b}\right)\left[0.145+\ln\left(2-\frac{4y_0-L}{2b}\right)-0.137\left(2-\frac{4y_0-L}{2b}\right)^2\right] \quad (4\text{-}28)$$

Case 2:

In this case, $S_R = PXYZ + PY + PYX$

The *PXYZ* component is calculated by Eq. 4-24.

The *PY* component:

$$PY=\frac{6.28b^2}{ah}\frac{\sqrt{k_xk_z}}{k_y}\left[\left(\frac{1}{3}-\frac{y_0}{b}+\frac{{y_0}^2}{b^2}\right)+\frac{L}{24b}\left(\frac{L}{b}-3\right)\right] \quad (4\text{-}29)$$

where y_0 is the midpoint coordinate of the well.

The *PYX* component:

$$PYX=\left(\frac{b}{L}-1\right)\left(\frac{6.28a}{h}\sqrt{\frac{k_z}{k_x}}\right)\left(\frac{1}{3}-\frac{x_0}{a}+\frac{{x_0}^2}{a^2}\right) \quad (4\text{-}30)$$

The productivity equation of Babu & Odeh was extracted from a very complex and general solution. According to the authors the error in using this simple equation is less than 3 percent, in most, if not all cases of interest. It is applicable for any drainage volume dimensions, for any permeability anisotropy, and for any length and location of the horizontal well.

4.2.4 Conclusions

The difference between the three methods is in their mathematical solution methods and the boundary conditions used. For example, Kuchuk & Goode uses an approximate infinite-conductivity solution where the constant wellbore pressure is estimated by averaging pressure values of the uniform-flux solution along the wellbore length. Because of the well boundary condition assumptions, Kuchuk & Goode generally gives the highest flow rate and Babu & Odeh gives the lowest rate of the three methods. However, the difference in the calculated flow rates using different methods is normally very small ($\pm$ 5 %). All of these three models are available in software PROSPER. The comparison of the models using the well HGSP-001 follows in section 4.2.6. For further IPR calculations the model Kuchuk & Goode is used.

4.2.5 Description of reservoir model options used for horizontal wells in PROSPER

To construct IPR curves for horizontal wells PROSPER offers two options, namely *Horizontal Well – dP Friction Loss in Wellbore* and *Horizontal Well – No Flow Boundaries*. The option *Horizontal Well – dP Friction Loss in Wellbore* can be used along with all three models discussed above, whereas the option *Horizontal Well – No Flow Boundaries* is based on the Kuchuk and Goode model.

4.2.5.1 Horizontal Well – dP Friction Loss in Wellbore

High permeability reservoir usually results in higher well production rate and thus higher velocity. To adequately model horizontal well inflow in high permeability reservoirs, it is necessary to account for pressure loss along the horizontal section. PROSPER divides the horizontal section into up to 20 sections and a network algorithm solves for zone production and wellbore pressure. Pressure loss between zones is accounted for. Along with this model a horizontal well model must be defined. The three available models are: Kuchuk & Goode, Goode & Wilkinson, and Babu & Odeh.

The model couples the reservoir inflow with the horizontal section of wellbore from the heel to the toe. The solution process is iterative and begins by establishing the flow potential using the input parameters describing the overall well length and spatial geometry along with vertical and horizontal anisotropy. The model assumes pseudo-steady state flow conditions. In addition, the model is not designed to handle massive hydraulic fractures perpendicular to the horizontal section to be simulated with very high negative skins. Depending on the specific reservoir characteristics at hand, use of high negative skins per zone, the model can become unstable with meaningless results[6].

4.2.5.2 Horizontal Well – No Flow Boundaries

The *Horizontal Well – No Flow Boundaries* model in PROSPER is based on the work of Kuchuk and Goode. The inflow model used here assumes that the horizontal well is draining a closed rectangular drainage volume with sealing upper and lower boundaries. The well can be placed anywhere in the drainage region. Pressure drops along the wellbore itself are not taken into account[6].

4.2.6 Comparison of the models for horizontal storage wells in withdrawal phase

To build IPR curves for horizontal wells the following reservoir models were applied and analyzed:

- Horizontal Well Model with Friction dp Loss
- Horizontal Well – No Flow Boundaries

IPR curves for HGSP-001 with dp-Friction loss model

The figures below illustrate the *dp-Friction loss* IPR models calculated with Kuchuk & Goode, Goode & Wilkinson, and Babu & Odeh methods at reservoir pressures of 91, 55 and 43 [bara] which are critical pressures on the withdrawal profile, for more detail see chapter 5, section 5.5. The plots are zoomed to gas rates between 0 and 100000 [m³(Vn)/h], which is in the range of practical application.

Table 4-7: Input data

Reservoir pressure	91	[bara]
Reservoir Temperature	41	[℃]
permeability	200	[md]
porosity	0,25	fraction
skin	7	[-]
Wellbore radius	4,25	[inches]
Well length	738,54	[m]
Reservoir thickness	8	[m]
Reservoir length	1400	[m]
Reservoir width	500	[m]
Length distance to reservoir edge	350	[m]
Width distance to reservoir edge	250	[m]
Bottom of reservoir to well center	3	[m]
Pipe roughness	0,0001	[m]
Horizontal anisotropy	1	
Vertical anisotropy	0,1	

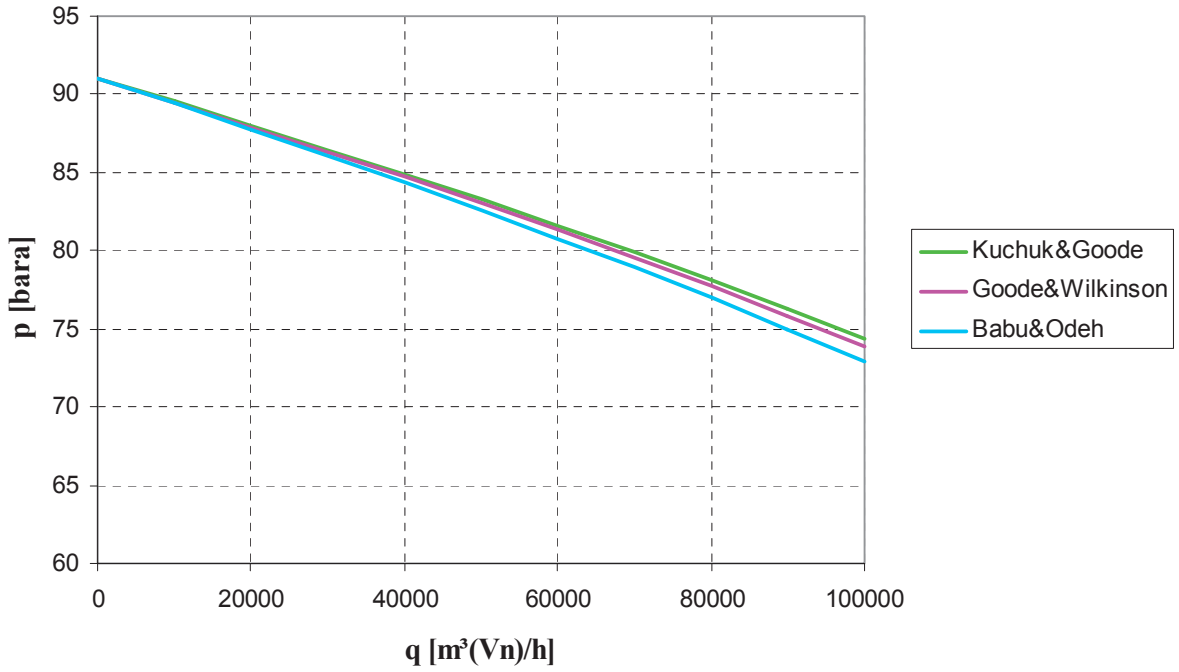

Figure 4-11: Comparison of IPR model for HGSP-001 at p_{res}=91 [bara]

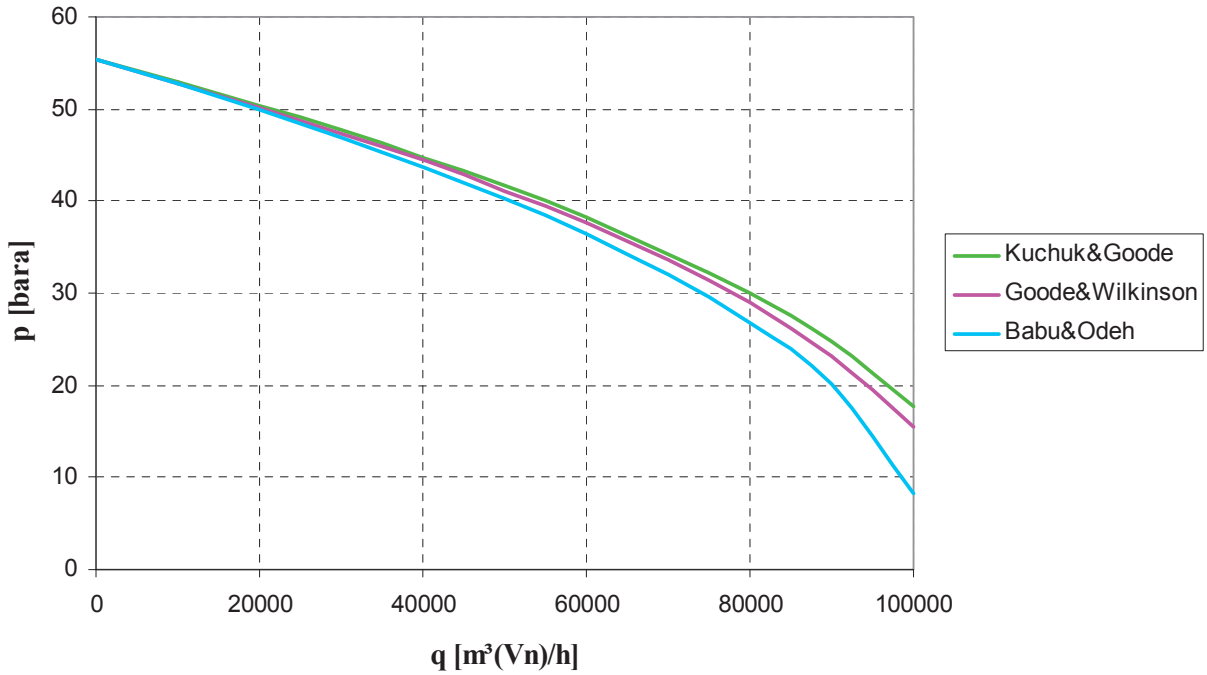

Figure 4-12: Comparison of IPR model for HGSP-001 at p_{res}=55 [bara]

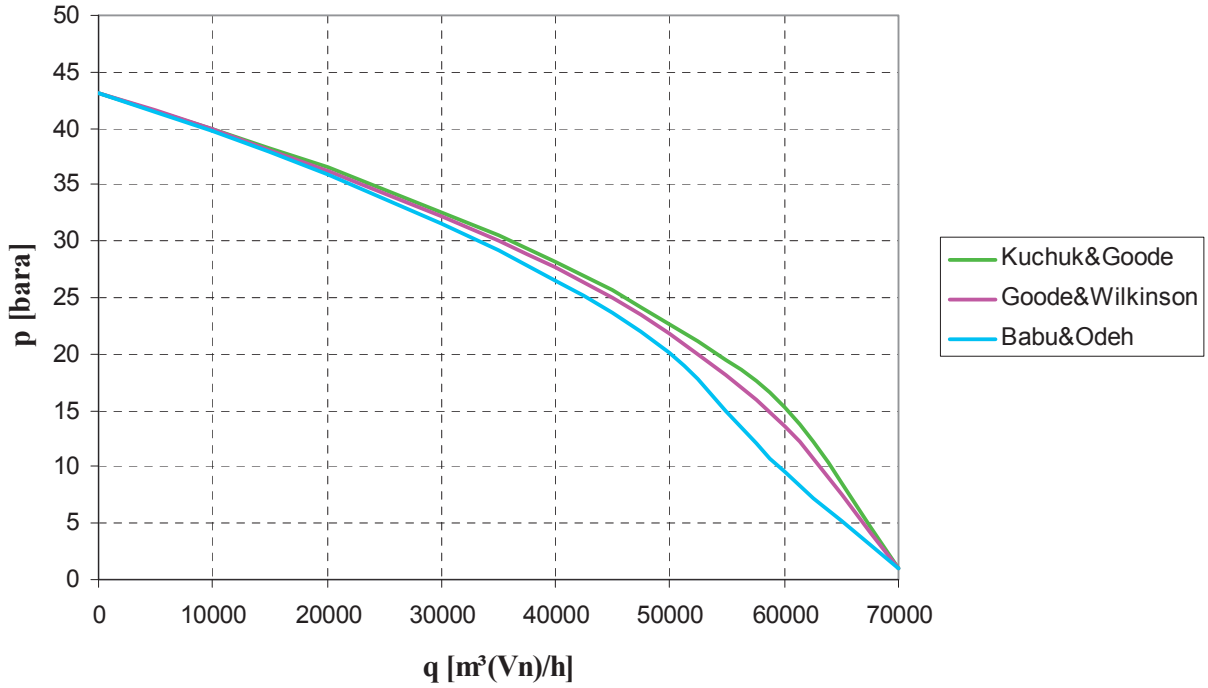

Figure 4-13: Comparison of IPR model for HGSP-001 at p_{res}=43 [bara]

4.2.6.1 Discussion of dp-Friction loss model results

All of the models used with *dp-friction loss* result in almost same IPR curves. The Kuchuk & Goode, Goode & Wilkinson, and Babu & Odeh give the following AOFs for reservoir pressure at 91 bara, 260248 [m³(nV/h)], 256081 [m³(nV/h)], and 248246 [m³(nV/h)], respectively. The Goode & Wilkinson model follows the same trend as the Kuchuk & Goode model since it is an expanded version of the Kuchuk & Goode. The difference is that the Goode & Wilkinson model includes the effects of having only a portion of the well open, whereas Kuchuk & Goode uses the total half-length of the well for the calculations. Therefore, Kuchuk & Goode delivers a slightly higher IPR curve as compared to Goode & Wilkinson.

Comparison of IPR curves for HGSP-001 with No Flow Boundaries and dp-Friction Loss with Kuchuk & Goode model

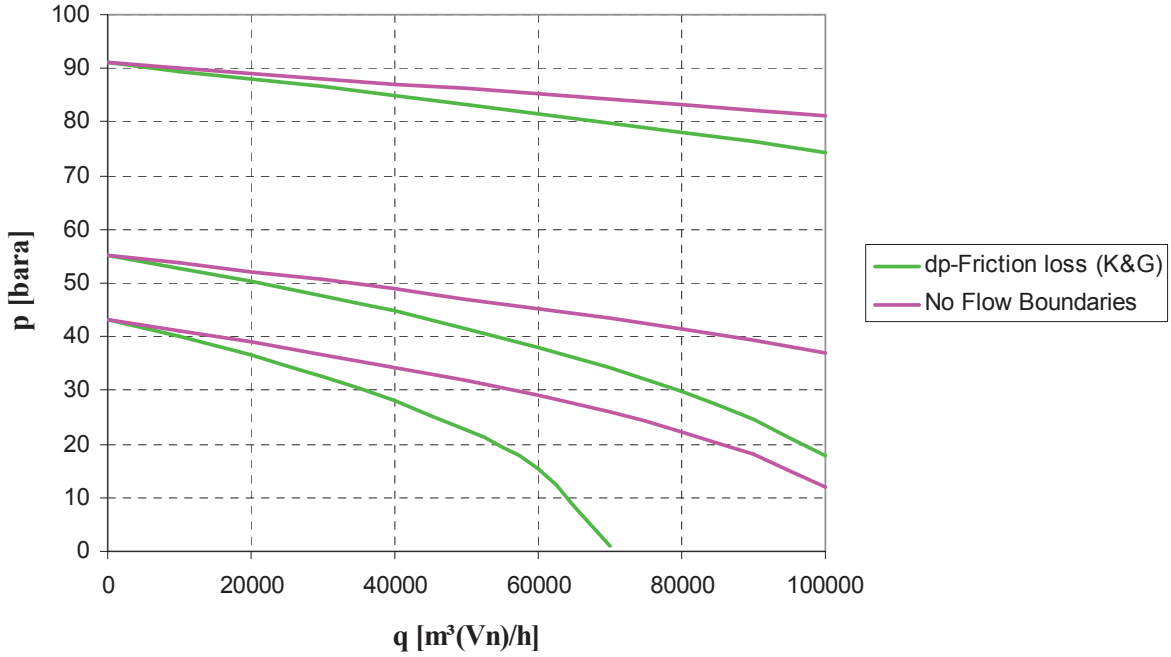

Figure 4-14: Comparison of IPR curves for HGSP-001 with two different reservoir models

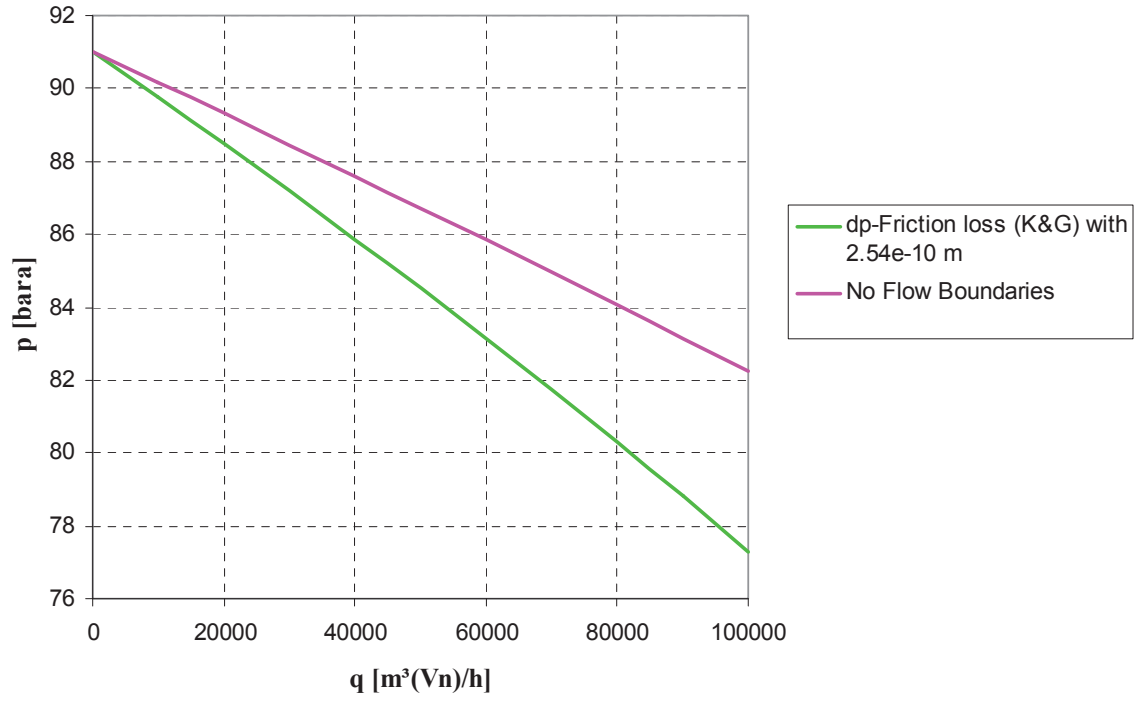

Figure 4-15: Comparison of IPR models for HGSP-001

4.2.6.2 Discussion of comparison results

Fig. 4-14 shows the IPR curves using two different reservoir models, namely *Horizontal Well - No Flow Boundaries* and the *Horizontal Well - dp-Friction Loss* with well model Kuchuk and Goode for a pipe roughness of 0.0001 [m]. Theoretically, the *No Flow Boundaries* model should result in less productivity compared to *dp-Friction Loss* model since the pressure at the boundary is not supported.

However, the *Horizontal Well – No Flow Boundaries* gives an AOF of 486563 [m³(Vn)/h] at reservoir pressure of 91 [bara], and the other model has an AOF of 260248 [m³(Vn)/h] at same reservoir pressure, which is almost the half of the *No Flow Boundaries'* AOF.

Both models are based on the work of Kuchuk and Goode, the only difference is that the *Horizontal Well – No Flow Boundaries* does not take into consideration the pressure drops along the well bore. Therefore, a comparison of the same reservoir models was done, where the pipe roughness of the *Horizontal Well - dp-Friction Loss* model was set to 2.54×10^{-10} [m], which should practically result in no friction pressure loss (Fig 4-15). Still the result is exactly in opposite to the expectation, which led to the conclusion that there is an error in the implementation of the model in the software. A request at software manufacturer in this case led to no satisfying results, therefore it is recommended not to use the *Horizontal Well - No Flow Boundaries* model for practical applications.

Results of HGSP-002 and HGSP-003

The same models were compared for HGSP-002 and HGSP-003 in the same manner. The results and the trends in differences are not reported since they were very similar to those of HGSP-001.

4.3 Sensitivity Analysis

The influences of different values of skin, permeability and effective well length on productivity were determined. The illustrated evaluations are based on HGSP-001. The impacts of the same parameters on performance of HGSP-002 and HGSP-003 are similar as in case of HGSP-001.

4.3.1 Skin

Different skin values were used with Kuchuk and Goode model to study skin's impact on IPR curves. The influence of skin is illustrated in Fig. 4-16. In this figure Kuchuk & Goode model was run for two different skin values of 0 and +7 at different pressures. The difference

between the two curves with different skin values at reservoir pressure 91 [bara] is about 2 % for rate 60000 [m³(Vn)/h]. Differences for the other curves at lower reservoir pressures of 55 and 43 [bara] are 7 % and 30 %, respectively. As shown, the difference is not very large, which underlines the fact that the skin is not the main influencing parameter. Not all of the related results are shown in this work.

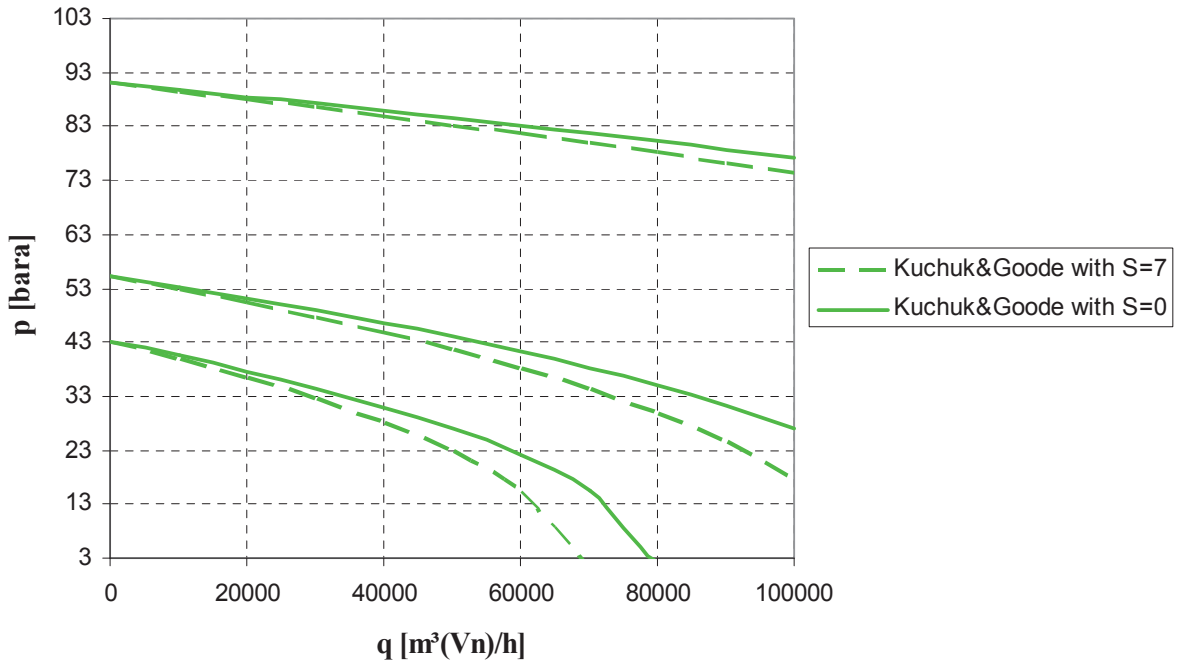

Figure 4-16: Skin influence with Kuchuk & Goode model

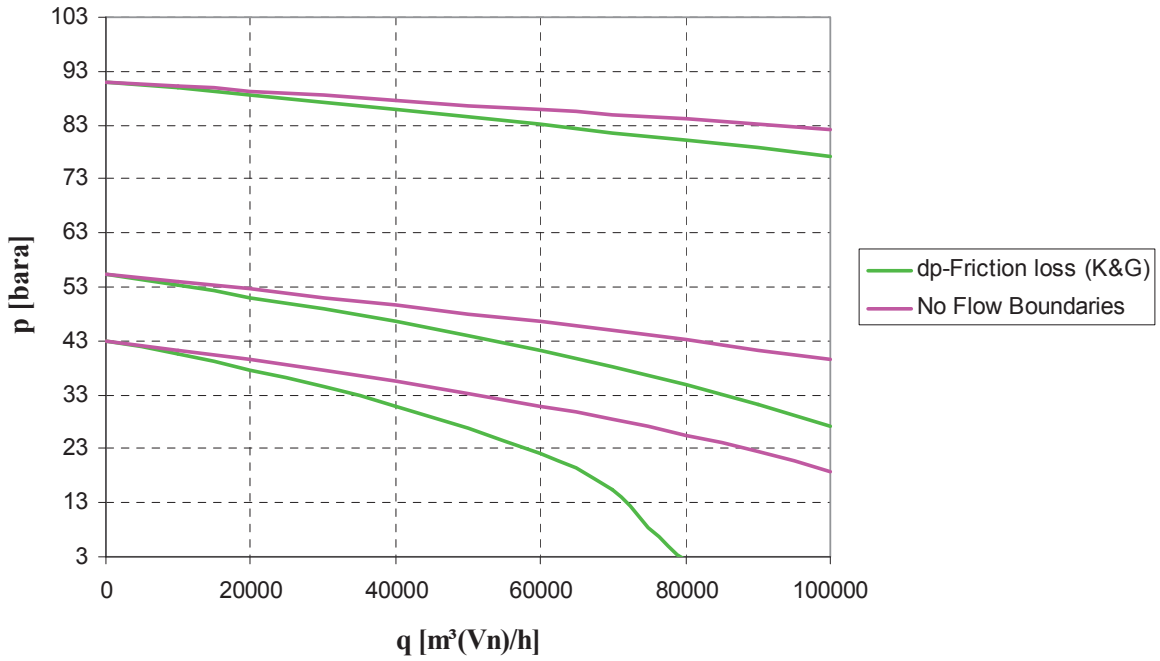

Figure 4-17: Comparison of two models with skin value 0

In the above figure the two reservoir models are compared again with skin value 0. It shows the same result, namely large difference with any skin value. This again indicates the less affect of skin on productivity of these storage wells.

4.3.2 Permeability

Horizontal Well – dp-Friction Loss model with well model Kuchuk & Goode were compared for different permeability values. The plot below shows the results for permeability values of 80, 150 and 200 [mD] at three different reservoir pressures. These IPR curves were calculated with a skin value of 0.

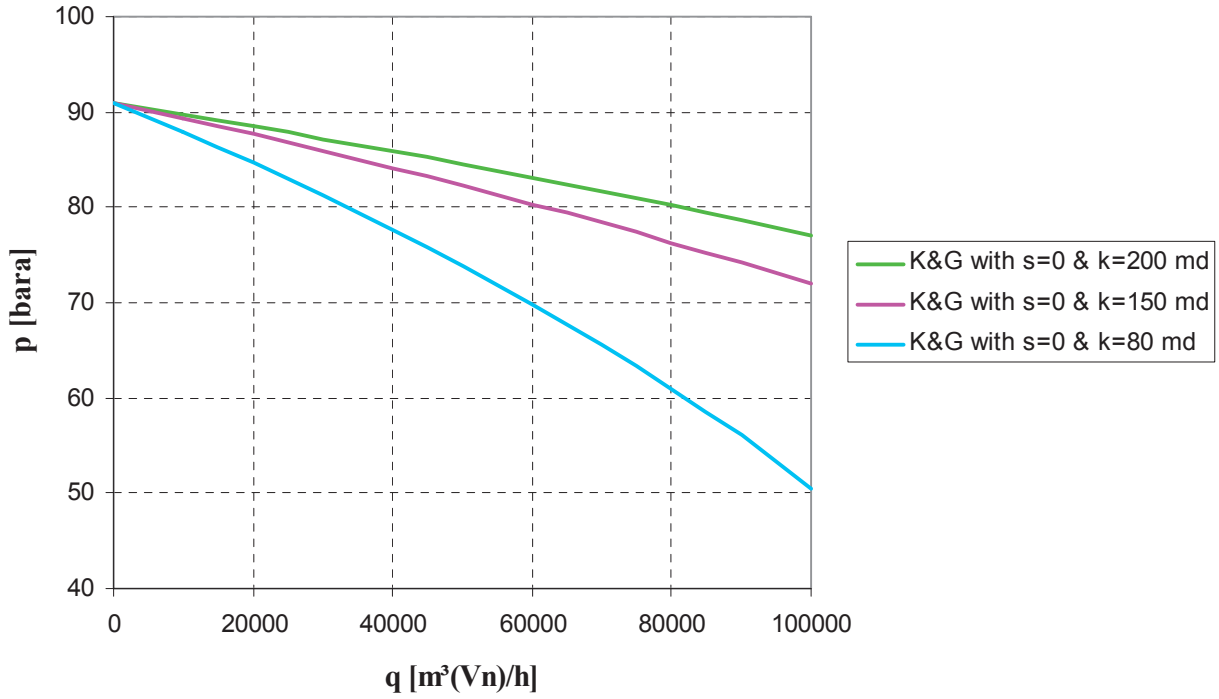

Figure 4-18: Comparison of IPR curves for HGSP-001 with different k at p_{res}=91 [bara]

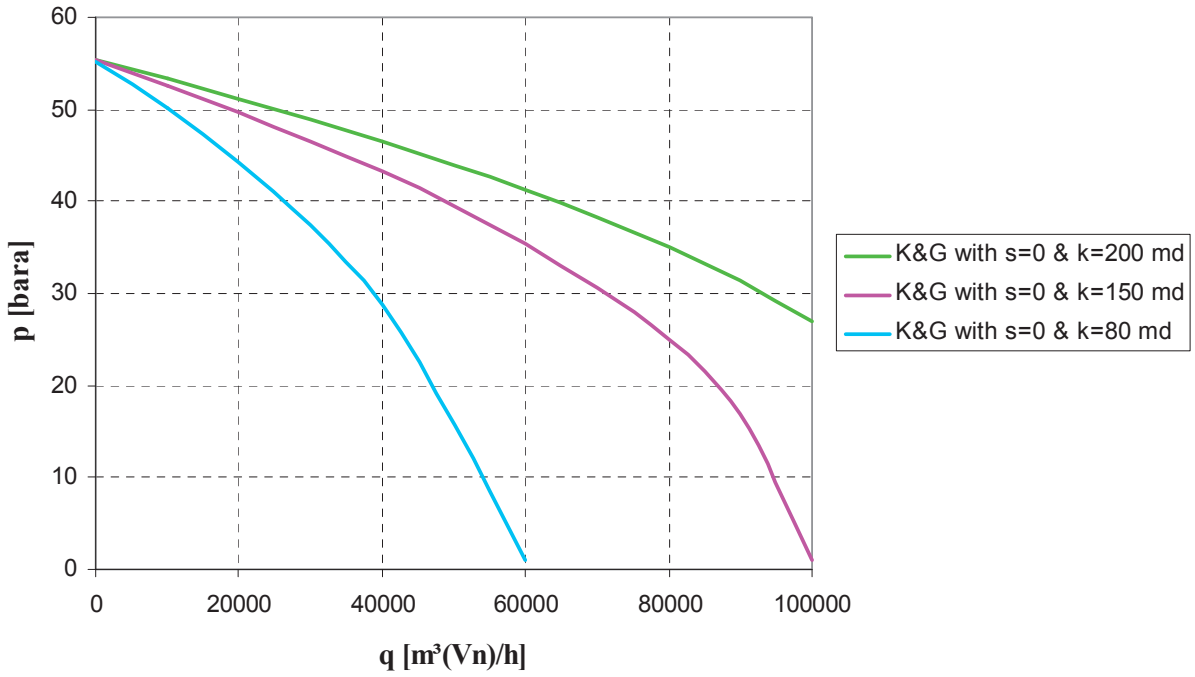

Figure 4-19: Comparison of IPR curves for HGSP-001 with different k at p_{res}=55 [bara]

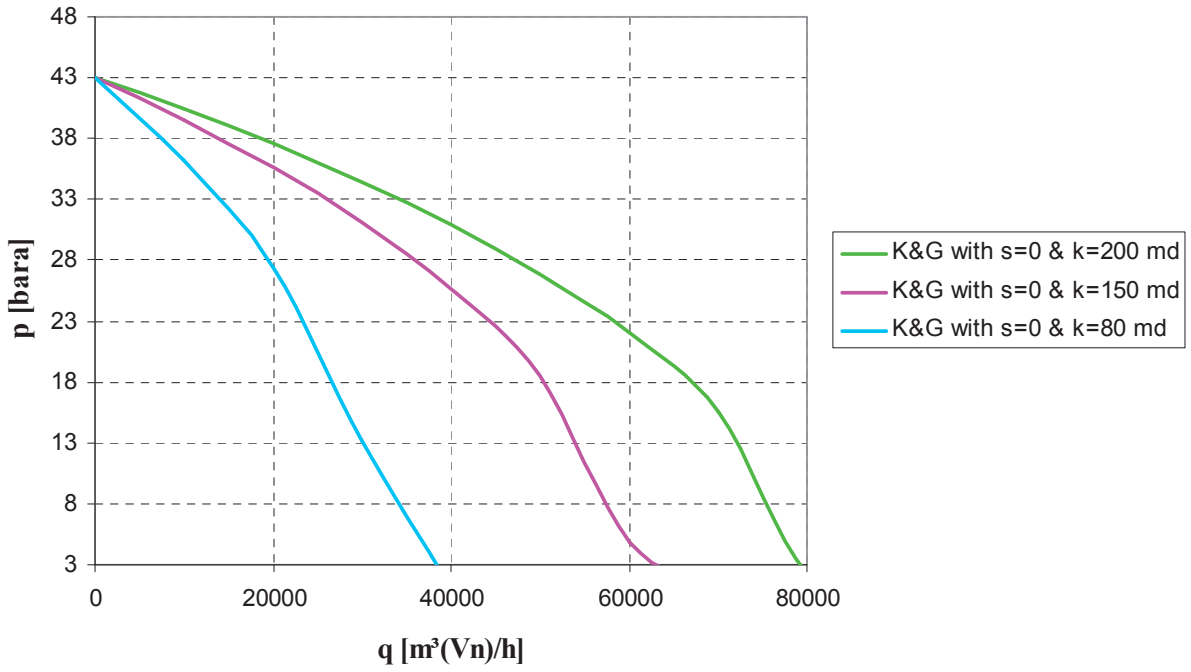

Figure 4-20: Comparison of IPR curves for HGSP-001 with different k at p_{res}=43 [bara]

The same comparison was done with the *Horizontal Well – No Flow Boundaries* model. In both cases, the strong influence of permeability is noticeable. In contrast to skin, permeability is the more influencing parameter.

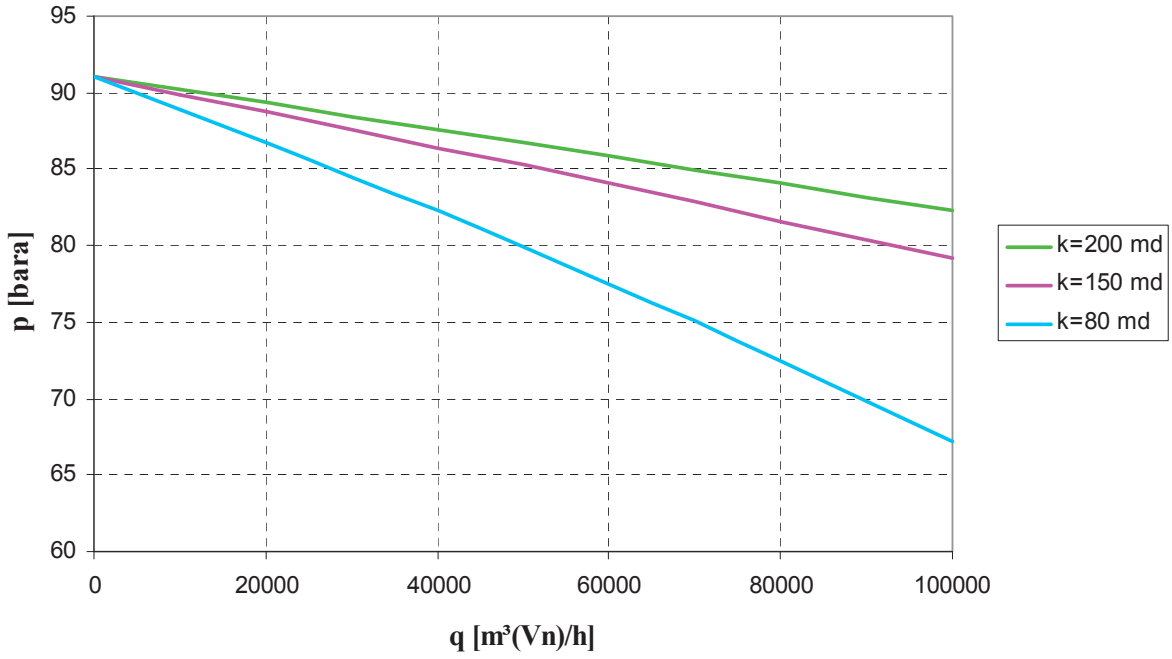

Figure 4-21: The influence of permeability on IPR curve with No Flow Boundary model

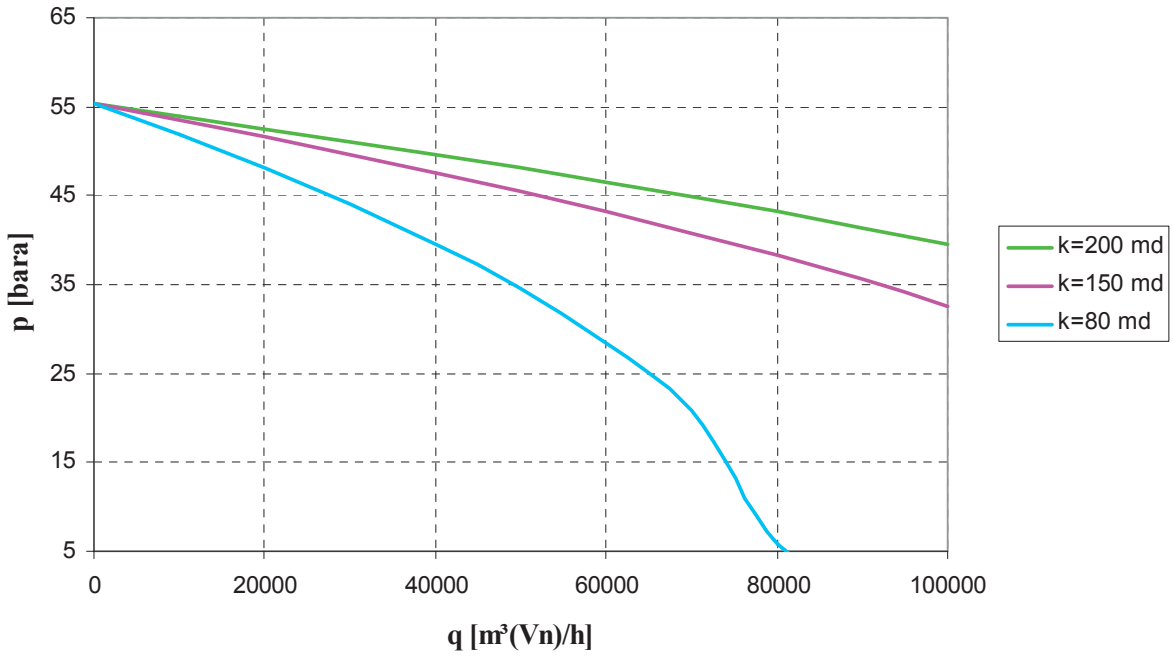

Figure 4-22: The influence of permeability on IPR curve at p_{res}=55 [bara]

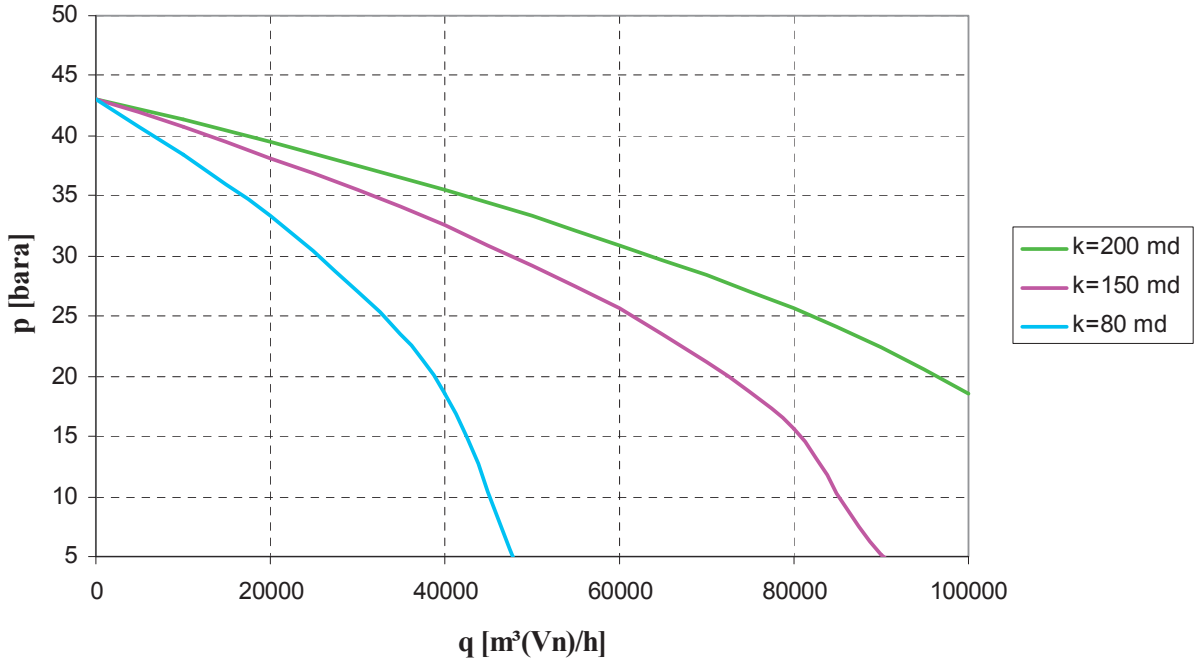

Figure 4-23: The influence of permeability on IPR curve at p_{res}=43 [bara]

4.3.3 Effective well length

The influence of effective well length on well productivity is examined using Horizontal Well – dp-Friction loss model with Kuchuk & Goode. The following figures show the results for three different reservoir pressures.

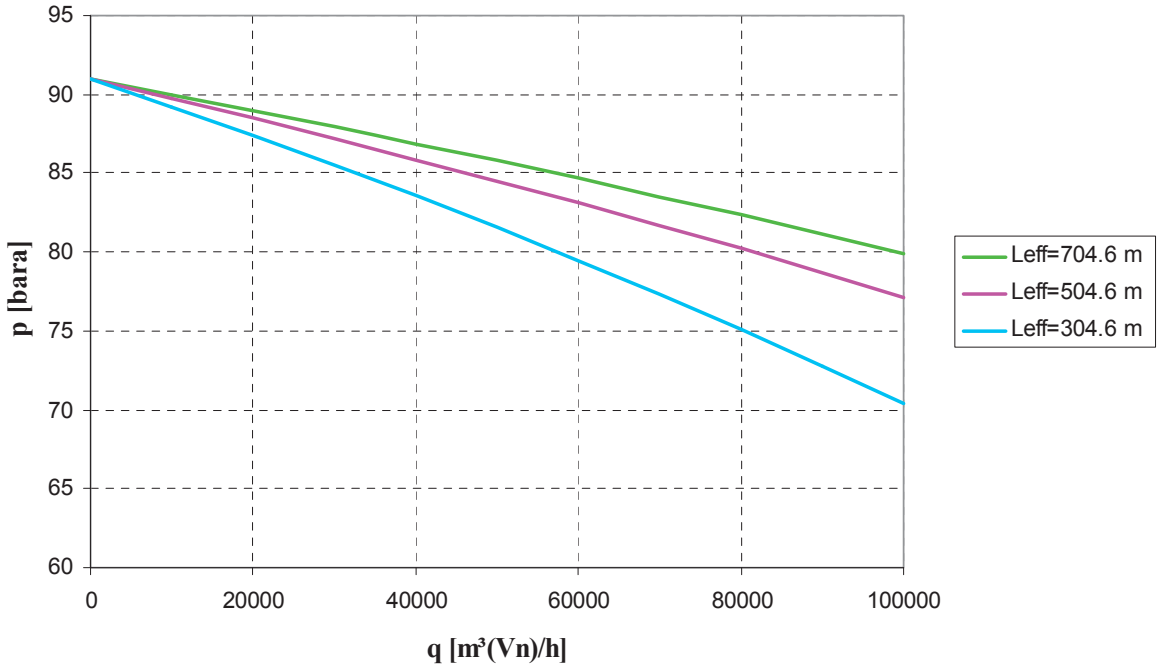

Figure 4-24: The impact of different effective well length on IPR curve at p_{res}=91 [bara]

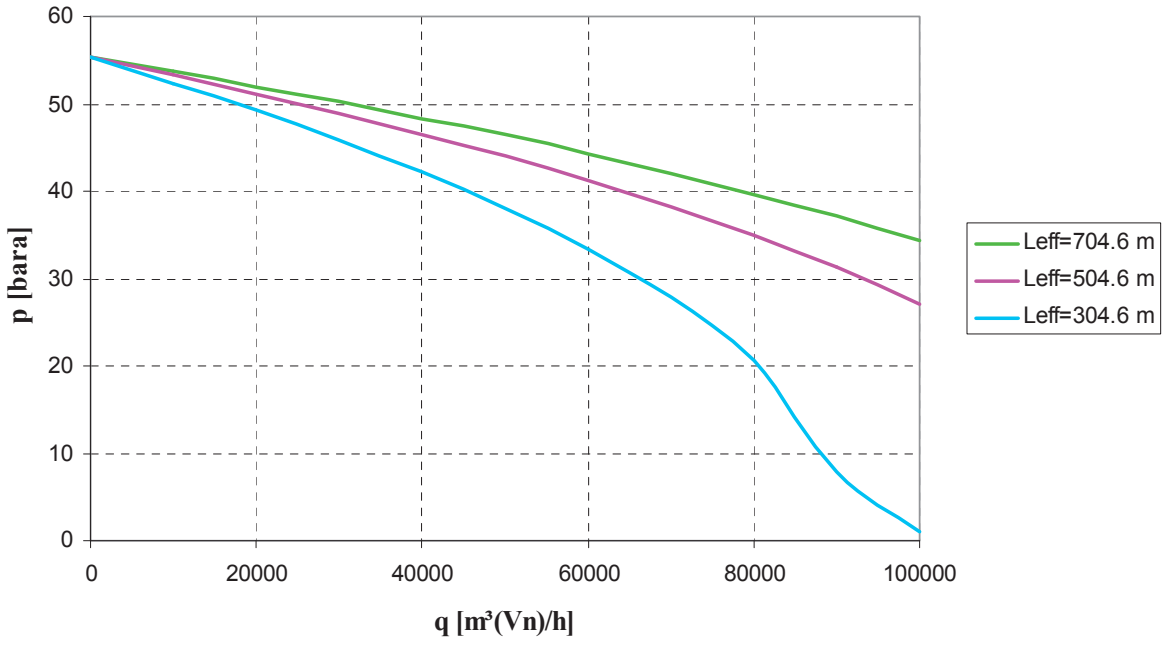

Figure 4-25: The impact of different effective well length on IPR curve at p_{res}=55 [bara]

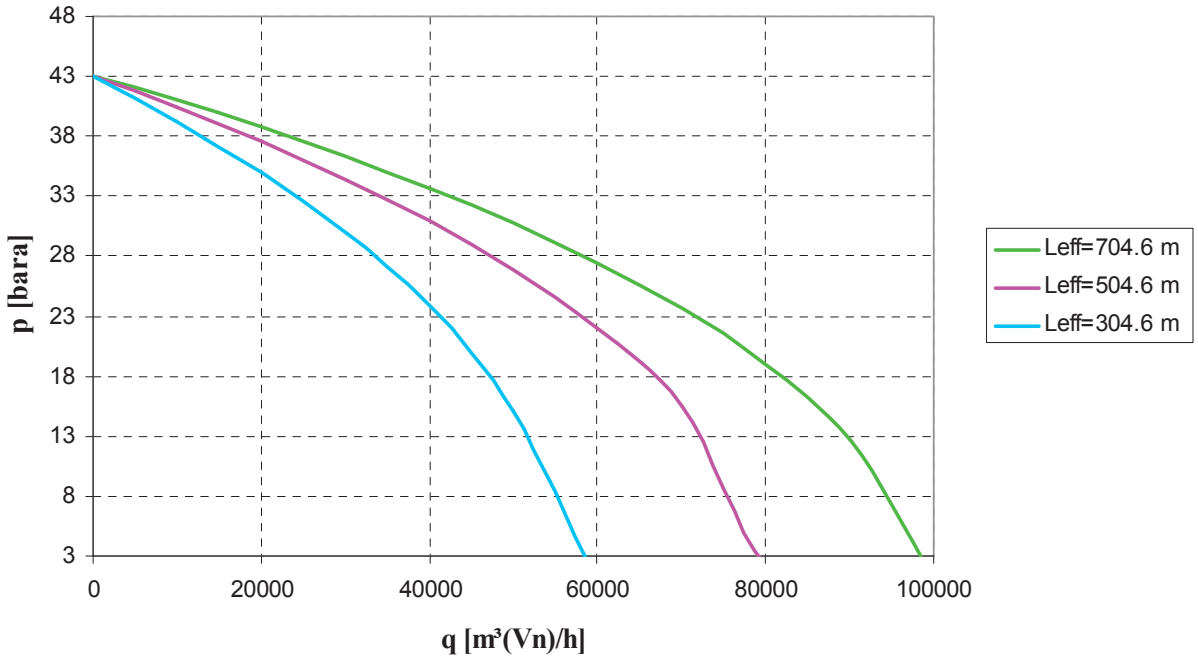

Figure 4-26: The impact of different effective well length on IPR curve at p_{res}=43 [bara]

The actual effective well length of HGSP-001 is 504.6 [m]. The impact of effective well lengths of 704.6 [m] and 304.6 [m], which are 200 [m] longer and shorter than the actual effective well length of HGSP-001, were evaluated. At reservoir pressures 91 [bara] and 55 [bara] one can observe similar trends for differences. In general, it is stated in literatures that effective well length has usually large effect on productivity up to a certain length depending on the given reservoir and well. Above this length only a negligible further increment in performance can be obtained. In the figures above we notice that this statement applies to storage wells of Haag field as well, where it is remarked that over the effective well length of 504.6 [m] the difference between IPR curves becomes smaller.

Another fact to be noticed in all of these sensitivity analyses is that the difference between the IPR curves is smaller at higher reservoir pressures compared to differences at lower reservoir pressures. This is due to friction in the wellbore, and it is velocity dependent. For instance, a specific volume has a smaller velocity at high pressures than the same volume at lower pressures. For detailed calculations of friction pressure losses in the wellbore see Chapter 8.

5 WELL PERFORMANCE AND PRODUCTIVITY – NUMERICAL APPROACH

5.1 Dynamic simulation

The numerical reservoir simulation model is based on the in-house geological model built in Petrel by Dr. Ralph Hinsch in RAG Company. The ECLIPSE Blackoil simulator is used for the dynamic simulation. It can model extensive well controls and support efficient field operations planning.

5.2 Numerical model construction

The simulation model has the dimension of 128 by 58 by 65 grid blocks in x, y and z directions respectively with average areal grid block sizes of 50 x 50 [m] and less than 1 [m] in the vertical direction. Grid block properties porosity and permeability have been generated within the static model based on log data, core measurements and analogies to nearby fields. Direct simulation of the model was possible without the necessity for upscaling, therefore the full field dynamic simulation model was constructed directly from the static model without the process of upscaling geological properties. Further dynamic parameters such as PVT and rock properties were assigned to the numerical model.

5.3 History Match

5.3.1 History match strategy and parameters

The distribution of porosity and consequently the pore volume distribution are well known due to enough well log data. Initializing the model with original log derived capillary curve resulted in a GIIP error of less than 3%. Therefore only the capillary pressure curve was slightly adjusted to final match the GIIP.

The second strategy was to modify the global porosity-permeability correlation to match the measured gas production rates. The applied modification was shift of the correlation curve to increase the permeability of low porosity values. The shifted curve was well within the range of the used porosity-permeability correlation cloud. The correlations are plotted in the following figures.

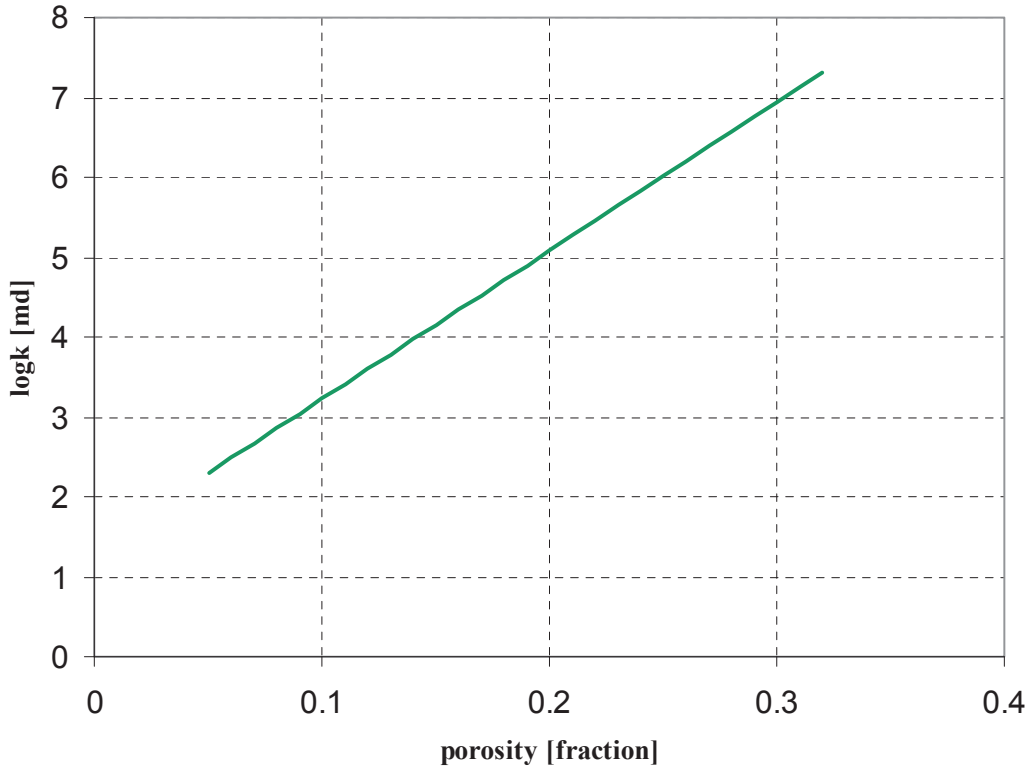

Figure 5-1: Linear relationship of modified permeability and porosity

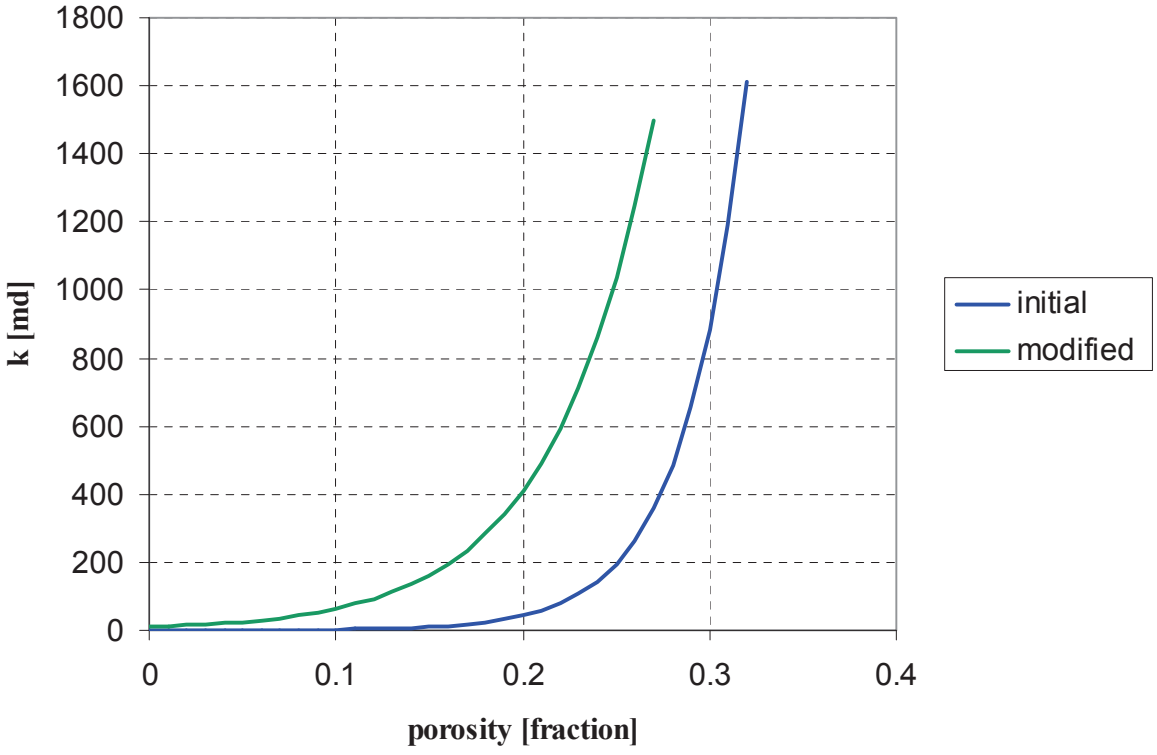

Figure 5-2: Permeability-porosity correlations

5.3.2 History match results

The dynamic pressure and gas production history match for the Haag wells are shown in Figures 5-3 – 5-8. The reservoir behavior is fully volumetric with the pressure declining rapidly with the cumulative production. The pressure distribution in the model from 1983 to 2008 at every 10 year interval is shown in the Appendix D as pressure distribution maps.

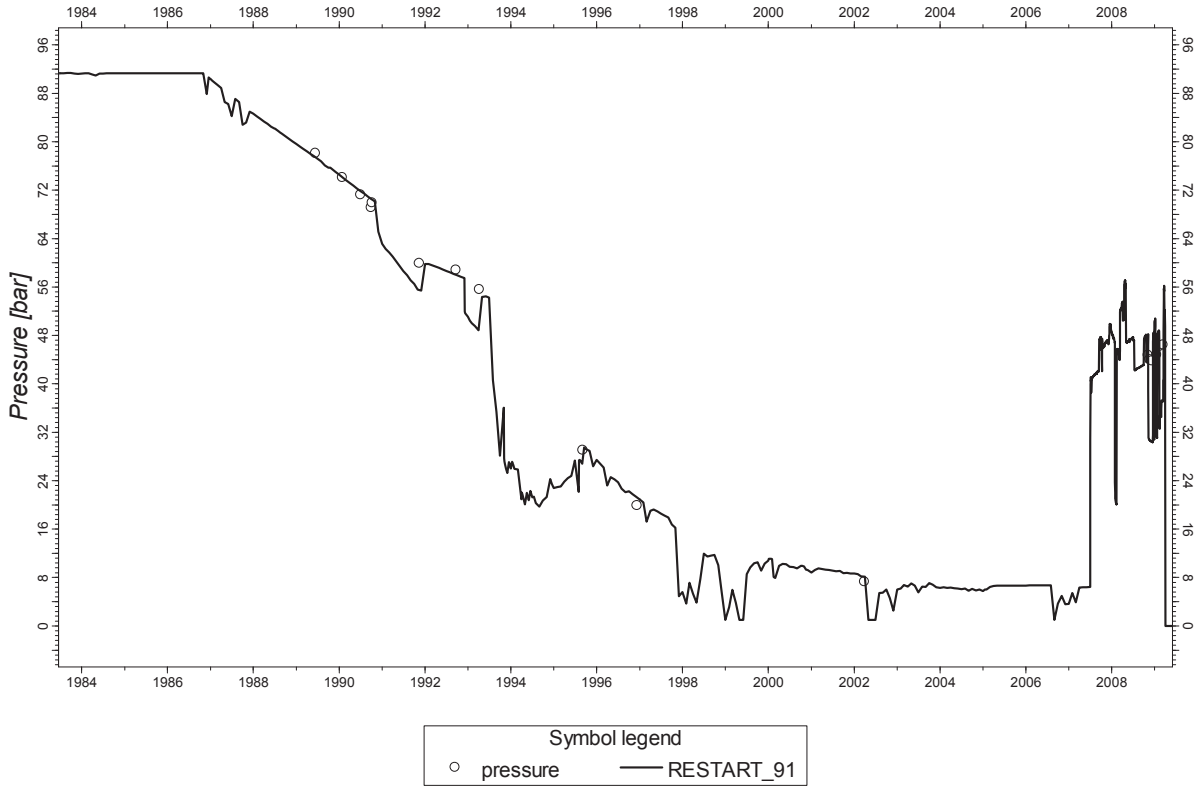

Figure 5-3: Pressure history match, HAAG-001

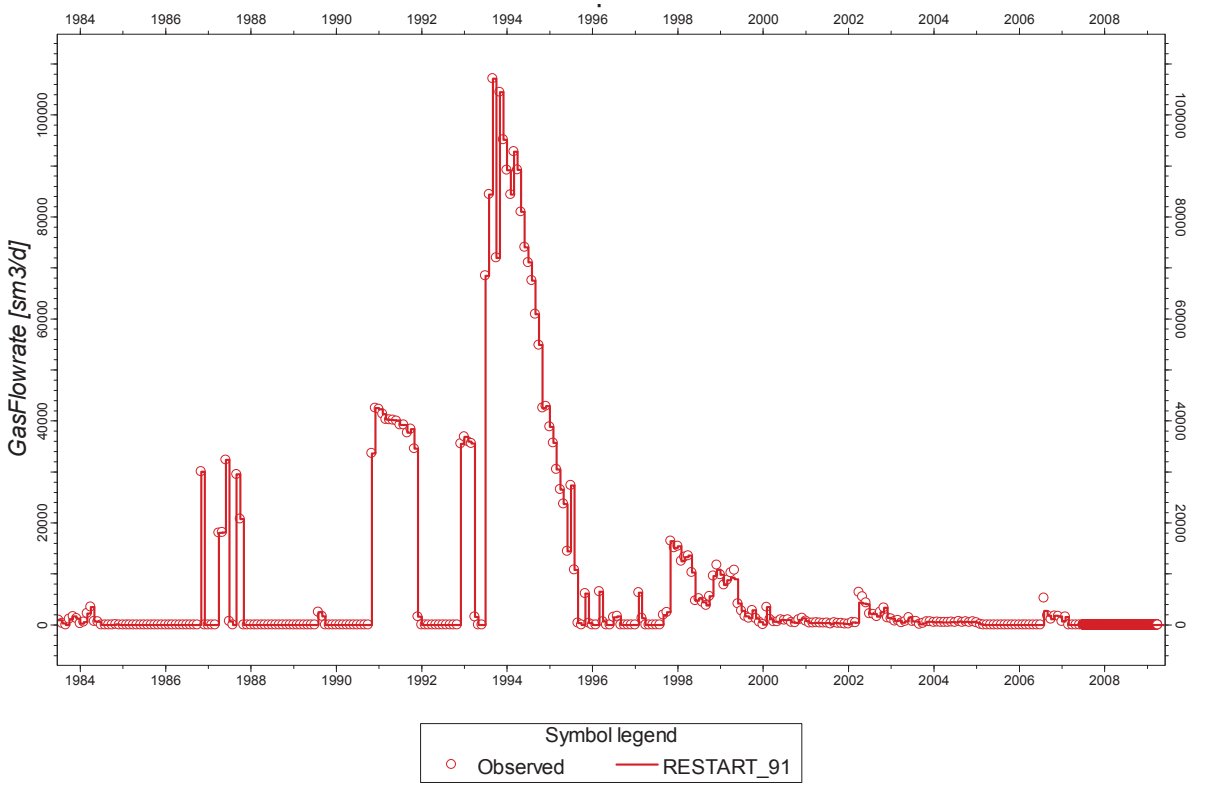

Figure 5-4: Gas production rate history match, HAAG-001

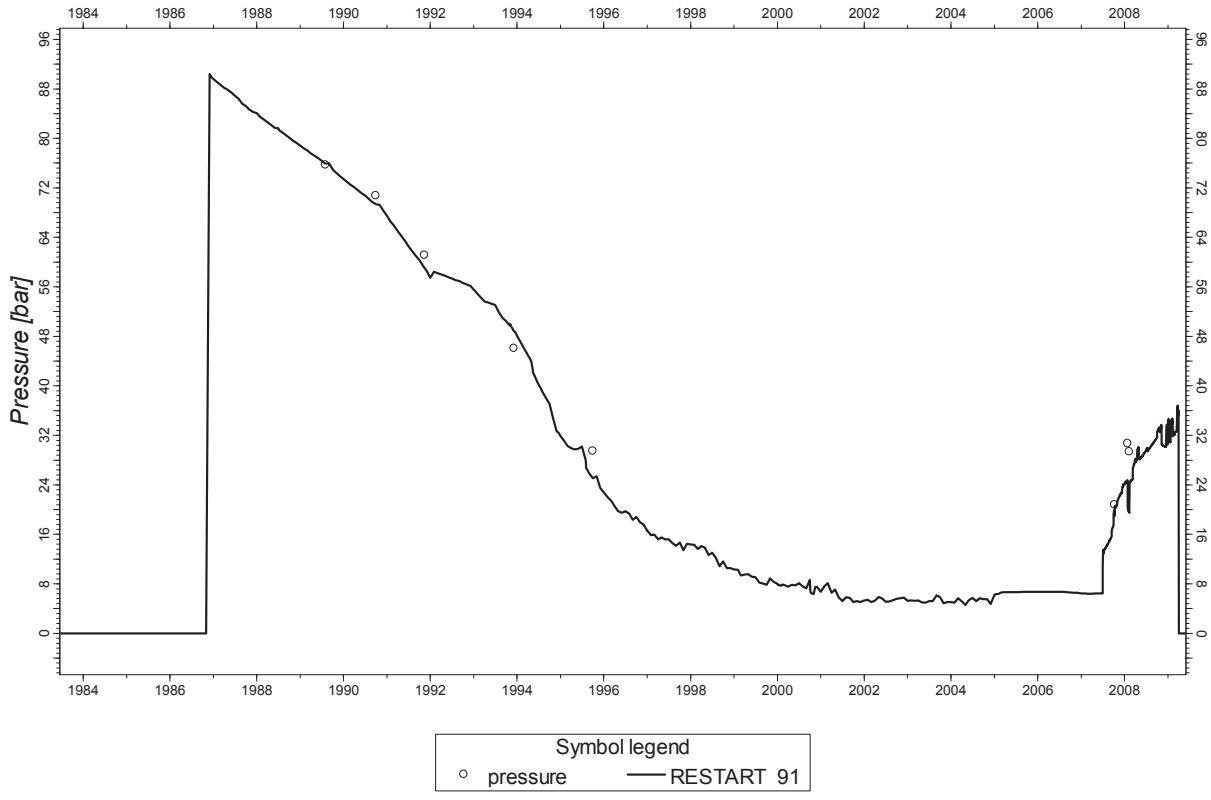

Figure 5-5: Pressure history match, HAAG-002

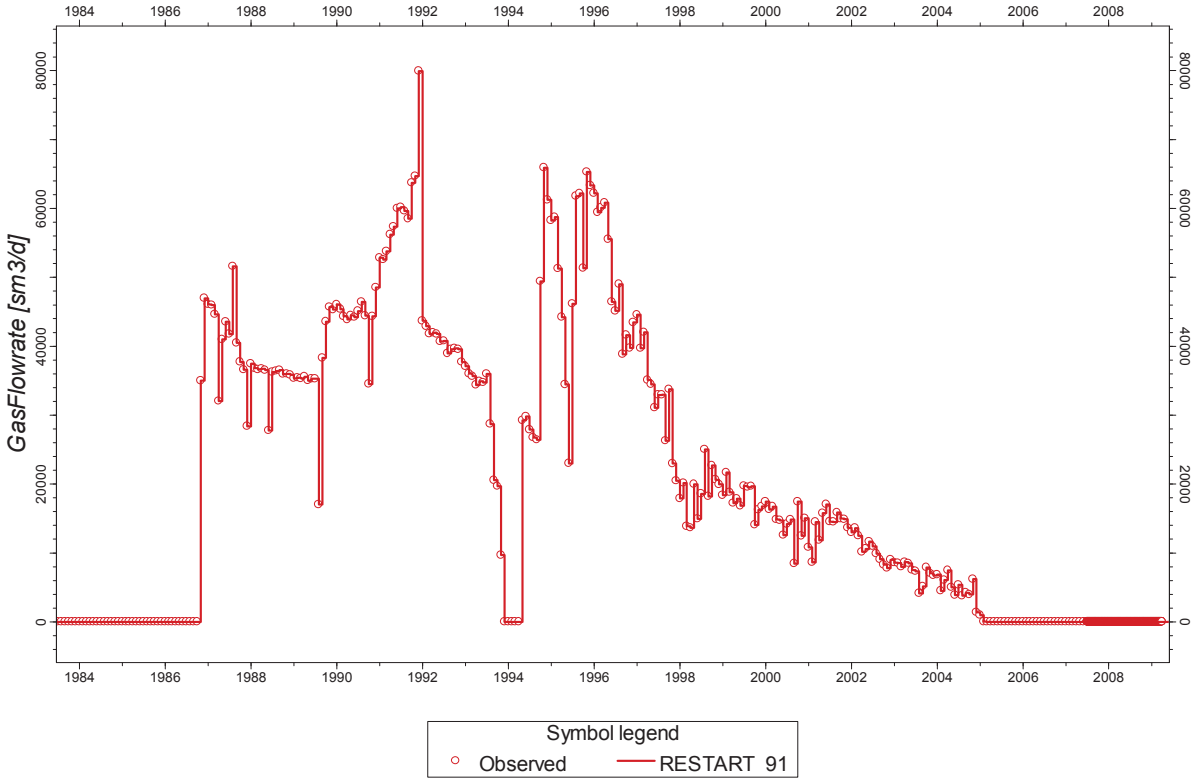

Figure 5-6: Gas production rate history match, HAAG-002

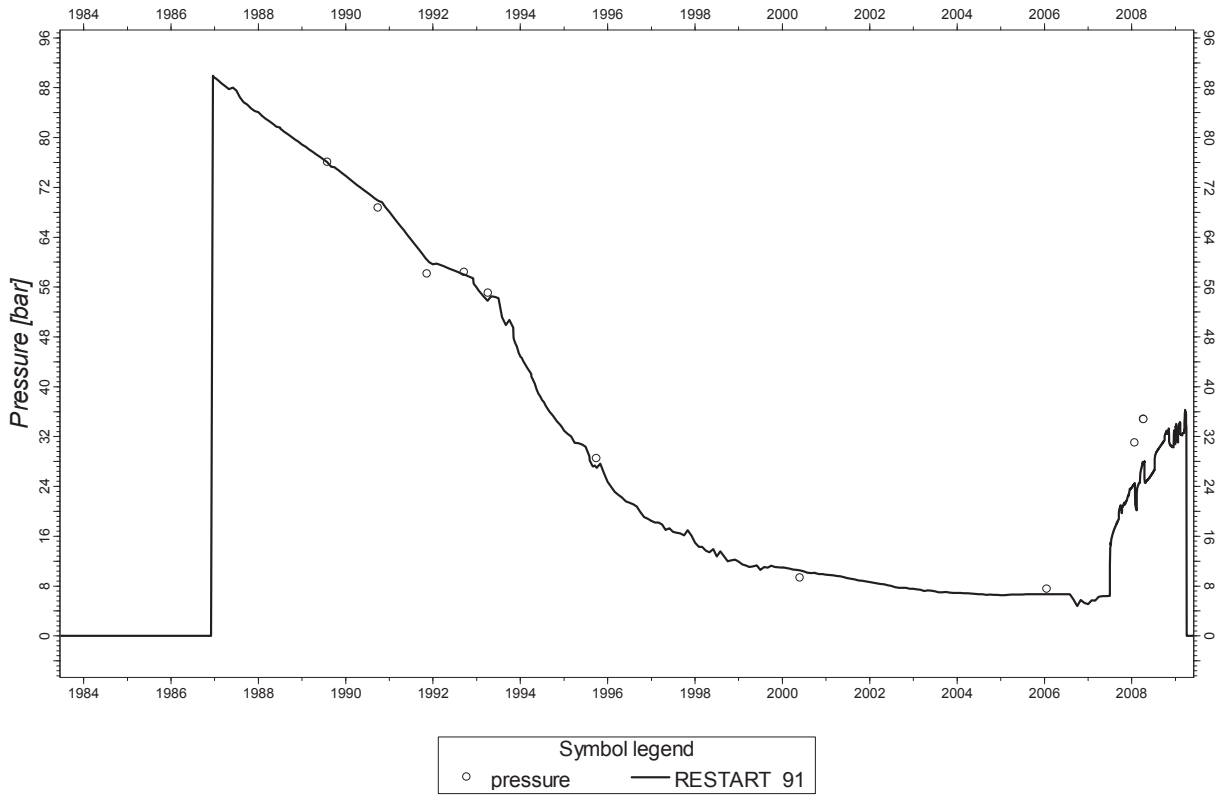

Figure 5-7: Pressure history match, HAAG-003

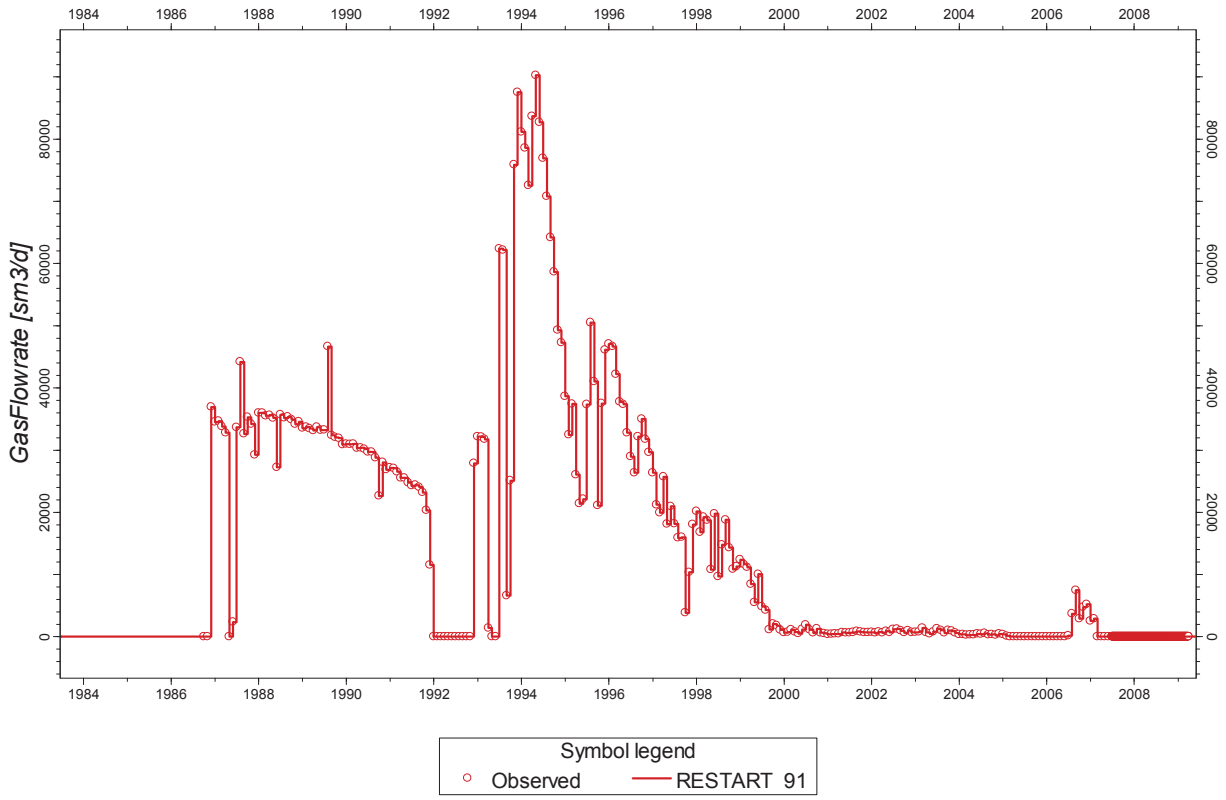

Figure 5-8: Gas production rate history match, HAAG-003

A good pressure match was achieved and the calibrated model is suitable for use in predictive mode.

5.4 Horizontal well techniques in ECLIPSE

There is no public available information about the implementation of horizontal wells in reservoir simulation package ECLIPSE of Schlumberger SIS.

5.5 Well performance calculations

Important parameters for the well performance calculation are determined by the planed withdrawal profile. The following diagram illustrates the withdrawal profile for the Haag underground storage facility. Turn-over-volume (TOV) of 190 Mio. [m³(Vn)] has been determined based on the feasibility study. The target withdrawal rate is 40000 [m³(Vn)/h] per well, which results in 120000 [m³(Vn)/h] for three storage wells. This rate is required to be kept until 70 % of TOV has been produced.

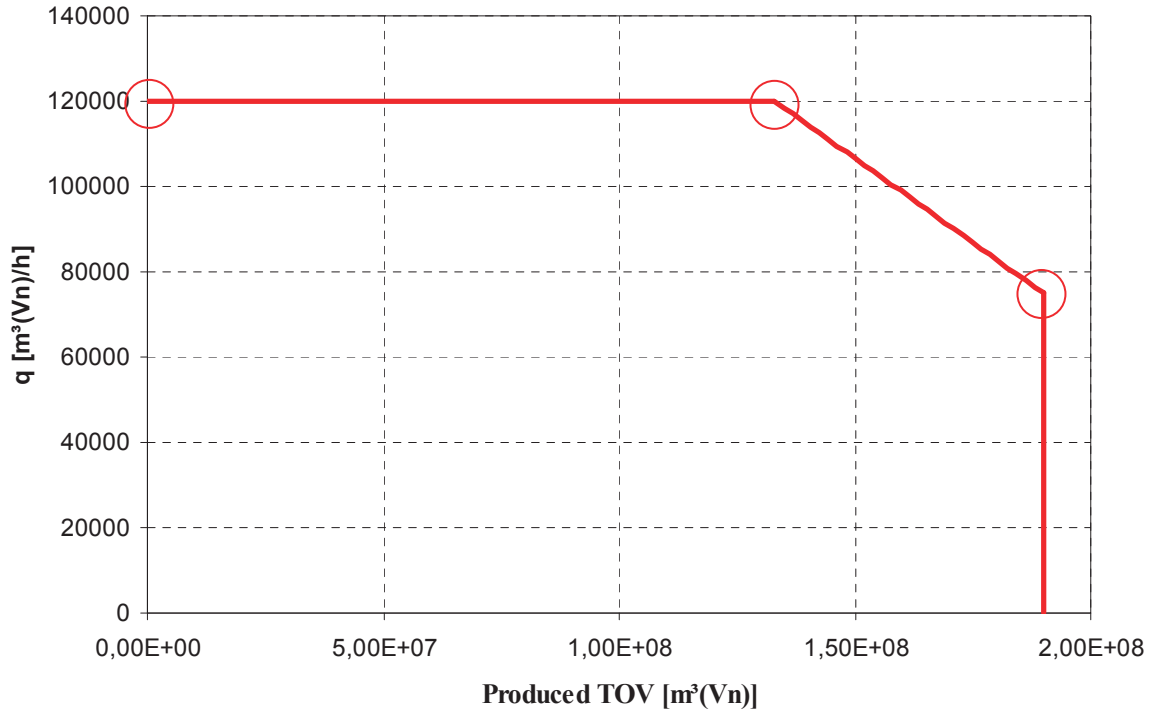

Figure 5-9: Withdrawal profile for Haag underground storage facility

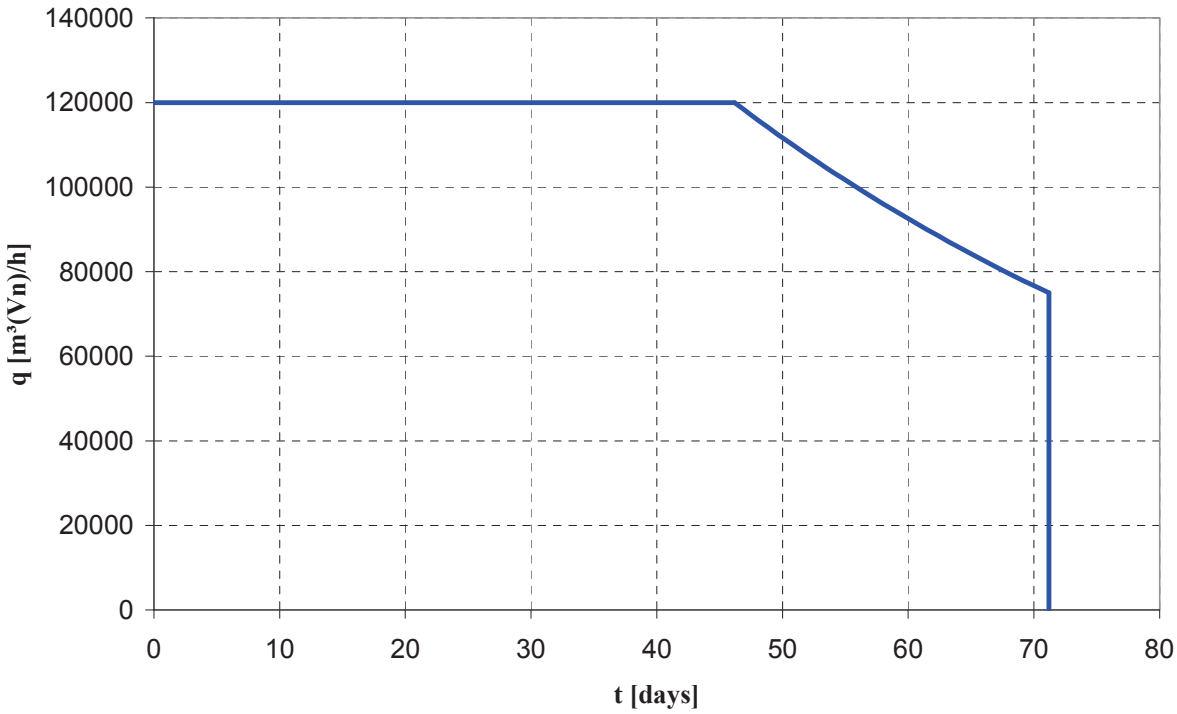

Figure 5-10: Withdrawal profile vs. time

Fig. 5-10 depicts the withdrawal profile as a function of time. The 70 % of TOV is produced on 46th day of withdrawal.

The 70 % of TOV is equal to 133 Mio. [m³(Vn)]. Producing above this volume requires reduction of the withdrawal rate due to surface facilities' constraints. Therefore the rate must be reduced down to 62.5 %. The trend in flow rate decrease is 1.5% per 1 % TOV reduction. Based on this withdrawal profile (see Fig. 5-9) there are three pressures that are significant for the storage cycles. They are the initial pressure at full storage, the pressure at 30 % of TOV in the storage, and at the end of the withdrawal cycle at cushion gas level. These corresponding reservoir pressure values are 91, 55 and 43 [bara], respectively, determined from history matched simulation model and confirmed by the p/Z-plot according to the corresponding volume present in the reservoir.

The well performance calculations are based on the history matched model. For a given reservoir pressure and different flow rates the bottom hole flowing pressures are calculated and compared to the corresponding values of the analytical approach. This is done for the three significant reservoir pressure levels and various flow rates. The results of the comparisons are reported in the next chapter.

5.6 Sensitivity Analysis

5.6.1 Skin

The impact of skin on inflow performance calculations are evaluated by running the simulator for different skin values. As mentioned above the bottom hole flowing pressures at different flow rates are calculated and an IPR curve was constructed by plotting these pressures against appropriate flow rates. The figures below show the results for skin values of 0 and 7 at three different reservoir pressures for HGSP-001. All of these plots depict the less influence of skin value on calculated bottom hole flowing pressures. It shows the similar trend as in case of analytical approach, namely underlining the fact that skin is less significant influencing parameter.

As skin is the only, in reality, changeable parameter (by means of well stimulation) compared to well length and reservoir permeability, the sensitivity analysis was done without these two parameters.

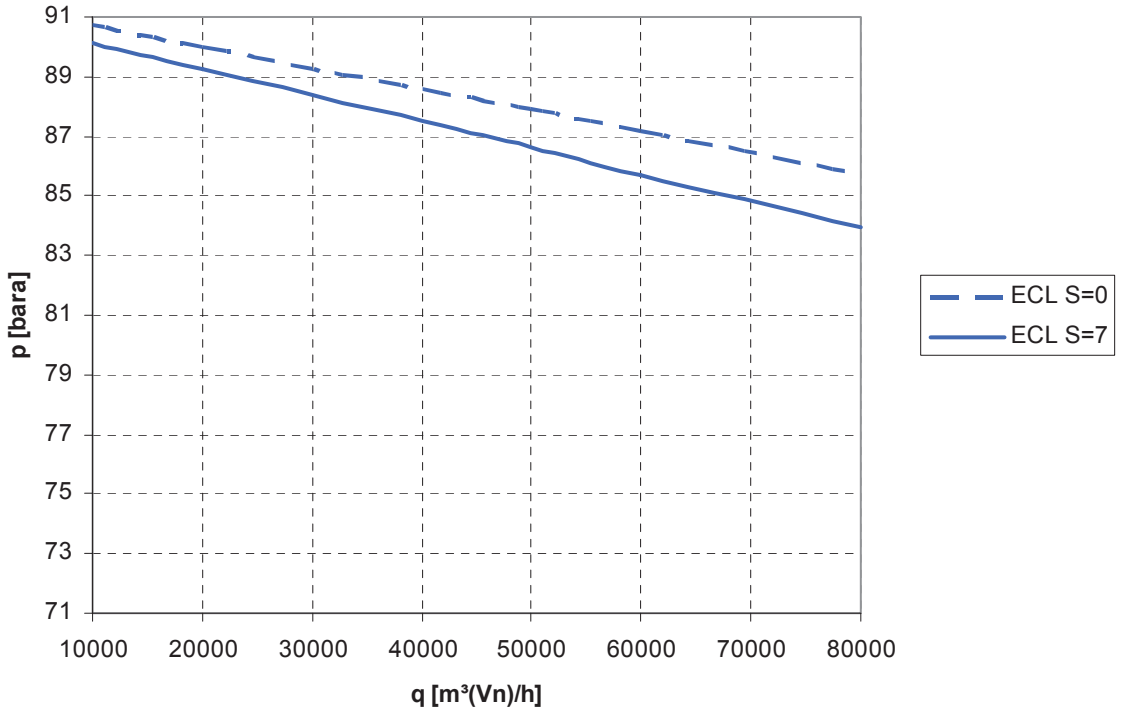

Figure 5-11: Influence of different skin values at p_{res}=91 [bara]

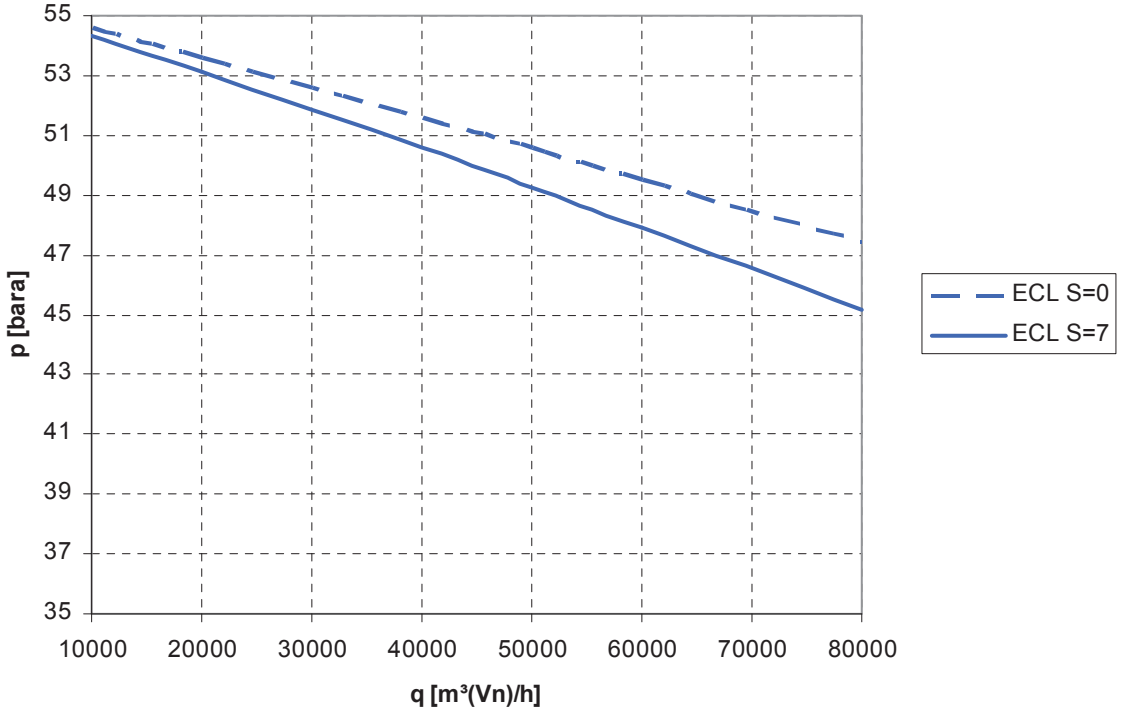

Figure 5-12: Influence of different skin values at p_{res}=55 [bara]

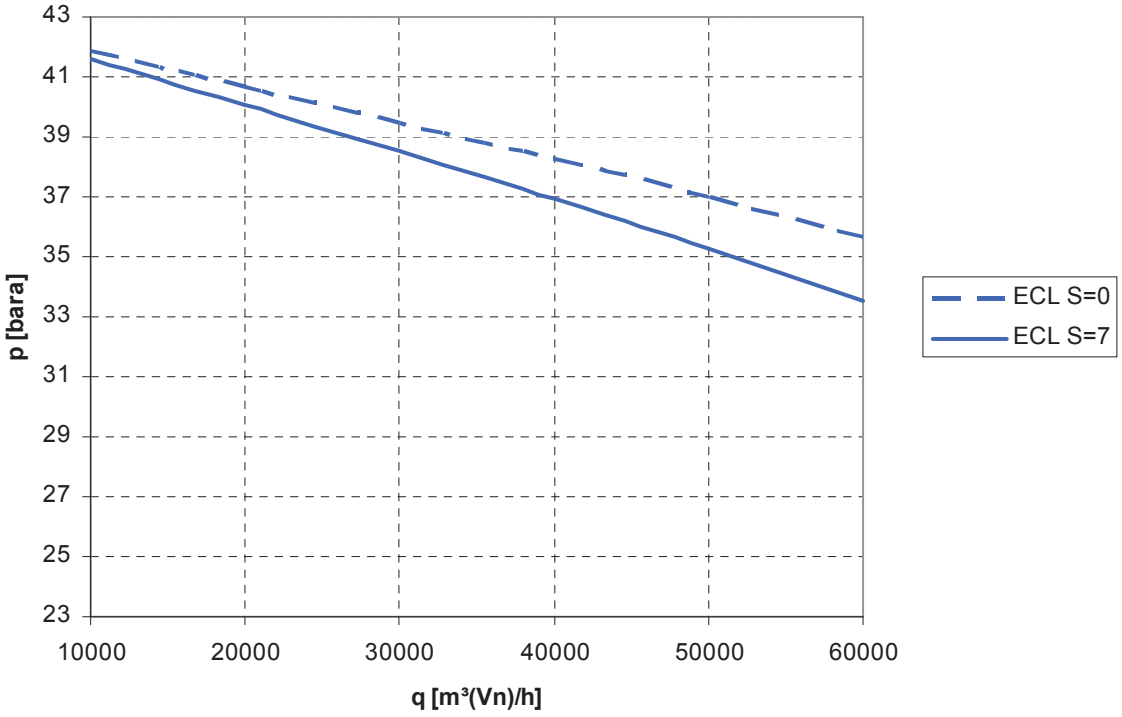

Figure 5-13: Influence of different skin values at p_{res}=43 [bara]

6 COMPARISON OF RESULTS

In this chapter the results of semi-analytical and numerical approaches are compared. The well model used in PROSPER is Kuchuk and Goode along with the reservoir model option *Horizontal Well – dp Friction Loss in Wellbore*.

6.1 Comparison of ECLIPSE and PROSPER based on HGSP-001

The comparisons are done for the three pressure values. The significant input data used in ECLIPSE are listed in Table 6-1. The input parameters for PROSPER are tabulated in Table 6-2.

Table 6-1: Comparable input data used in ECLIPSE

Average permeability	210	[md]
Average porosity	0.21	fraction
Skin	0	[-]

Table 6-2: Input data for PROSPER

Permeability	200	[md]
Porosity	0.25	fraction
Skin	0	[-]
Wellbore radius	4.25	[inches]
Well length	738.54	[m]
Reservoir thickness	8	[m]
Reservoir length	1400	[m]
Reservoir width	500	[m]
Length distance to reservoir edge	350	[m]
Width distance to reservoir edge	250	[m]
Bottom of reservoir to well center	3	[m]
Pipe roughness	0.0001	[m]

The parameters porosity and permeability for the analytical approach have been derived from the numerical model. The skin value in both models is 0.

6.1.1 Comparison without productivity multiplier

The figures below show the results of the PROSPER model and the original ECLIPSE simulation.

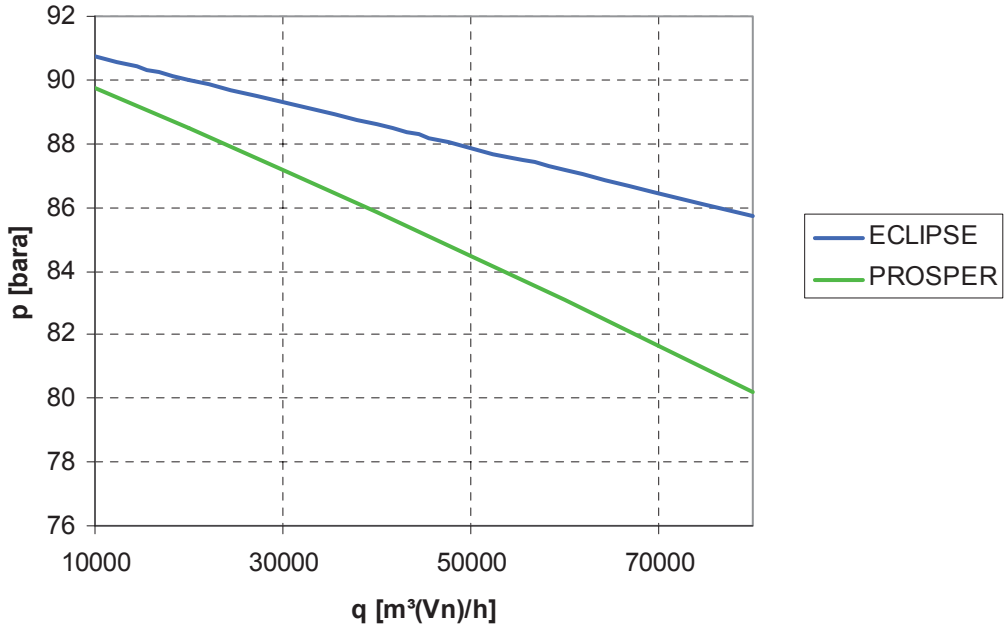

Figure 6-1: Comparison of results at p_{res}=91 [bara] for HGSP-001

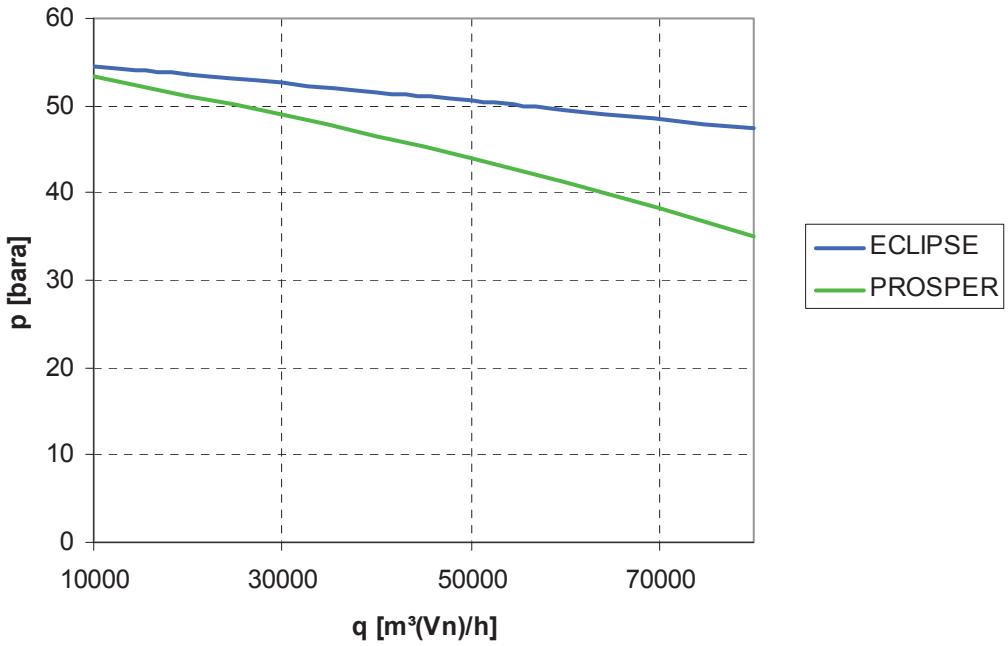

Figure 6-2: Comparison of results at p_{res}=55 [bara] for HGSP-001

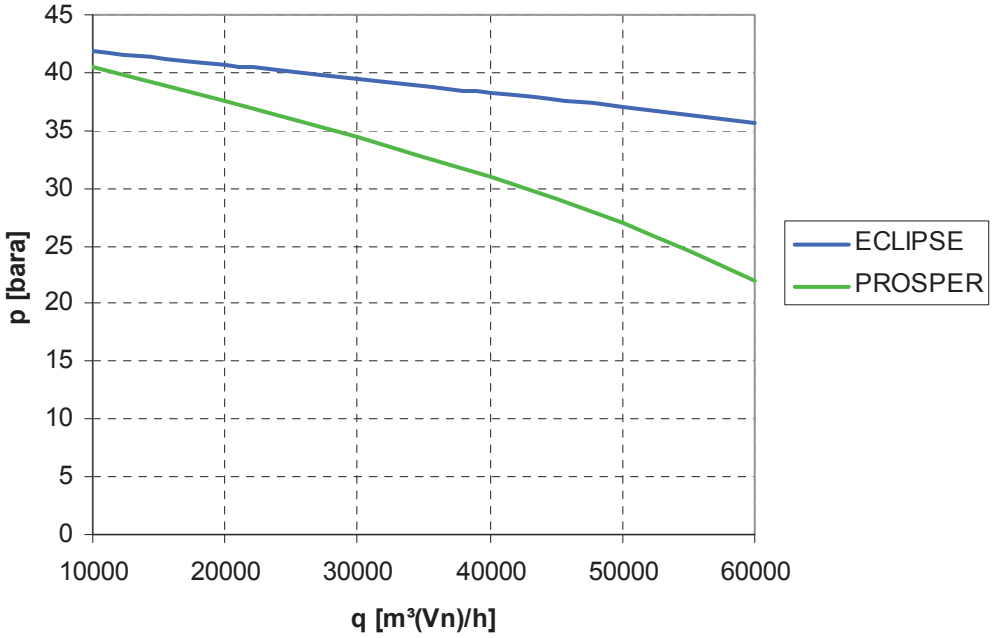

Figure 6-3: Comparison of results at p_{res}=43 [bara] for HGSP-001

6.1.2 Comparison with productivity multiplier

The following figures show the corrected results of ECLIPSE model with the correct productivity multiplier for the three different reservoir pressures. For detailed discussion see section 6.3.

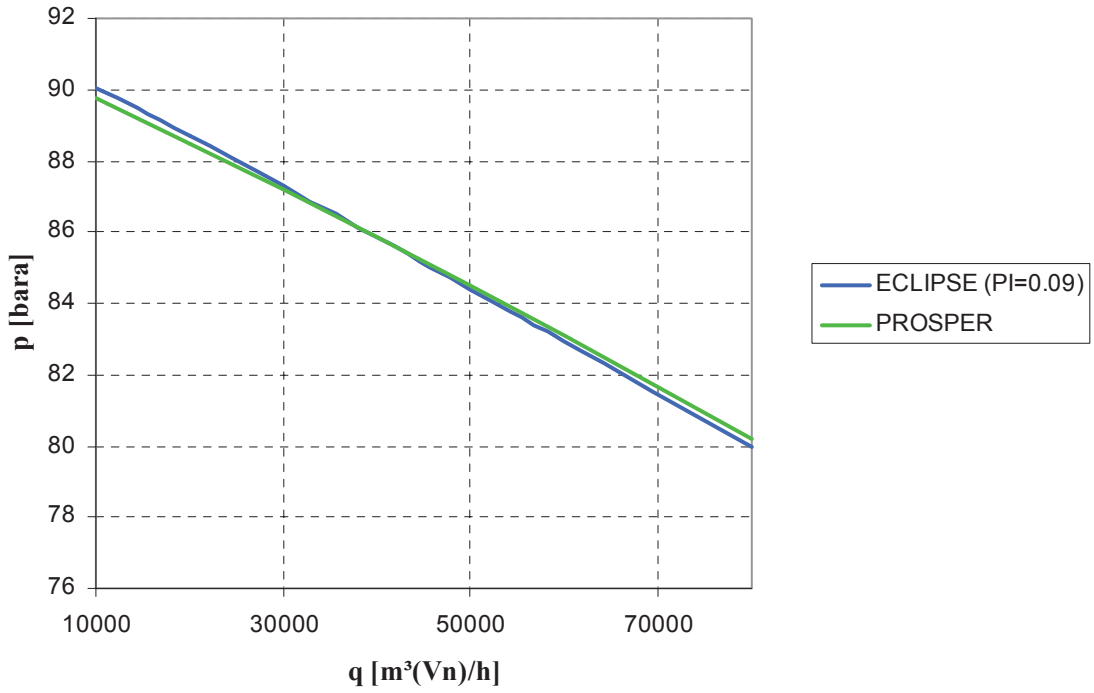

Figure 6-4: Comparison of the PROSPER IPR curve with corrected curve from ECLIPSE

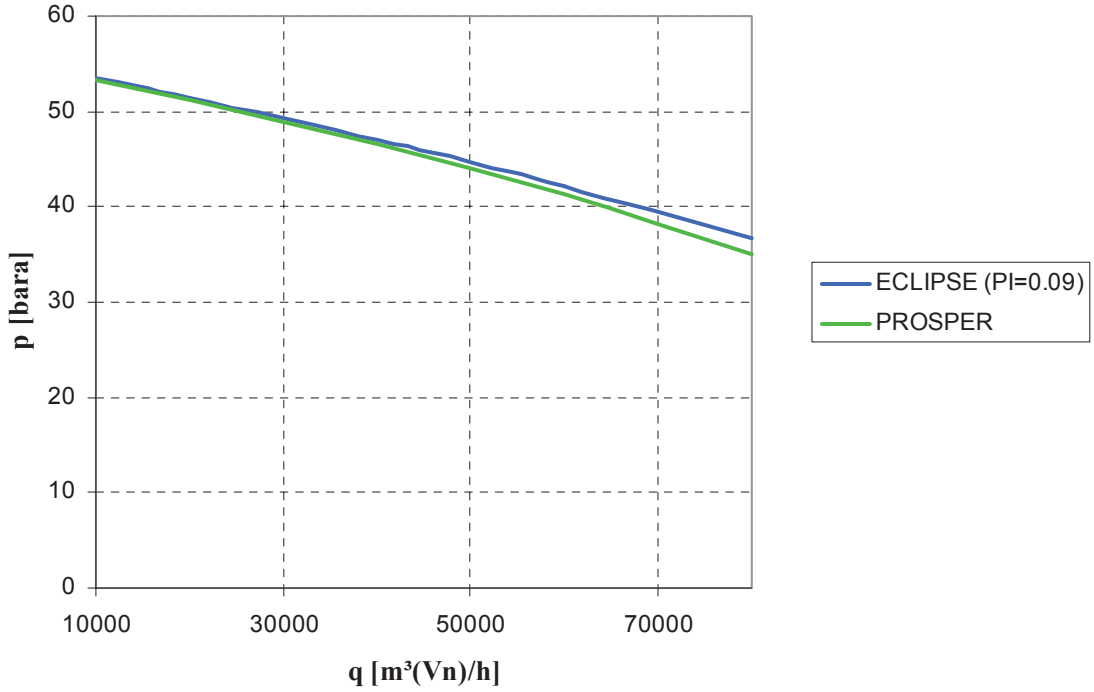

Figure 6-5: Comparison of the corrected curve at p_{res}=55 [bara]

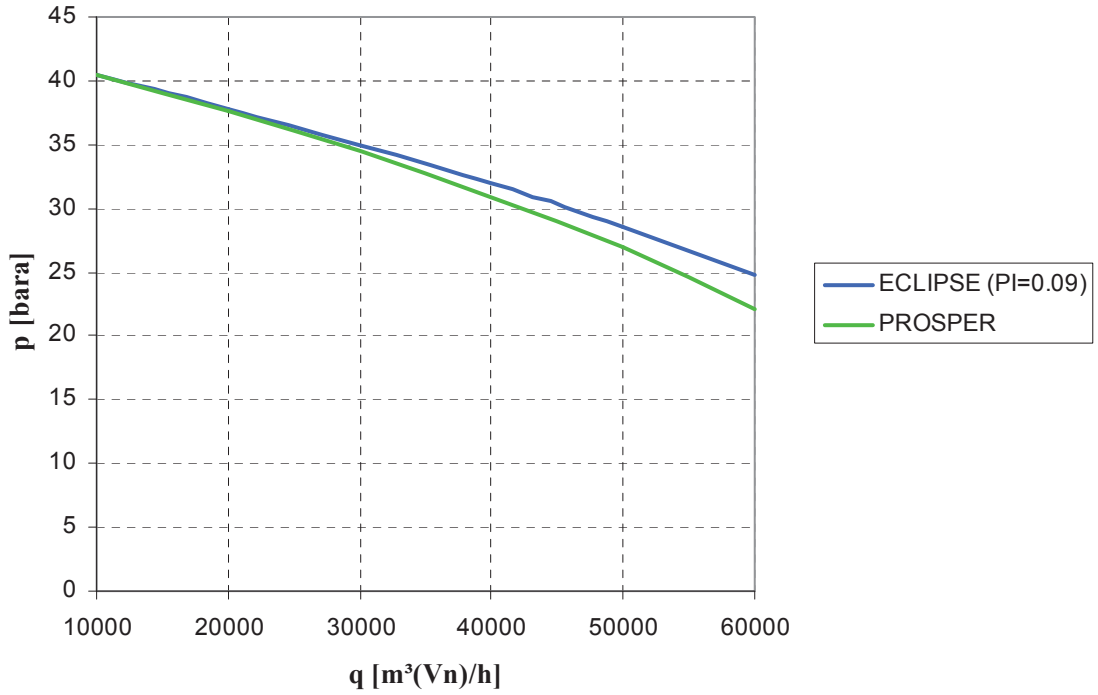

Figure 6-6: Comparison of the corrected curve at p_{res}=55 [bara]

6.2 Comparisons based on HGSP-002 and HGSP-003

The same approach as for well HGSP-001 was applied to HGSP-002 and HGSP-003 and it was possible to find a correct productivity multiplier for each well to match the corresponding analytical data.

However, these correct productivity multipliers are different for each well and no correlation to well properties can be found. The value for HGSP-002 is 0.65 and for HGSP-003 is 0.25.

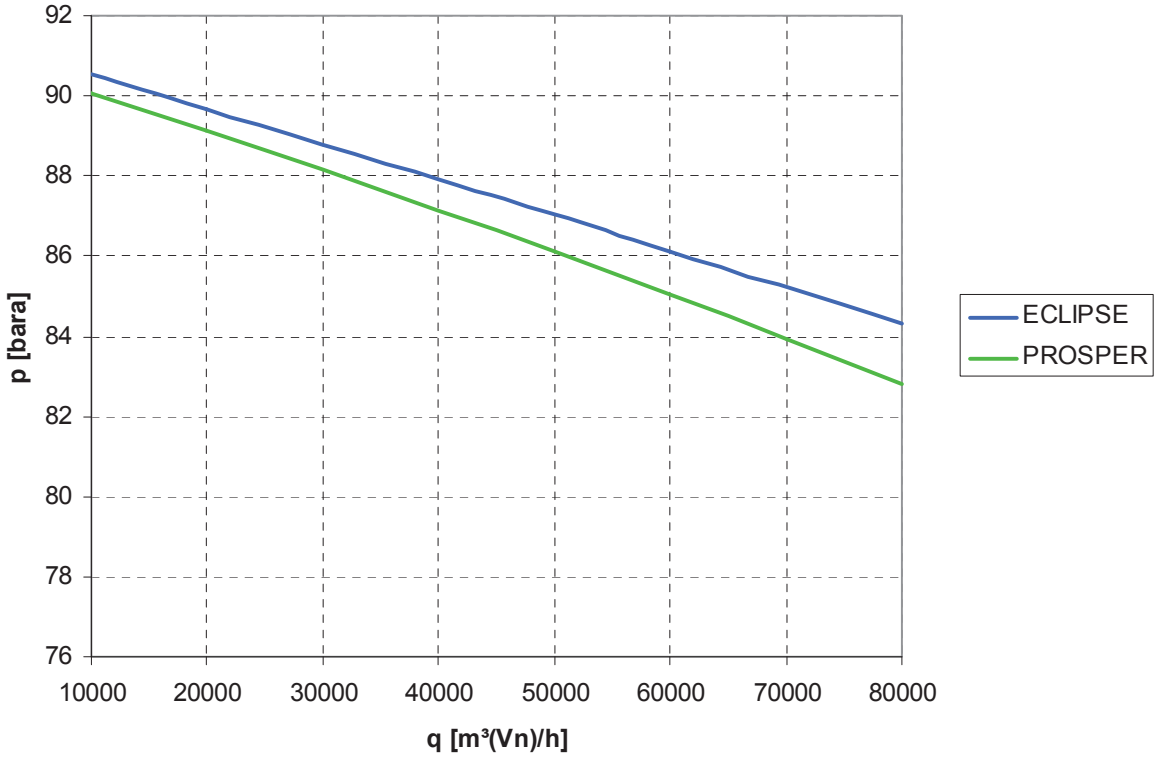

Figure 6-7: IPR without productivity multiplier at p_{res}=91 [bara] for HGSP-002

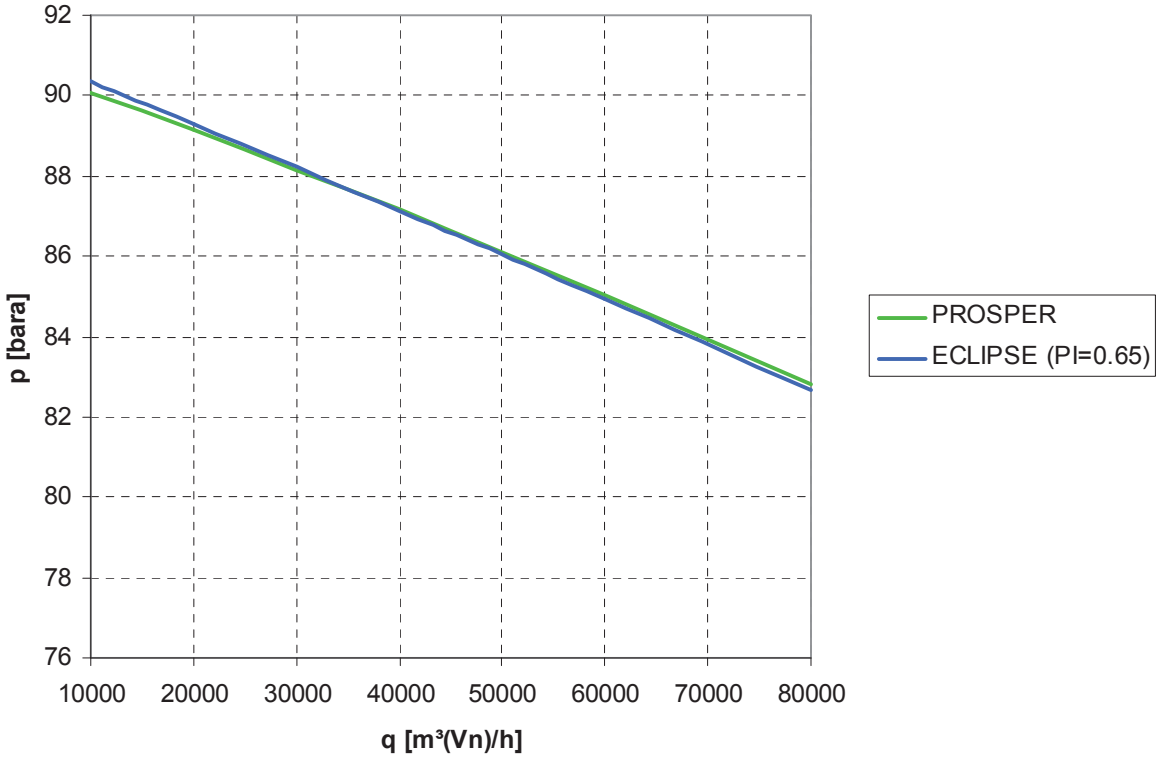

Figure 6-8: IPR with productivity multiplier at p_{res}=91 [bara] for HGSP-002

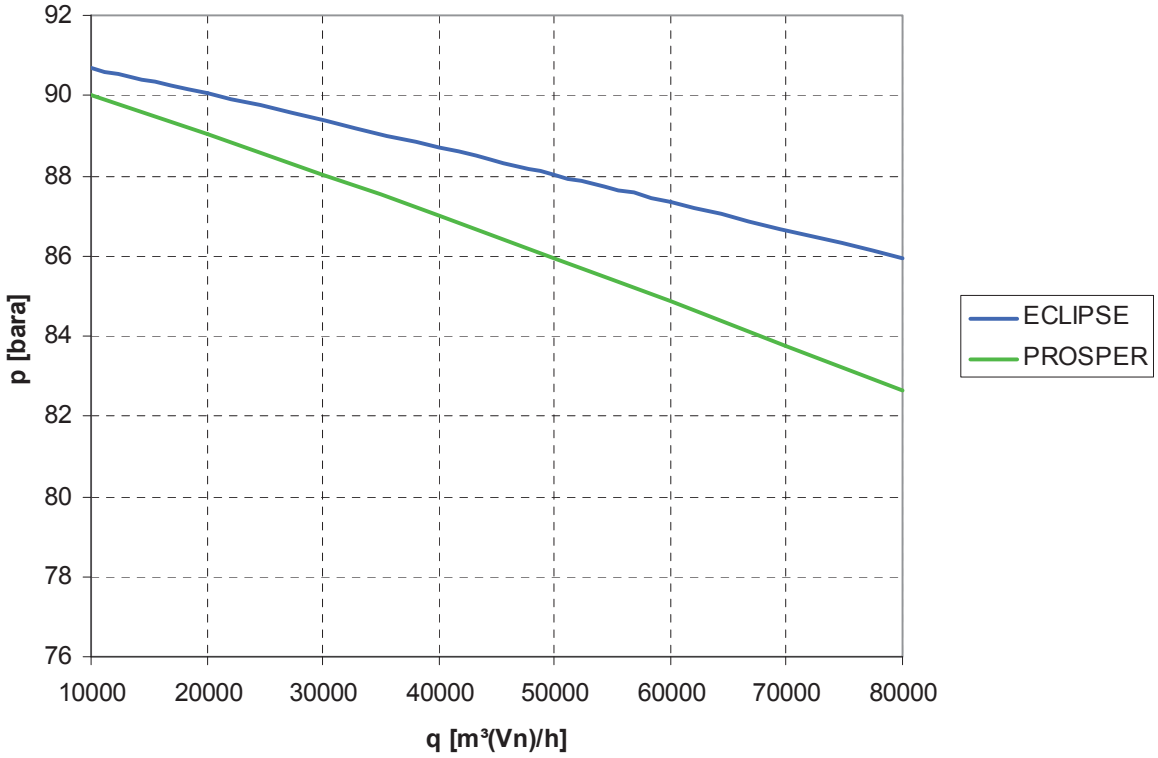

Figure 6-9: IPR without productivity multiplier at p_{res}=91 [bara] for HGSP-003

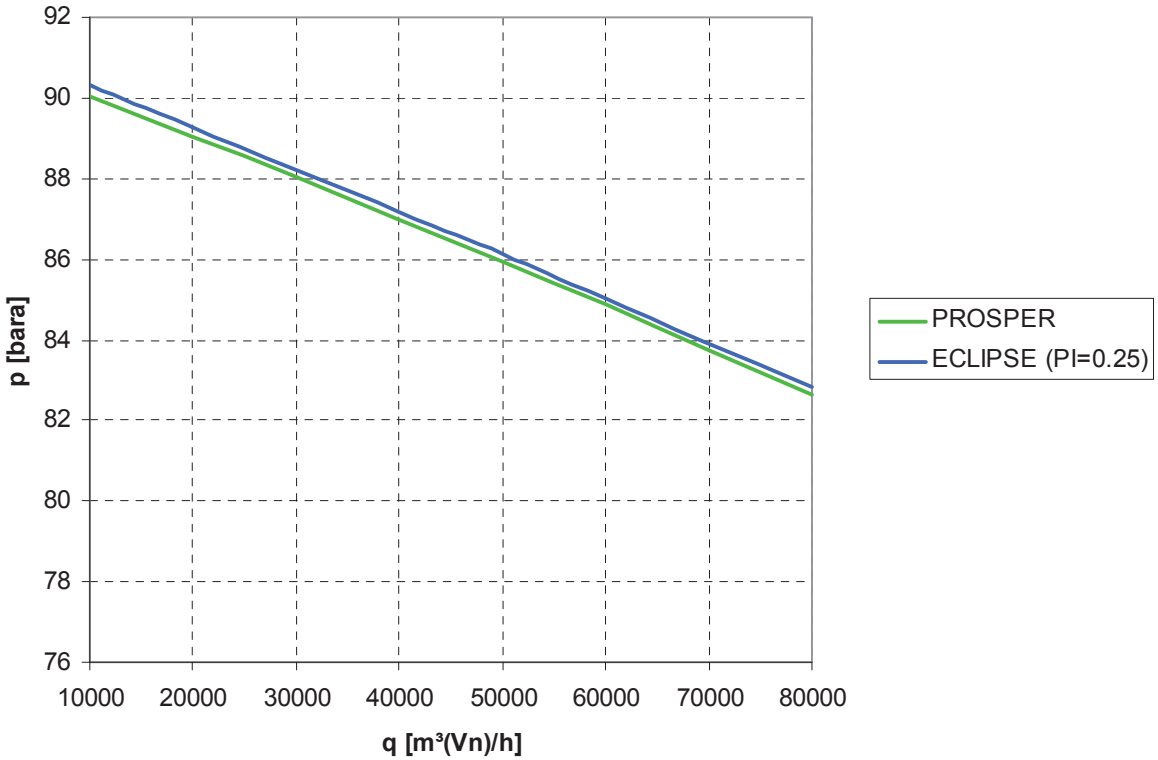

Figure 6-10: IPR with productivity multiplier at pres=91 [bara] for HGSP-003

6.3 Discussion of results

As seen on the Fig. 6-1 through Fig.6-3, the difference between the two models is large. The ECLIPSE model yields too optimistic results. Since the calculation method of ECLIPSE for horizontal wells is unknown, it was not possible to gain any information about it, so it is assumed that ECLIPSE does not use a dedicated horizontal well model to calculate the horizontal well inflow.

The semi-analytical approach delivers more reliable inflow performance calculations; because these calculations are based on certain researched well models, which have been constructed specifically for horizontal wells. Therefore, the calculations of numerical approach must be modified based on the results of the semi-analytical approach.

This is done by artificially modifying the well productivity within the numerical approach. ECLIPSE offers the possibility of using a productivity multiplier, which changes the entire well potential. The value of this multiplier has to be found through trial and error.

The results achieved based on an individual well were excellent. The determined value of the productivity multiplier delivers perfect matches of both approaches for the investigated pressure range in the given well. However, it was identified that the same productivity multiplier cannot be used for other wells. Therefore, the value of the productivity multiplier must be evaluated separately for each single well.

7 FULL FIELD MODEL

There are basic requirements called performance properties in the operation of underground storage reservoirs. These are:

- Verification of inventory
- Assurance of deliverability

The inventory represents the gas inside the storage horizon. It is made up of two parts:

- Base gas (more commonly referred to as cushion gas)
- Top gas (or working gas or Turn-Over-Volume, TOV)[11]

The working gas shares the reservoir with base gas. While both consist of the same gas, their role is different in storage.

The working gas is regularly withdrawn and injected whereas the cushion gas constantly remains in the reservoir and provides the pressure necessary to deliver the working gas. The larger cushion gas volume, the higher one would expect the deliverability of gas from storage. The deliverability is a storage characteristic which relates to the ability of the storage to deliver the gas to its dedicated customers. It strongly depends on the equalized pressure dominating in the reservoir. Since the pressure is a function of the amount of gas in the storage container, it simply follows that deliverability is a function of inventory.

In case of the Haag field the withdrawal profile constructed according to the full field simulation model with ECLIPSE, without productivity multiplier, seems to have a correct profile (see Fig. 7-1), which would fully satisfy contractual requirements.

After comparing the semi-analytical with numerical approach, the numerical simulation was run with corresponding correct productivity multipliers, which represents the correct well performances.

The withdrawal profiles built according to simulation runs with and without productivity multipliers were compared as depicted in Fig. 7-1. As shown in the figure, the withdrawal profile with productivity multiplier has shorter period of maximum deliverability i.e. deliverability is reduced to some point and afterwards it follows the same trend as the withdrawal profile without productivity multiplier for certain period of time then it decreases again. That means the deliverability rate of working gas to the customer is less than contractual deliverability rate, and consequently the TOV is also less than the TOV in agreement.

The possible measure that can be taken in order to fulfill the agreement by providing 100 percent deliverability and TOV is to increase the volume of base gas. Whether this measure is viable must first be proven by considering economic as well as technical reasons.

As already mentioned above, the base gas volume provides the reservoir pressure necessary to conduct storage operations, which means increasing the amount of base gas increases the inventory and consequently pressure in the reservoir increases as well. If the overall equalized pressure remains under initial pressure, this measure is technically possible. However, in terms of economic considerations it reduces the value of the project.

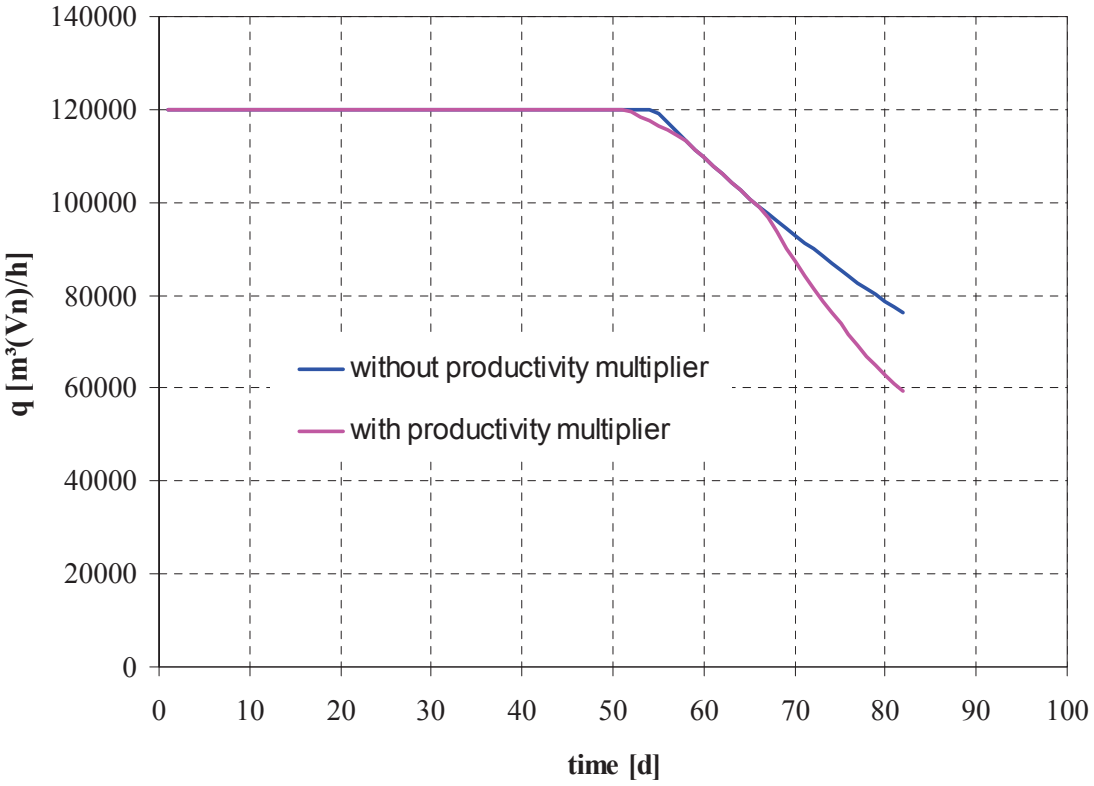

Figure 7-1: Withdrawal profiles with and without productivity multipliers

8 PRESSURE DROP CALCULATIONS

From the reservoir engineering standpoint, a horizontal wellbore is assumed as an infinite-conductivity fracture, i.e., the pressure drop along the well length is very small and is negligible[12]. Thus, horizontal well represents a long wellbore where well pressure throughout the wellbore is constant. In practice, some pressure drop from the tip of the horizontal wellbore to the producing end is important to maintain fluid flow within the wellbore (see Fig. 8-1). The question addressed is, "What is the expected pressure drop along the length of the gas well?"

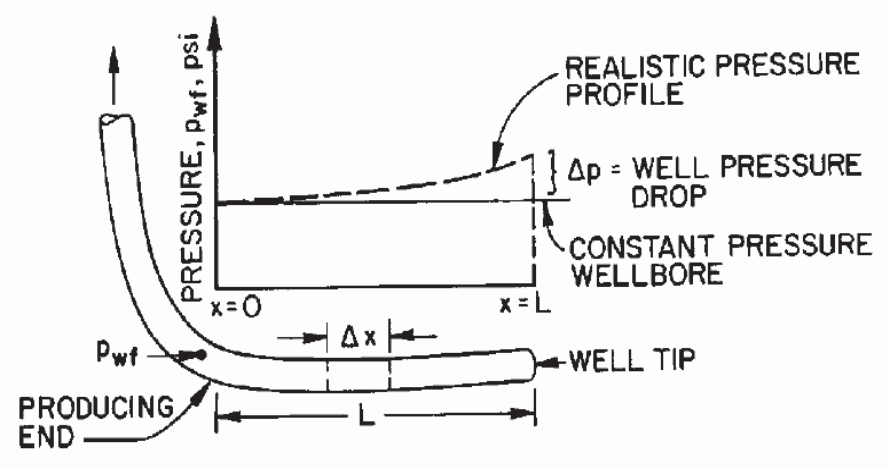

Figure 8-1: A schematic diagram of pressure loss along the well length[12]

Assuming that a horizontal wellbore can be considered as a horizontal pipe, the equation for pressure drop calculation in a pipe can be written using the laws of mass, momentum, and energy conservation as

$$\frac{dp}{dL} = \left(\frac{dp}{dL}\right)_{gravity} + \left(\frac{dp}{dL}\right)_{friction} + \left(\frac{dp}{dL}\right)_{acceleration} \tag{8-1}$$

where dp … pressure drop, and

dL … incremental length

With the further assumption of gravity and acceleration terms being negligible in the horizontal section of the pipe and the flow being fully developed, the equation would reduce to

$$\frac{dp}{dL} = \left(\frac{dp}{dL}\right)_{friciton} = -\frac{f_m \cdot \rho \cdot v^2}{2 \cdot g_c \cdot d} \tag{8-2}$$

For single-phase flow through a horizontal wellbore, the above equation can be rewritten in terms of U.S. field units as[11]

$$\Delta p = (1.14644 \times 10^{-5}) f_m \rho q^2 L / d^5 \quad \text{(in U.S. field units)} \tag{8-3}$$

where f_m … Moody's friction factor, dimensionless

ρ … Fluid density, [g/cm³]

Δp … Pressure drop, [psia]

q … Flow rate at Reservoir conditions, [RB/day]

L … Horizontal length, [ft]

d … Pipe diameter, [inches] => represents the internal pipe diameter

$$f_m = \{1.14 - 2\log|(\varepsilon / d) + 21.25\,\mathrm{Re}^{-0.9}|\}^{-2} \qquad \text{for turbulent flow} \tag{8-4}$$

where ε … Pipe roughness [inches]

Re … Reynolds number [dimensionless]

The Reynolds number is defined as

$$\mathrm{Re} = \frac{q \cdot D}{\vartheta \cdot A} \quad \text{or} \quad \mathrm{Re} = \frac{\upsilon \cdot D}{\vartheta} \tag{8-5}$$

q … Flow rate [m³/s]

D … Inner diameter of pipe [m]

ϑ … Kinematic viscosity [m²/s] which equals to μ/ρ;

where μ … Dynamic viscosity [Pa.s] and ρ … density [kg/m³]

A … cross-sectional area that the flow is going through [m²]

$\upsilon = \frac{q}{A}$ … Velocity [m/s]

For the case of Haag field i.e. three horizontal wells, HGSP-001, HGSP-002 and HGSP-003 the calculations are as following:

First of all, the flow regime is determined using the Eq. 8-5 for bottom hole flowing pressure of 37 [bara] and reservoir temperature 39 [°C].

1) Inner diameter of tubing = 6.19 [inches] = 0.157226 [m]
2) $A = \pi \cdot r^2 \Rightarrow A = \pi \cdot 3.095^2 = 30.09339457$ [in²] = 0.0194151 [m²]
3) $\frac{p \cdot V}{z \cdot T} = \left(\frac{p \cdot V}{z \cdot T}\right)_{Norm}$

   p_N = 1 [atm]

   T_N = 273.15 [K]

V_N = 40000 [m³(Vn)] … the planned amount of gas that should be injected/produced per hour

z_N = 1

p_{wf} = 37 [bara] = 36.51 [atm]

T = 39 [°C] = 312.15 [K]

z = 0.9477 @ 37 [bara] & 39 [°C] (Standing)

$$\frac{36.51 \cdot V}{0.9477 \cdot 312.15} = \frac{1 \cdot 40000}{1 \cdot 273.15} \Rightarrow V = 1186.53 \text{ [m³] per hour}$$

1 hr = 3600 s

$$q = \frac{1186.53}{3600} = 0.3295 \text{ [m³/s]}$$

Velocity in tubing is $\upsilon = \frac{0.3295}{0.0194151} = 16.97$ [m/s]

4) $\vartheta = \frac{\mu}{\rho}$

$\mu = 0.0115$ [cp] = 0.0115×10^{-3} [Pa.s] @ 37 [bara], 39 [°C] (Standing)

$\rho = 23.53$ [kg/m³] @ 37 [bara], 39 [°C]

$$\vartheta = \frac{0.0115 \times 10^{-3}}{23.53} = 4.89 \times 10^{-7} \text{ [m²/s]}$$

The following figures illustrate the viscosity and density trends as a function of pressure. The viscosity is identified according to Standing method.

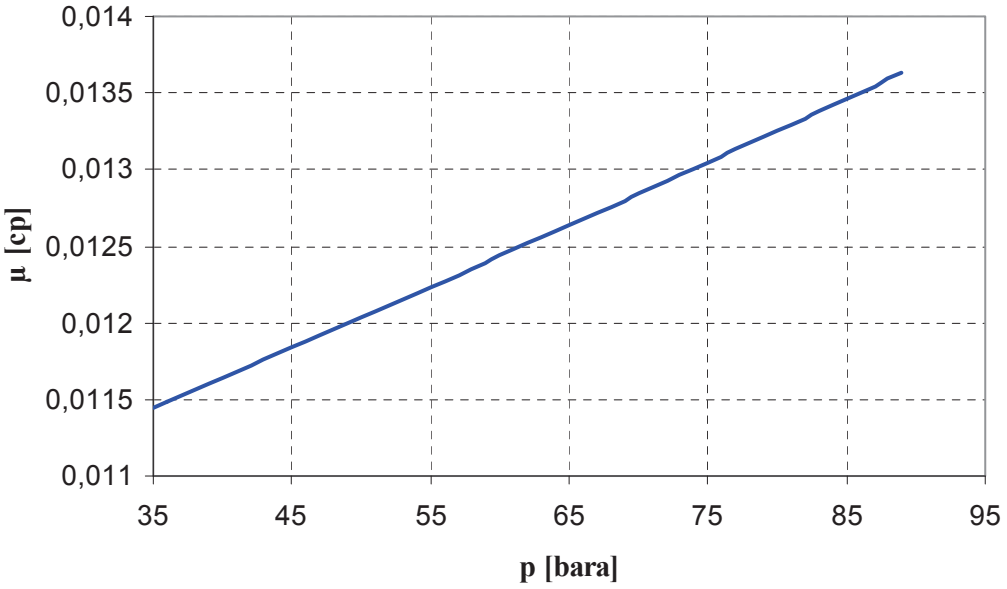

Figure 8-2: Viscosity vs. pressure

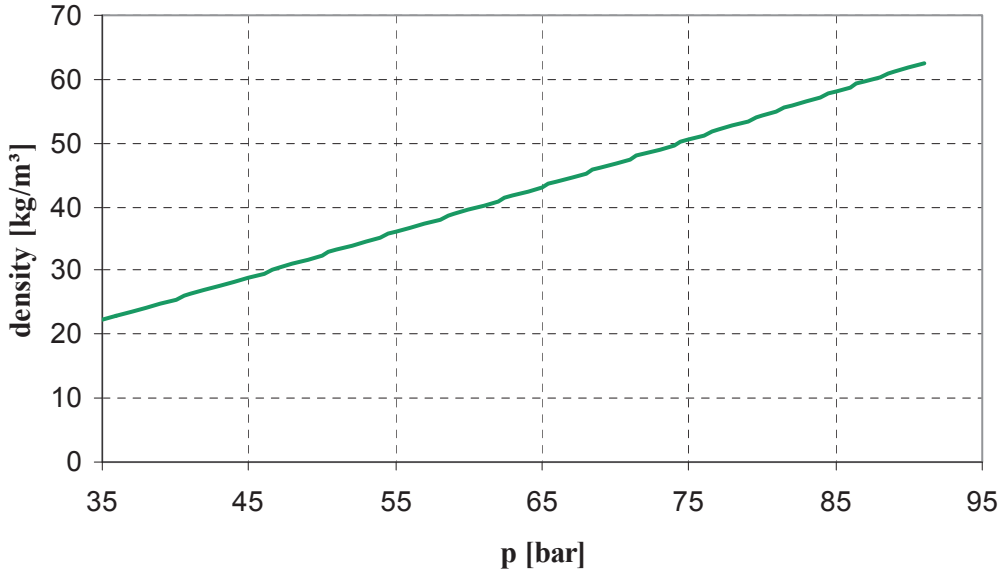

Figure 8-3: Density vs. pressure

The Reynolds number is

$$\mathrm{Re} = \frac{0.3295 \cdot 0.157226}{4.89 \times 10^{-7} \cdot 0.0194151} = 5456715.27 \Rightarrow \mathrm{Re} > 4000 \Rightarrow \text{flow regime} = \text{turbulent!}$$

The following figures show the Reynolds number and velocity in tubing vs. pressure, respectively:

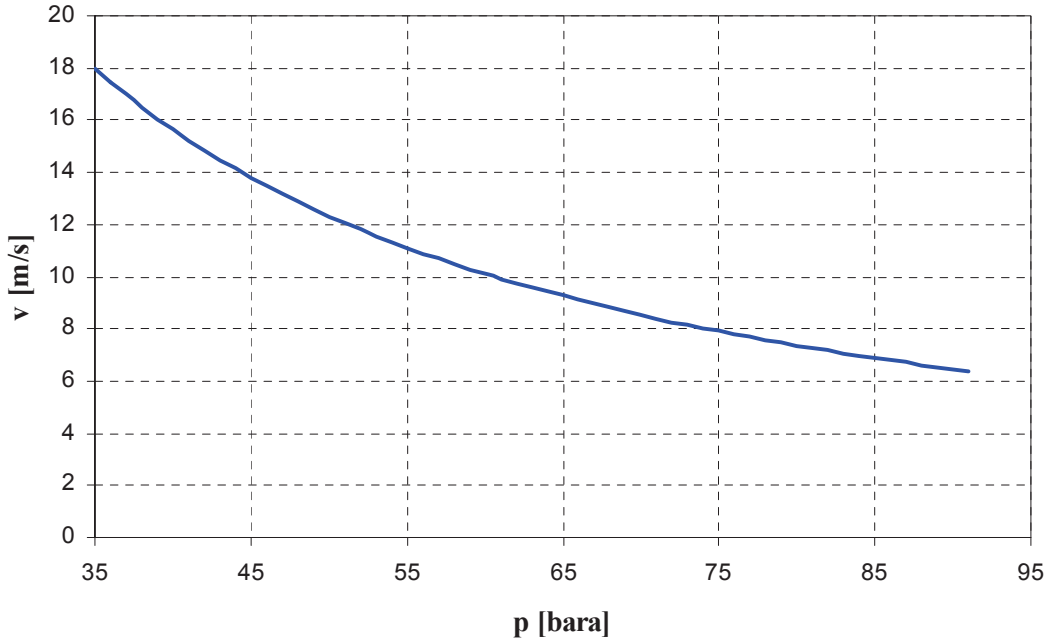

Figure 8-4: Velocity in the tubing vs. pressure

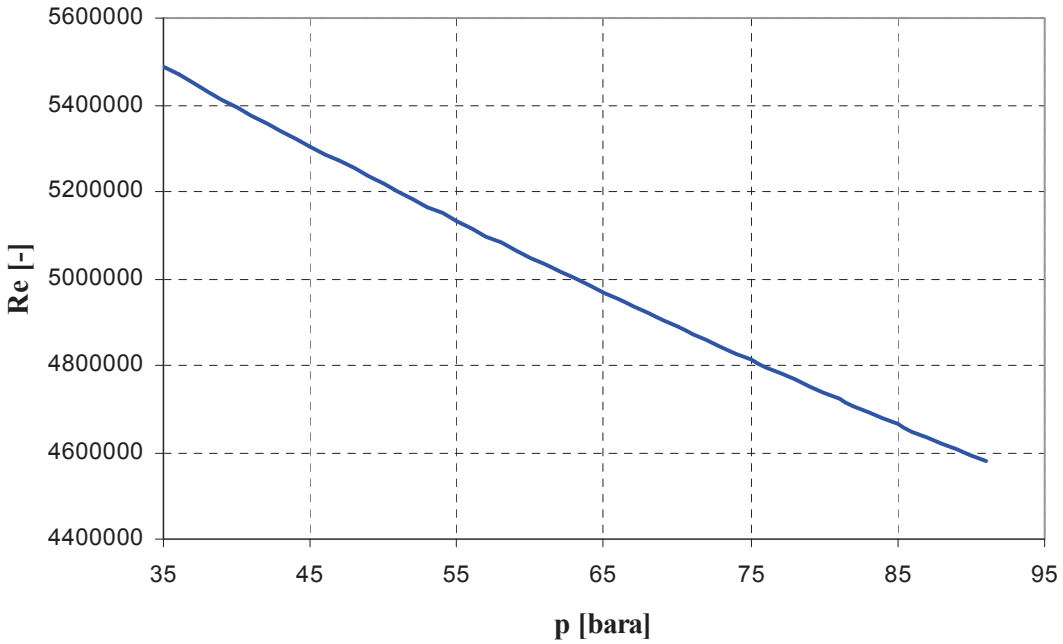

Figure 8-5: Reynolds number (tubing) vs. pressure

Now, the pressure drop due to friction in the tubing is calculated using the Eq. 8-3.

$\varepsilon = 0.0006\,[\text{Inches}]$ … pipe roughness

$\varepsilon / d = 0.0006 / 6.19 = 9.69 \times 10^{-5}$

$f_m = \{1.14 - 2\log\left|9.69 \times 10^{-5} + 21.25 \cdot 5456715.27^{-0.9}\right|\}^{-2} = 0.0123003619$

The well length differs for each well; therefore the parameters are inserted into the Eq. 8-3 for individual well as following:

HGSP-001:

L = 738.54 [m] = 2423.03 [ft]

$\rho = 23.52$ [kg/m³] = 0.02352 [g/cm³] @ 37 bara; 39 °C

$q = 1186.53$ [m³/h] = 179113 [bbl/d] @ 37 bara; 39 °C

$$\Delta p = (1.14644 \times 10^{-5}) \cdot 0.0123003619 \cdot 0.02352 \cdot 179113^2 \cdot 2423.03 / 6.19^5$$

$\Delta p = 28.37$ [psia] = **1.95 [bar]** pressure drop due to friction at lowest bottom hole flowing pressure possible (37 bara).

HGSP-002:

L = 805.48 [m] = 2642.65 [ft]

$\rho = 23.52$ [kg/m³] = 0.02352 [g/cm³] @ 37 bara; 39 °C

$q = 1186.53$ [m³/h] = 179113 [bbl/d] @ 37 bara; 39 °C

$$\Delta p = (1.14644 \times 10^{-5}) \cdot 0.0123003619 \cdot 0.02352 \cdot 179113^2 \cdot 2642.65 / 6.19^5$$

$\Delta p = 30.94$ [psia] = **2.13 [bar]** at bottom hole flowing pressure 37 bara.

HGSP-003:

L = 806.56 [m] = 2646.19 [ft]

$\rho = 23.52$ [kg/m³] = 0.02352 [g/cm³] @ 37 bara; 39 °C

$q = 1186.53$ [m³/h] = 179113 [bbl/d] @ 37 bara; 39 °C

$$\Delta p = (1.14644 \times 10^{-5}) \cdot 0.0123003619 \cdot 0.02352 \cdot 179113^2 \cdot 2642.65 / 6.19^5$$

$\Delta p = 30.98$ [psia] = **2.13 [bar]** pressure drop due to friction at lowest bottom hole flowing pressure of 37 bara.

The highest fluid velocity occurs near the wellbore, where flow converges. Usually the fluid velocity near the wellbore can be minimized by increasing perforated producing length[12]. The flow regime through perforations can be calculated to check the above statement for the three horizontal wells of Haag field.

All three wells were completed with pre-drilled liners. The well HGSP-001 has 7 perforations per feet with a diameter of $1^{3/4}$ [in]. The perforated zones, their lengths and the number of perforations are tabulated in the following table.

Table 8-1: Perforation data of HGSP-001

Perforated zone	Length [ft]	Perforations
1	81,069	567
2	608,46	4259
3	965,98	6762
	Total	**11589**

The Eq. 8-5 is used to determine the Reynolds number, in which the perforation diameter is used for the calculation.

1. Diameter of a perforation is 1.75 [inches] = 0.04445 [m]

2. $A = \pi \cdot r^2 \Rightarrow A = \pi \cdot \left(\frac{1.75}{2}\right)^2 = 2.405281875\,[\text{in}^2] = 0.00155179\,[\text{m}^2]$

3. $\frac{p \cdot V}{z \cdot T} = \left(\frac{p \cdot V}{z \cdot T}\right)_{Norm}$

   $p_N = 1$ [atm]

   $T_N = 273.15$ [K]

   $V_N = 40000$ [m³(Vn)] … the planned amount of gas that should be injected/produced per hour

   $z_N = 1$

   p = 37 [bara] = 36.51 [atm] … the lowest possible bottom hole flowing pressure

   T = 39 [°C] = 312.15 [K] … reservoir Temperature

   z = 0.9477 @ 37 [bara] & 39 [°C] (Standing)

   $\frac{36.51 \cdot V}{0.9477 \cdot 312.15} = \frac{1 \cdot 40000}{1 \cdot 273.15}$ => V = 1186.53 [m³] per hour

   1 hr = 3600 s

   $q = \frac{1186.53}{3600} = 0.3295\,[\text{m}^3/\text{s}]$

   I assumed an even flow distribution from reservoir into the tubing.

   q per perforation: $q = \frac{0.3295}{11589} = 2.84412 \times 10^{-5}$ [m³/s] per perforation.

   Velocity: $\upsilon = \frac{q}{A} \Rightarrow \upsilon = \frac{2.84412 \times 10^{-5}}{0.00155179} \frac{m^3/s}{m^2} = 0.01832$ [m/s] per perforation

4. $\vartheta = \frac{\mu}{\rho}$

$\mu = 0.0115$ [cp] = 0.0115x10^{-3} [Pa.s] @ 37 [bara], 39 [°C] (Standing)

$\rho = 23.53$ [kg/m³] @ 37 [bara], 39 [°C]

$$\vartheta = \frac{0.0115 \times 10^{-3}}{23.53} = 4.89 \times 10^{-7} \text{ [m²/s]}$$

Putting all the parameters above into the Eq. 8-5 gives

$$\text{Re} = \frac{2.88412 \times 10^{-5} \cdot 0.04445}{4.89 \times 10^{-7} \cdot 0.00155179} = 1666.2 \quad \Rightarrow \text{Re} < 2300 \Rightarrow \text{flow regime = laminar!}$$

The well HGSP-002 has 36 perforations per feet with a diameter of ½ [in]. The perforated zones, their length and the number of perforations are tabulated in Table 8-2.

Table 8-2: Perforation data of HGSP-002

Perforated zone	Length [ft]	Perforations
1	243,27	8758
2	122,08	4395
3	81,69	2941
4	282,87	10183
5	811,06	29198
	Total	**55475**

The same calculation steps were done to calculate the Reynolds number for HGSP-002 and HGSP-003.

$$\text{Re} = \frac{5.9412 \times 10^{-6} \cdot 0.0127}{4.89 \times 10^{-7} \cdot 12.66 \times 10^{-5}} = 1218.07 \quad \Rightarrow \text{Re} < 2300 \Rightarrow \text{flow regime = laminar!}$$

The HGSP-003 has 7 perforations per feet with a diameter of $1^{3/4}$ [in]. The perforated zones, their length and the number of perforations are tabulated in the table below.

Table 8-3: Perforation data of HGSP-003

Perforated zone	Length [ft]	Perforations
1	910,4	6373
2	356,4	2495
3	199,3	1395
4	518,2	3627
	Total	**13890**

$$\text{Re} = \frac{2.3722 \times 10^{-5} \cdot 0.04445}{4.89 \times 10^{-7} \cdot 0.00155179} = 1389.57 \quad \Rightarrow \text{Re} < 2300 \Rightarrow \text{flow regime = laminar!}$$

The figure below shows the Reynolds number vs. pressure for the three wells.

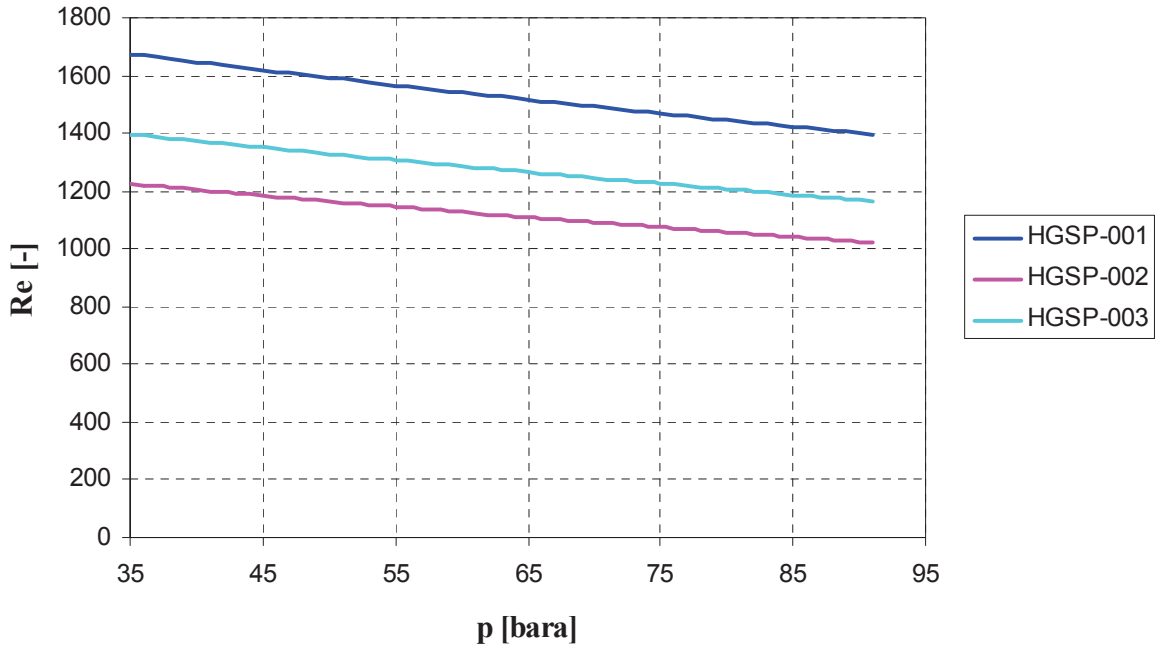

Figure 8-6: Reynolds number (perforation) vs. pressure

All three wells have laminar flow through a perforation for bottom hole flowing pressure ranging between 35 and 91 [bara].

The following figure depicts the velocity trend in a perforation for the three wells.

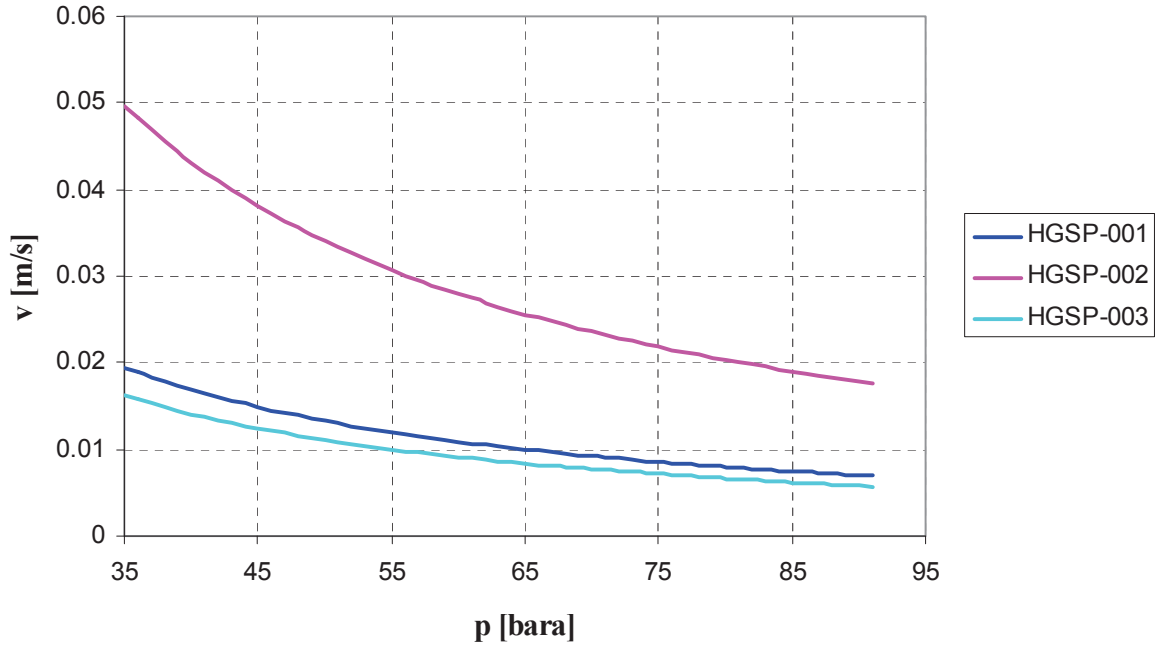

Figure 8-7: Velocity in the perforation vs. pressure

The flow regime in the perforation is laminar since the total flow rate of the fluid into the well is divided by the large number of perforations (up to 55475). Consequently, the velocity of the fluid entering the perforation drops drastically. The only assumption considered for the calculations of flow regime through a perforation, is the evenly distribution of flow into the well from all directions along the well length.

The flow after perforations i.e. in the tubing is turbulent for pressures between 35 and 91 [bara], since the Reynolds number is above 4000. The pressure losses due to friction are calculated as above. However, as seen from the results there is no significant pressure drop (maximum 2.13 bar) at these conditions.

RECOMMENDATIONS

The well inflow calculated by numerical approach is higher than the well inflow calculated semi-analytically for the same reservoir conditions. The inflow calculation method used in the software package, ECLIPSE, is unknown. The semi-analytical calculations are more reliable because the methods behind the semi-analytical approach are known and well researched and tested.

The difference between the two approaches i.e. the failure in the numerical approach is not negligible.

As a consequence, the results of the numerical approach must be matched to the results of the semi-analytical approach. However, a general usable matching parameter or matching equation does not exist and therefore the matching procedure has to be done on a well by well base.

Therefore, it is recommended to construct semi-analytically inflow performance models for each horizontal well parallel to the numerical approach to be able to correct the numerical calculations.

REFERENCES

1. Schlumberger: *Underground Gas Storage Feasibility Study for the Hall Formation HOF-3 Reservoir, Haag Field*.
2. Kuhlemann, J., Kempf. O., 2002, *Post-Eocene evolution of the North Alpine Foreland Basin and its response to Alpine tectonics, Sedimentary Geology*, 152, 45-78.
3. Nachtmann, W., Wagner, L., 1987, Mesozoic and Early Tertiary evolution of the Alpine Foreland in Upper Austria and Salzburg, Austria, Tectonophysics, 137, 61-76.
4. Borowski, K., Strauss, C., Hinsch, R., 2008, *Lithofacies and depositional environment in the upper Hall Formation, Alpine Molasse basin, Upper Austria, Pangeo* 2008, Journal of Alpine Geology, Vol. 49, p.13.
5. Hinsch, R., 2008, *New Insights into the Oligocene to Miocene Geological Evolution of the Molasse Basin of Austria,* Oil & Gas European Magazine, V34 (3), p. 138-143.
6. *PROSPER Reference Manual*, Petroleum Experts Ltd., Edinburgh, UK (2009)
7. Jones, L. G., Blount, E. M., and Glaze, O. H.: "*Use of Short Term Multiple Rate Flow Tests to Predict Performance of Wells Having Turbulence,*" SPE ATCE (Oct. 1976)
8. Goode, P. A. and Kuchuk, F. J.: "*Inflow Performance of Horizontal Wells,*" SPE Reservoir Engineering (Aug. 1991) 319-323.
9. Goode, P. A. and Wilkinson, D. J.: "*Inflow Performance of Partially Open Horizontal Wells,*" JPT (Aug. 1991) 983-987.
10. Babu, D. K. and Odeh, A. S.: "*Productivity of a Horizontal Well,*" RR870902-1FR September 2, 1987.
11. Tek, M. R., *Natural Gas Underground Storage, Inventory and Deliverability*, PennWell Publishing, 1996.
12. Joshi, S. D., *Horizontal Well Technology*, PennWell Publishing, 1991.
13. Ho, C.K., and Webb, S. W., *Gas Transport in Porous Media*, Springer, 2006.
14. Whitson, C. H. and Brule, M. R., *Phase Behavior*, SPE Monograph Series V20, 2000.

APPENDIX

Appendix A: Brooks and Corey System[13]

$$S_e = \frac{S_l - S_{l,r}}{1 - S_{l,r}} \tag{A-1}$$

$$k_{r,l} = S_e^{(2+3\lambda)/\lambda} \tag{A-2}$$

$$k_{r,g} = (1 - S_e)^2 \left(1 - S_e^{(2+\lambda)/\lambda}\right) \tag{A-3}$$

where S_e … Effective saturation

$k_{r,l}$ … Liquid relative permeability

$k_{r,g}$ … Gas relative permeability

λ … pore-size index

Appendix B: Z-factor calculation with Standing and Katz method[14]

Standing and Katz (1942) has developed a generalized Z-factor chart (see Fig. A-1), which has become an industry standard for predicting the volumetric behaviour of gases. Standing presents the following correlations to determine pseudocritical properties for dry hydrocarbon gases ($\gamma_{gHC} < 0.75$),

$$T_{pcHC} = 168 + 325\gamma_{gHC} - 12.5\gamma^2{}_{gHC} \tag{A-4}$$

$$p_{pcHC} = 667 + 15\gamma_{gHC} - 37.5\gamma^2{}_{gHC} \tag{A-5}$$

T_{pcHC} … Hydrocarbon-component pseudocritical temperature in a gas [°R]

p_{pcHC} …Pseudocritical pressure of hydrocarbon components only in a gas [psia]

γ_{gHC} … Gas specific gravity of hydrocarbon components in a gas mixture

$$T_{pr} = \frac{T}{T_{pcHC}} \tag{A-6}$$

$$p_{pr} = \frac{p}{p_{pcHC}} \tag{A-7}$$

T_{pr} …pseudoreduced Temperature

T … Temperature [°R]

p_{pr} …pseudoreduced pressure

p … Pressure [psia]

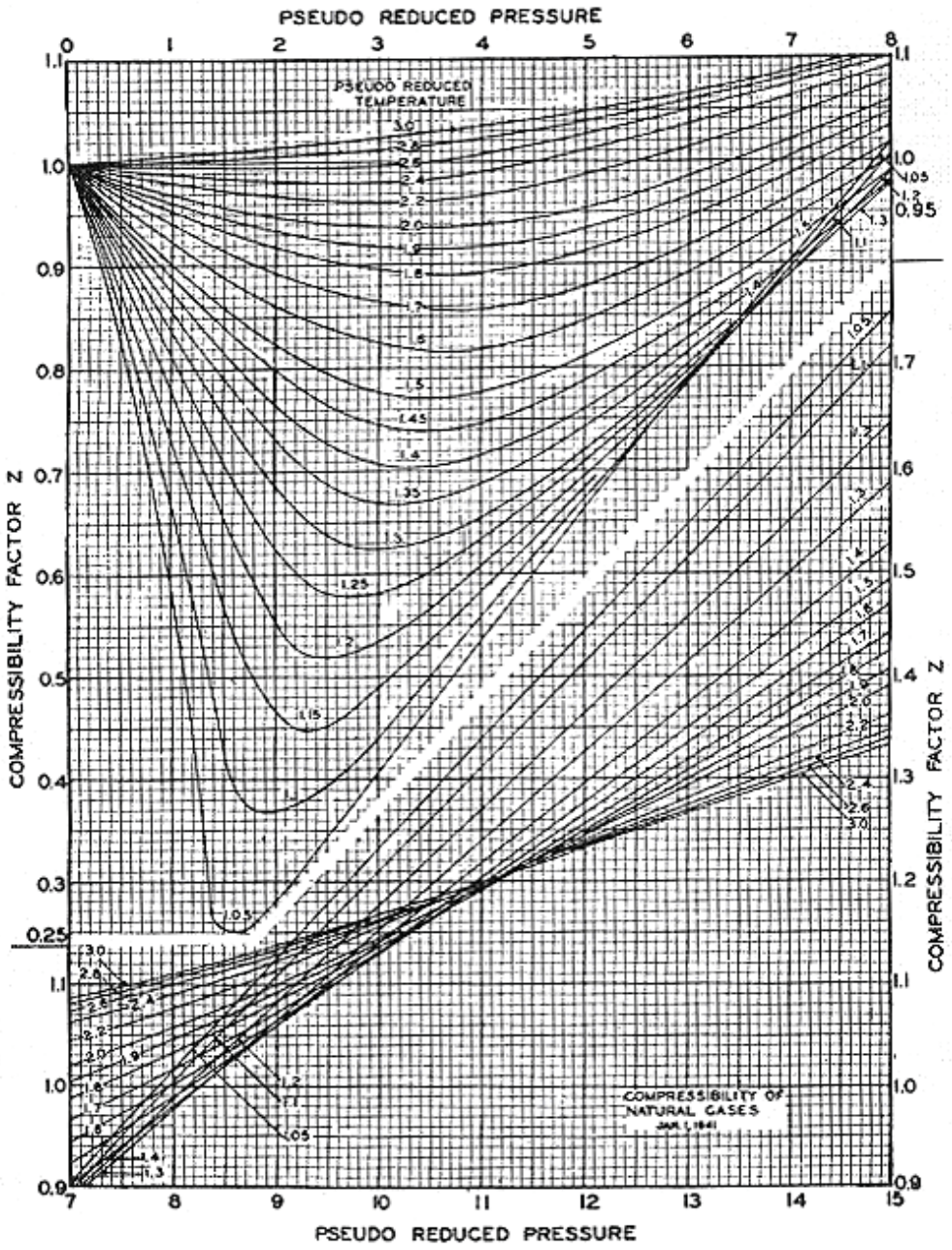

Figure A- 1: Standing-Katz Z-factor chart[14]

Appendix C: Calculation of Formation Volume Factor[14]

The gas formation volume factor B_g is defined as the ratio of gas volume at specified p and T divided by the ideal gas volume at standard conditions.

$$B_g = \left(\frac{p_{sc}}{T_{sc}}\right)\frac{zT}{p} \qquad \text{(A-8)}$$

p_{sc} … Pressure at standard conditions

T_{sc} … Temperature at standard conditions

For p in [bar] and T in [°C] this result in:

$$B_g = 0.0037085 \cdot z \cdot \frac{T}{p} \text{ [m³/Sm³]}$$

Appendix D: Pressure distributions in the field

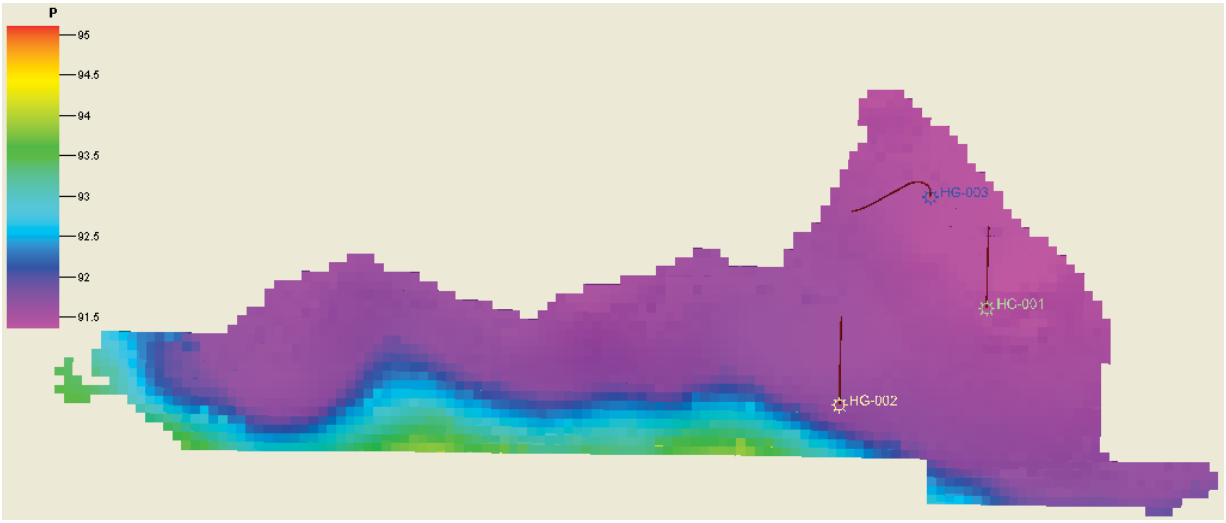

Figure A- 2: Pressure distribution in the Haag reservoir – 1983

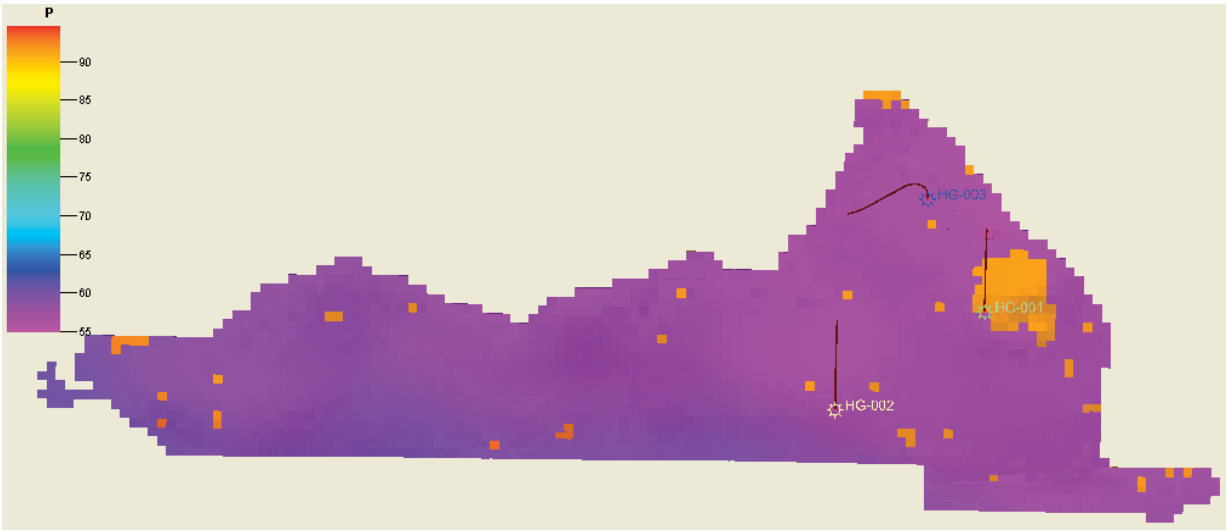

Figure A- 3: Pressure distribution in the Haag reservoir – 1993

The blocks with orange/red colour, in the figure above and in the figures below, represent non-permeable shale blocks with less than 3 % porosity. These blocks exhibit initial pressure, but they do not have communication with neighbour blocks.

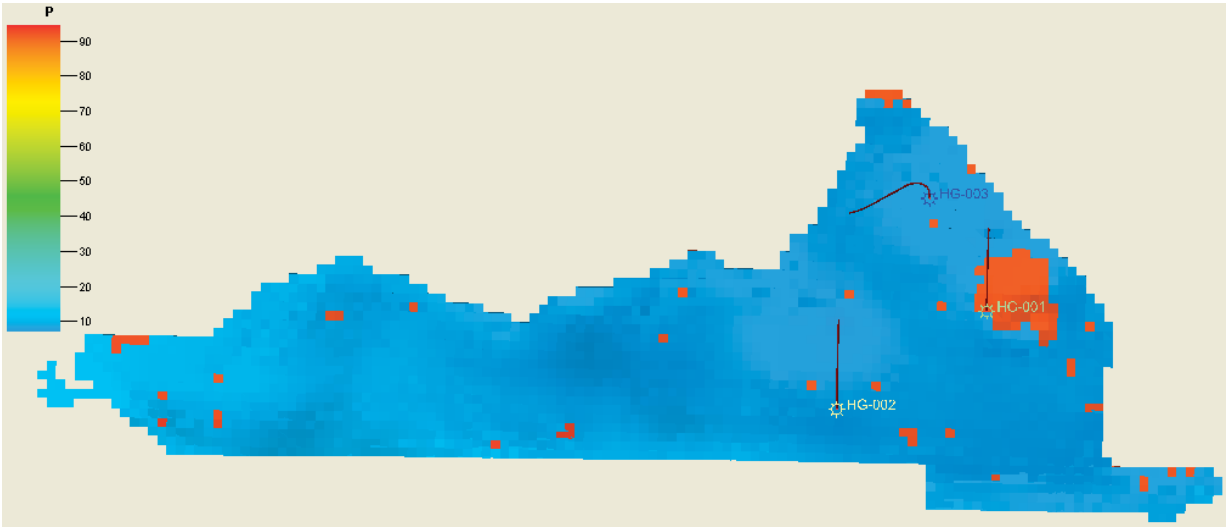

Figure A- 4: Pressure distribution in the Haag reservoir – 2003

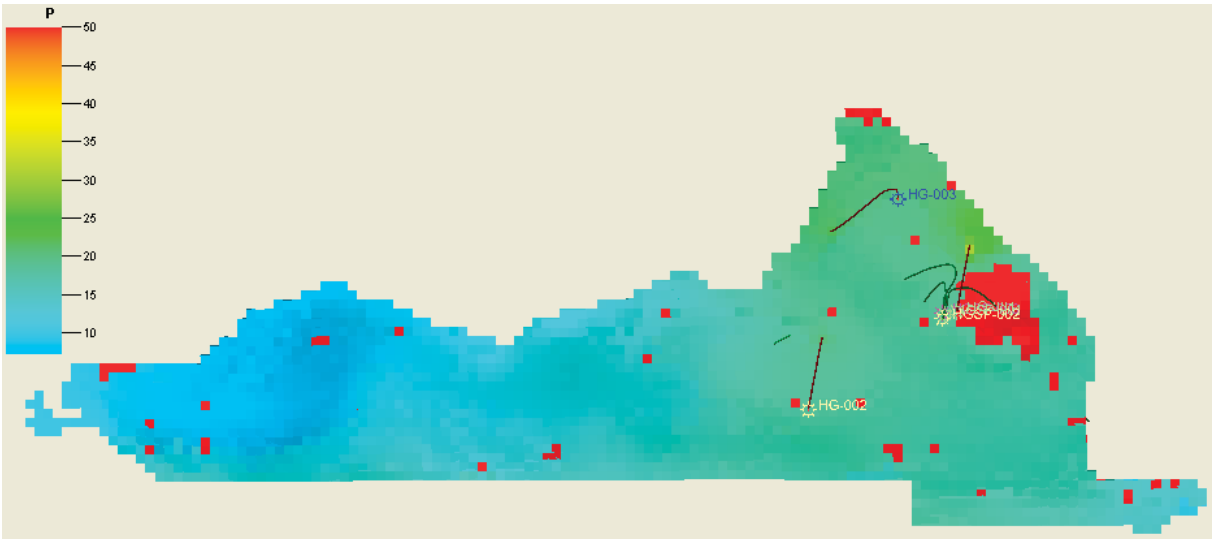

Figure A- 5: Pressure distribution in the Haag reservoir – 2008

In July 2007 injection through vertical wells for pressure build-up was started. In the figure above one can see the development of pressure build-up around the wells in January, 2008.